# REMOTE MEASUREMENT OF GRAVEL-BED RIVER DEPTHS AND ANALYSIS OF THE GEOMORPHIC RESPONSE OF RIVERS TO CANALS AND SMALL DAMS

by

SUZANNE CORINNA WALTHER

A DISSERTATION

Presented to the Department of Geography
and the Graduate School of the University of Oregon
in partial fulfillment of the requirements
for the degree of
Doctor of Philosophy

December 2010

DISSERTATION APPROVAL PAGE

Student: Suzanne C. Walther

Title: Remote Measurement of Gravel-bed River Depths and Analysis of the Geomorphic Response of Rivers to Canals and Small Dams

This dissertation has been accepted and approved in partial fulfillment of the requirements for the Doctor of Philosophy degree in the Department of Geography by:

| | |
|---|---|
| W. Andrew Marcus | Chairperson |
| Patricia F. McDowell | Member |
| Dan G. Gavin | Member |
| David W. Hulse | Outside Member |

and

| | |
|---|---|
| Richard Linton | Vice President for Research and Graduate Studies/Dean of the Graduate School |

Original approval signatures are on file with the University of Oregon Graduate School.

Degree awarded December 2010

DISSERTATION ABSTRACT

Suzanne C. Walther

Doctor of Philosophy

Department of Geography

December 2010

Title: Remote Measurement of Gravel-bed River Depths and Analysis of the Geomorphic Response of Rivers to Canals and Small Dams

Approved: _____
W. Andrew Marcus

This dissertation investigates the potential impacts of canals and small dams on gravel-bed rivers and methods for documenting those impacts. First, I evaluate the potential for mapping channel depths along the McKenzie River, OR, using 10 cm resolution optical aerial imagery with a hydraulically-assisted bathymetry (HAB-2) model. Results demonstrate that channel depths can be accurately mapped in many areas, with some imagery limitations. The HAB-2 model works well in the majority of the river ($R^2$=0.89) when comparing modeled to observed depths, but not in areas of shadow, surface turbulence, or depths >1.5 m. Next, I analyze the relative effects of a small dam and two diversion canals on sediment distribution along bars of the lower McKenzie River. The typical pattern of downstream fining is disrupted at each feature and several tributaries, particularly in the "reduced water reaches" below canal outtakes. Most modeled discharge values necessary to mobilize bar sediments fall at or below the 2-year flood return interval, with the remaining at or below the 5-year flood return interval, generally reflecting the $D_{50}$ values at each bar (20-115 mm). The third analysis investigates the potential to document geomorphic impacts of small dams in Oregon at ecoregion extents using air photos and

publically available data sets. This analysis highlights data disparity with respect to the collecting agency's mission and the difficulty of using remote sensing for small dams. Though the imagery was not useful in evaluating small dam impacts due to resolution and feature size, the data were useful in mapping the small dam distribution across Oregon and each ecoregion. Sixty-one percent of Oregon land is located in the catchment of at least one small dam and the greatest number of dams per area is in the Willamette Valley ecoregion. Overall, this research suggests that, while the application of these techniques must be improved, our ability to observe, study, and understand rivers is enhanced by remote sensing advancements and the combined use of these methods in river restoration and management.

This dissertation includes previously published and co-authored material.

CURRICULUM VITAE

NAME OF AUTHOR: Suzanne C. Walther

GRADUATE AND UNDERGRADUATE SCHOOLS ATTENDED:

University of Oregon, Eugene
University of Virginia
University of California, Santa Barbara

DEGREES AWARDED:

Doctor of Philosophy, 2010, University of Oregon
Master of Science, 2006, University of Oregon
Master of Science, 2003, University of Virginia
Bachelor of Arts, 1992, University of California, Santa Barbara

AREAS OF SPECIAL INTEREST:

Fluvial geomorphology
Human impacts on river systems
Remote sensing of rivers

PROFESSIONAL EXPERIENCE:

Researcher, Willamette River Environmental Flows Monitoring, US Army Corps of Engineers (USACE) and The Nature Conservancy (TNC), 2010

Course Instructor, Department of Geography, University of Oregon,
Hydrology and Water Resources Winter 2010
The Natural Environment Spring 2009, Summers 2008, 2009
GEOG 360 Watershed Science and Policy Winter 2008

EWEB research representative and Lane Council of Governments researcher, McKenzie River Project, University of Oregon and Eugene Water and Electric Board (EWEB), 2008-2009

Course Instructor, International Studies Office, University of Virginia,
Study Abroad in Southern Africa, People, Culture and the Environment of southern Africa, 2007, 2008

Graduate Teaching Fellow, Department of Geography, University of Oregon, Physical Geography, Global Environmental Change, Advanced GIS, Remote Sensing, Fluvial Geomorphology and Watershed Science and Policy Fall 2006-Fall 2007, Spring 2008, Spring 2010

Researcher, Sprague River Project, University of Oregon, Summer 2007

Teaching Assistant International Studies Office, University of Virginia, Study Abroad in Southern Africa, People, Culture and the Environment of southern Africa, 2002, 2003, 2006

Tutor, Services for Student Athletes, University of Oregon, 2006-2007

Graduate Teaching Fellow, Department of Geological Sciences, University of Oregon, Introductory Geology sequence, 2003-2006

Teaching Assistant, Department of Environmental Sciences, University of Virginia, Geology Labs, 2000-2003

Associate, California-American Water Company, Chula Vista, California, 1999-2000

Research Assistant, Department of Geological Sciences, California State University, Long Beach, 1997-1998

Enviro-Grants Administrator and Associate, Patagonia Corporation, Boston, Washington, D.C., Santa Monica, and Munich, Germany, 1994-1999

GRANTS, AWARDS, AND HONORS:

ASPRS William A. Fischer Memorial Scholarship, 2009

UO College of Arts and Sciences Charles A. Reed Graduate Fellowship, 2009

GSA Robert K. Fahnestock Memorial Award, 2008

University of Oregon Women in Graduate Science Travel Award, 2008

SAVANA Travel Grant, 2008

University of Oregon Summer Research Grant, 2007

SAVANA Research Grant, 2007

Gamma Theta Upsilon, Theta Kappa Chapter, 2006

Moore Research Award, 2003

UVA Graduate Fellowship, 2001-2002 and 2002-2003

GSA Graduate Research Grant, 2002

UVA Department Exploratory Research Grant, 2002

US Rowing Collegiate All-American, 1992

Western Region and NCAA Scholar-Athlete, 1991 and 1992

PUBLICATIONS:

Walther, S.C., and Neumann, F., in review. Sedimentology, isotopes and palynology of late Holocene cores from Lake Sibaya and the Kosi Bay system (KwaZulu-Natal, South Africa). *South African Geographical Journal*.

Walther, S.C., Marcus, W.A., and Fonstad, M., in press 2010. Evaluation of high resolution, true colour, aerial imagery for mapping bathymetry in clear water rivers without ground-based depth measurements. *International Journal of Remote Sensing*.

Walther, S.C., Roering, J.J., Almond, P.W., and Hughes, M.W., 2009. Long-term biogenic soil mixing and transport in a hilly, loess-mantled landscape: Blue Mountains of southeastern Washington. *Catena*, 79 (2): 170-178.

Swap, R.J., Walther, S.C., and Annegarn, H.J., 2008. SAVANA: Implementation and Evolution of an International Research and Education Consortium. *IIENetwork*, 2008. http://www.iienetwork.org/page/133528/

# ACKNOWLEDGMENTS

I would first like to thank my advisor Andrew Marcus for his generosity, kindness and especially his patience, even when I had none. I am extremely grateful that I took your river modeling course just before my academic career nearly ended--it turned out to be a much better fit in the end. We fell into the McKenzie River, so to speak, and took the research much farther than expected. I learned a lot from the collaborative experience between the University, Eugene Water and Electric Board (EWEB), and various agencies. Many thanks to Pat McDowell for introducing me to fluvial geomorphology and to teaching watershed science and policy, and for including me in the Willamette project. I have learned a lot from you both. I would like to thank my other committee members for their help during this process: Dan Gavin for his thoughtfulness and David Hulse for his flexibility. Thanks also go to Mark Fonstad for his insight and collegiality.

I would like to thank Karl Morgenstern at EWEB for funding and logistical support. He is integral to the vision and collaboration efforts to improve the future of the McKenzie River. Thanks to Bob DenOuden at the Lane Council of Governments (now at EWEB) for the time and space to write. Thanks to the McKenzie Fire and Rescue, who provided logistical support on the McKenzie River. Thank you to Paul Blanton, Russ Harrel, Karl Morgenstern, David Donohue, Steve Vandecoevering, JD Fountain, Jack Kyle, Stephani Michelson-Correa, Matt Landers, and Doug Caven who helped collect field data, to Jacob Bartruff for help in applying HAB-2 in ArcMap, and to Amanda Reinholtz for tackling ArcHydro in no time and helping graph with R.

Thanks to my initial cohort and to my first real office mate: Ingrid Nelson--to adventures on that side in the future. Thanks to my awesome office mates and River

Club: Paul Blanton, Polly Lind, Didi Martinez, Stephani Michelson-Correa, Amanda Reinholtz, Denise Tu, and Sarah Praskievicz. We managed to form a real working/thinking group and had fun in the process.

Though this was a journey that could be called nothing but a struggle from beginning to end, as it was more an exercise in ingenuity and survival for my family, there are some people that made it so much better and added laughter to my life when it didn't feel like I could laugh. Thanks to the Perez-Jefferis family for everything. You guys are the reason we had a real life here. I will never forget that. Watching the boys grow up together has been awesome. Your friendship is pure gold. Thanks also to my fellow OAR rowers--you have no idea how much it meant to be able to "just row"--a release that has kept me *almost* sane. Special thanks to Kellers for invaluable support and friendship--Sally, I couldn't have kept it up without you.

Finally, thanks to Russ Harrel. There are no words that could express how grateful I am for you and your humor through this time and all it encompassed (Rio). Though I wasn't always sure that I'd make it through this, I knew you'd be there. You are a wonderful husband and dad. Rio and I are so lucky to have you.

This research was supported through the University of Oregon Department of Geography, EWEB, the American Society for Photogrammetry and Remote Sensing (ASPRS) William A. Fischer Memorial Scholarship, the Geological Society of America (GSA) Robert K. Fahnestock Memorial Award, the UO College of Arts and Sciences Charles A. Reed Graduate Fellowship, an ASPRS Summer Research Award, a UO Women in Graduate Sciences Travel Grant, and a SAVANA Research Grant.

To all the first generation college students who complete a graduate degree--
we are beating the odds…

TABLE OF CONTENTS

Chapter Page

Chapter Page

Chapter Page

LIST OF FIGURES

Figure Page

LIST OF TABLES

# CHAPTER I

## INTRODUCTION

Rivers are dynamic landscape features (Amoros and Petts, 1993) that scientists in both fluvial geomorphology (Kellerhals et al., 1976; Montgomery and Buffington, 1997; Schmitt et al., 2007) and ecology (Naiman et al., 1992; Chessman et al., 2006) have long attempted to explain by way of reducing the complexity of fluvial features (Kondolf et al., 2003). Historically, the study of rivers has focused on field measurements at the reach scale, yet today we are still unable to answer questions of interactions and linkages that occur at larger scales. Advances in optical remote sensing of rivers have produced several methods for bathymetric (Fonstad and Marcus, 2005; Carbonneau et al. 2006) and grain-size (Carbonneau et al. 2004) mapping at reach extents. At the same time, network-scale variability of fluvial forms and processes has long been investigated by field-based data, but these studies focus on fewer sites because of the time needed to collect the data (Schmitt et al. 2007). However, geomorphic responses to change can occur over long timescales and vary as a function of local channel characteristics and distance from the change of interest (e.g. sediment source, dam reduced hydrology or sediment supply, development, water diversion). Because remote sensing data with medium to high spatial resolution are now available at a national scale (digital elevation model, aerial orthophotographs), these newer methods can now begin to be applied at multiple scales

(Amos et al., 2008; Orr et al., 2008) to gain a new perspective for understanding complex water issues.

In addition to the shift in the scale of investigation, there has been a renewed focus on examining the human role in changing river systems. These changes in the river have occurred through engineering such as channelization, dams, diversions and culverts, and more recently restoration and dam removal (Gregory, 2006). Today, every variety of human use of water as a resource is ubiquitous in the landscape. In order to reduce or minimize negative human impacts of the river system, a better understanding of river processes and linkages, as well as the effects and responses of the river to changes, is needed. Sediment characteristics provide a measure for analysis. Sediment transport dynamics control channel form and geomorphic processes that help create and sustain aquatic habitat. Changes in flow and sediment supply change sediment transfer and, thus, channel stability and size distributions. Sediment movement is critical to the ecological health of the stream system. The sorting of sediment through transport processes creates habitat for spawning and for benthic organisms that provide food for other species. Both species diversity and abundance are affected by grain size, variety of sizes, stability, and the presence of organic detritus (Doyle and Stanley, 2006).

This dynamic character of rivers is a reflection of flow and sediment regimes interacting with landscape vegetative and physiographic features on varying spatial and time scales (Corenblit et al. 2007; Ward and Stanford, 1995). The result is diversity of habitat between and within river reaches that make up a complex ecosystem that is dependent on a continued broader, more inclusive view of river ecology and connectivity

that encompasses spatio-temporal heterogeneity and functional processes of both species and sedimentary dynamics in river systems for its maintenance and restoration.

The need to understand river systems has increased in conjunction with the growing population and expanding development. This dissertation examines methods of studying the river and investigates human impacts on the river. The technological developments in remote sensing have allowed for an entirely new scale at which the riverscape can be studied. In Chapter II, I evaluate the HAB-2 model, with thousands of sonar ground validation points, in the most extensive test to date of the model for its use in basin modeling and river management. The material in Chapter II is co-authored with W. Andrew Marcus and Mark A. Fonstad, and is in press in the International Journal of Remote Sensing (Walther et al., in press).

In Chapter III, I investigate the impacts of the Leaburg dam and the Leaburg and Walterville diversion canals on the sediment movement on the bars of the McKenzie River, Oregon. I use the grain size distribution and median diameter ($D_{50}$) of bar gravels based on count measurements, obtained from field data, to calculate the shear stress and stage height needed to move the median grain size of each bar. Next, I use the WinXSPRO model with sonar and LiDAR based cross-sections to estimate the discharge at the stage height at each bar cross-section. The results are compared against the return interval and the 1996 flood discharges to determine how often the modeled discharges that are needed to move the bar gravels occur. Ultimately, this information can be used to inform environmental flow plans to be implemented on the river for habitat improvement in the near future. This chapter includes material that will be published as a coauthored article with Patricia F. McDowell, who provided editorial assistance.

In Chapter IV, I map the distribution of small dams (30 ft. in height or less) in Oregon from the Oregon Water Resources Division (OWRD) dam and the Oregon Division of Fish and Wildlife (ODFW) fish passage barrier data sets. The density of dams differs with Level IV ecoregion within the state. In addition, I focus on the issues of mapping and evaluating small dam impacts using available datasets. This chapter includes material that will be published as a coauthored article with W. Andrew Marcus, who provided editorial assistance. Chapter V briefly summarizes the overall findings, applications, and significance of this dissertation research.

This research focuses on some of the important issues in river research and science today, including new technologies and techniques for studying and understanding the river system, the geomorphic component of human impacts and its application to the use of environmental flows in management, and the issues related to mapping small dams and evaluating their impacts. Future work will complement this research to provide more expansive gravel movement research on regulated rivers to inform management decisions, especially with respect to environmental flows in sediment supply limited rivers. The McKenzie River and Oregon as a whole can be used as a scale model to study rivers and human impacts within the river channel involving channel change, sediment movement, small dam impacts, and management. Insights gained from this study can be applied to other regions with regulated and/or gravel-bed rivers.

CHAPTER II

# EVALUATION OF HIGH RESOLUTION, TRUE COLOUR, AERIAL IMAGERY FOR MAPPING BATHYMETRY IN A CLEAR WATER RIVER WITHOUT GROUND-BASED DEPTH MEASUREMENTS

This chapter has been accepted for publication:
Walther, S.C., Marcus, W.A., and Fonstad, M.A., In press. Evaluation of high resolution, ture-colour, aerial imagery for mapping bathymetry in clear water rivers without ground-based depth measurements. *International Journal of Remote Sensing.*

## 1. Introduction

Bathymetric maps of rivers are useful for characterizing habitat (McKean, 2008; Legleiter et al. 2002, 2004; Marcus *et al.* 2003), documenting flow dynamics, predicting channel change (Lane *et al.* 2002), forecasting flooding (Brunner, 2002), and evaluating effects of management and restoration efforts (Steffler and Blackburn, 2002). Advances in optical remote sensing of rivers have produced several methods for bathymetric mapping at reach extents (Fonstad and Marcus, 2005; Carbonneau *et al.* 2006). This article evaluates the potential of the hydraulically-assisted bathymetry (HAB-2) model of Fonstad and Marcus (2005) to map channel depths throughout portions of the clear water McKenzie River, Oregon, which is deeper and provides a broader range of shadow,

depth, and turbulence than previous test rivers. HAB-2 is an image-based model that does not require in situ depth measurements to calculate bathymetry.

Specifically, we conduct the most rigorous test of the HAB-2 model to date using extensive sonar data and limited ground-based measurements to evaluate bathymetric maps developed with 10 cm and 0.5 m resolution film-based optical true colour imagery. We evaluated how the accuracies of modelled depths varied with:

- image resolution
- filtering
- different bands
- riffles and shadows, and
- comparison of results with Oregon digital orthophoto quad (DOQ) imagery.

The combined ground and image data allow us to demonstrate the applications of this image-based depth mapping for watershed scale water quality and quantity modelling.

## 2. Bathymetric mapping

### *2.1. General approaches*

Ground-based approaches to mapping bathymetry include rods or drop lines, staff gauges, sonar, and ground penetrating radar. If a large number of measurements are required along a river, these approaches can be time consuming, expensive, and dangerous. Alternatively, modelling approaches such as step backwater modelling can provide depth estimates at different discharges if there are existing survey data. One- and two-dimensional modelling approaches, however, interpolate along and between survey

points and do not capture the full range of flow hydraulics, leading to inaccuracies in depth estimates.

Optical remote sensing of river depths, though limited by the need to see through the water column, can provide more comprehensive data throughout clear water rivers (i.e., rivers in which one can see to the bottom). Remotely sensed bathymetric mapping techniques include those that require ground-based measurements and those that do not. The remote sensing techniques that require ground measurements correlate the image reflectance to depth (Winterbottom and Gilvear, 1997; Lorang *et al.* 2005; Carbonneau *et al.* 2006). The accuracy of correlation-based depth estimates can be improved by segmenting the stream into biotypes (e.g. pools, riffles, etc) (Marcus et al., 2003). Still, the need for ground measurements, even if lesser in number, reduces the gains of using remote sensing, especially when applied to large extents. The personnel costs and time needed to gather data limit the amount of data that can be collected at time-of-image-acquisition and the scale of the project. This often leads to the use of intensive, local data to characterize reach extents (~10s of meters to several hundred meters), or extensive, low density ground data to characterize larger extents, both of which fail to the capture the full range of depth variations in the river (Fonstad and Marcus, *2010*).

The techniques that do not require ground measurements, such as photogrammetry (Lane and Chandler, 2003; Westaway *et al.* 2001, 2003) and HAB (Fonstad and Marcus, 2005), eliminate those ground expenses. However, photogrammetric approaches, while useful for archival imagery, require stereo imagery and more complex and laborious processing. As of this time, the HAB-2 model is the only alternative that does not require ground measurements or stereo imagery. This

enables the bathymetric mapping of unobstructed stream areas over large spatial areas at different times and even with historical imagery, so long as the water is clear.

### *2.2. HAB-2 model background*

The HAB-2 model is based on the Beer-Lambert law that expresses the exponential absorption of light in a water column with minimal scattering:

$$I = I_0 e^{-\beta D} \tag{2.1}$$

where e is the base of natural logs, $I$ is the intensity of light at some water depth, $D$, $I_0$ is the intensity of light prior to entering the water column, and $\beta$ is a diffuse attenuation coefficient (Denny, 2003). The intensity ($I$) is unknown in most images, so the digital number ($DN$) value is substituted into equation (1):

$$DN = DN_0 e^{-\beta D}. \tag{2.2}$$

The distance of light passage $D$ is recognized as the depth of the water and solved for by rearranging equation (2):

$$D = \ln (DN/DN_0) / -\beta. \tag{2.3}$$

The value $DN_0$ is the $DN$ of the riverbed in the absence of water absorption, which is the $DN$ value of a pixel of just-wetted substrate near the channel edge.

The diffuse attenuation coefficient ($\beta$) is a constant that is typically measured with a secchi disk. However, shallow rivers and streams are not sufficiently deep to use this method and it requires ground-based measurements at the time of image acquisition, which obviates the utility of the HAB-2 method. Therefore, the value of the coefficient $\beta$ must be estimated. We do so by inputting a seed value of 1.0 for $\beta$ into equation (2.3), then calculating the depths at each pixel along the cross section. Next, the depth estimates

are combined to calculate the hydraulic radius ($R$) and the cross-sectional area ($A$). This enables us to back-calculate the discharge using the equation:

$$Q = AV = WD_aV \tag{2.4}$$

where area $A$ ($m^2$) is equal to the width ($W$) measured from the image cross section, times the average depth ($D_a$) calculated from the estimated depths using a value of one for $\beta$. $V$ is the average velocity (m/s), typically estimated using the Manning equation:

$$V = R^{2/3}S^{1/2}/n \tag{2.5}$$

where $R$ is the hydraulic radius (m) derived from the estimated cross section, $S$ is the longitudinal energy gradient of the flow (m/m) estimated using the local slope taken from topographic maps, and $n$ is the hydraulic resistance. In this study we use Jarrett's (1984) equation:

$$n = 0.32S^{0.38}R^{-0.16} \tag{2.6}$$

which was shown to be most accurate in high roughness mountain streams similar to the McKenzie River (Jarrett, 1987, Marcus et al. 1992, Wohl, 1998). Assuming $R$ equals $D_a$, we then substitute equations (2.5) and (2.6) into equation (2.4) to solve for $Q$:

$$Q = W\,(D_a^{1.83})\,(S^{0.12}) / 0.32. \tag{2.7}$$

The initial estimate of $Q$, based on the seed value of one for $\beta$, will not match the measured $Q$ value obtained from a local gage. However, an iteration of new values of $\beta$ can be input until the estimated $Q$ value equals the measured $Q$ value. Once the $\beta$ value is determined, equation (2.3) can be applied to the $DN$ values for the entire stream to create a bathymetric map. The model is run in a Microsoft Office Excel spreadsheet (Microsoft, 2009).

## 3. Study area

The McKenzie River is a sixth-order, 138 km long westward flowing tributary of the Willamette River in western Oregon (figure 2.1). The study area is in the lower two-thirds of the watershed where the river channel is mostly unconfined and the valley widens with distance downstream. The river in these reaches is characterised by a slope of less than 0.002, though there are large local variations across the reach characterized by riffle-pool morphology. The river usually has a single channel and long, relatively straight reaches with occasional large amplitude bends, mid-channel bars and islands that locally give the river a multithreaded character. In the study reach of the river, the channel is 40-60 m wide, with primarily Douglas fir, cedars, and cottonwood growing on the banks. Depending on the portion of river and sun angle the firs can cast shadows over the entire or much of the width of the channel. These variations in river and lighting conditions and the need to address them are discussed in section 6.1.4.

The sediment transport capacity is high relative to sediment supply, so the channel bed is predominantly cobble and boulders (EA Engineering, Science, and Technology, 1991). The river is the sole source of water for the city of Eugene, Oregon, and the source of power for the Leaburg Walterville Hydroelectric Project. The project on the lower McKenzie includes one dam, two diversion canals, and two power plants, all of which are run-of-the-river facilities (EWEB, 2007). The study area extends from Leaburg Dam to just below the Walterville tailrace (figure 2.1*c*). The results of this study are useful for ongoing flow routing and water quality models being developed by EWEB. Models, such as the MIKE-11 model developed by DHI Water & Environment, Inc., use cross-sections along the length of the river in the modelling flow processes. As with

many hydraulic models, the cross-sections used for the MIKE-11 model are often simplistic trapezoidal shapes. The cross-sections mapped from the HAB-2 model are being applied to create more realistic channel shapes for the flow model.

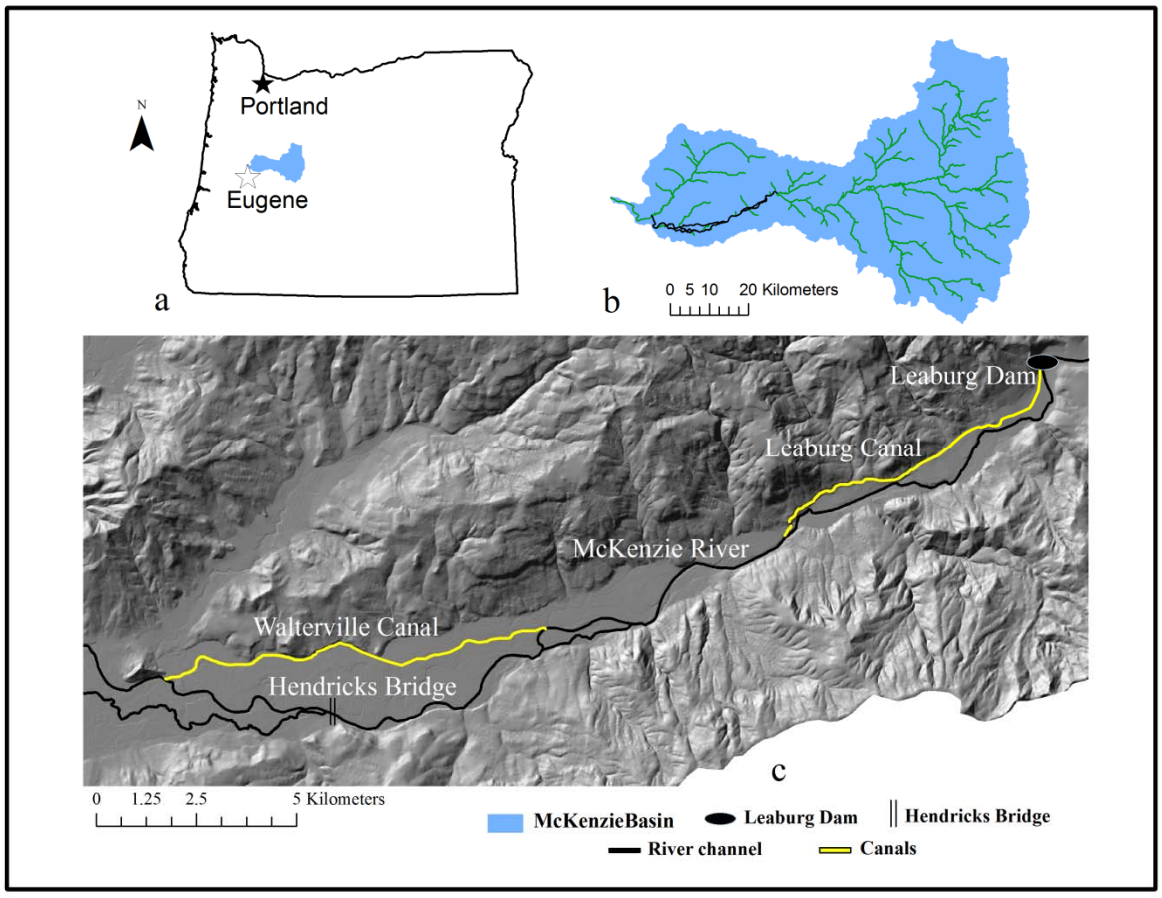


**figure 2.1.** Study area clockwise from top left: (*a*) Location of the McKenzie River Watershed in central western Oregon, (*b*) McKenzie River Watershed with major streams and study area outlined in black, and (*c*) the study area between Leaburg dam and the tailrace of the Walterville canal.

## 4. Methods

We evaluated the HAB-2 model in the McKenzie River using data sets from 2007 and 2008 (table 2.1). The 2007 data include 10 cm resolution imagery and sonar depth

measurements. The 2008 data included 0.5 m imagery and target depth measurements. Based on preliminary analyses, we ran the HAB-2 model using the red band on both sets of imagery, as well as evaluating the HAB-2 performance using the green band and areas of the river with different characteristics (riffles and shadows) for the 2008 imagery. The imagery and sonar/target points ultimately used were limited by colour-balance issues with scanned film imagery, shadows, loss of targets due to the river current, and potential inaccuracies in sonar measurements or locations, as is further discussed in section 6.1. In addition, we compared a cross-section modelled on the 2007 and 2008 imagery to a HAB-2 cross section at the same site on 0.5 m 2005 DOQ imagery (table 2.1). Although we did not have ground measurements from 2005, the comparison provides a qualitative indicator of the ability of the HAB-2 model to capture depth variations on historical imagery.

### *4.1. Data acquisition 2007*

The 2007 imagery were collected from a flight on October 28, 2007. The imagery was fine resolution (10 cm), three-band (red, green, blue), film-based aerial photographs over the entire extent of the study area. At the time of acquisition the stream bottom was clearly visible. We geo-referenced the 2007 aerial photography with 2005 half-meter resolution Oregon Imagery Explorer images (OIE, 2008) collected as part of the National Agricultural Imagery Program.

Prior to the 2007 flight, contractors for the U.S. Army Corps of Engineers (USACE) collected over 5,624 sonar data points in our study reach (~1 river km) from September 19, 2007 through October 1, 2007. The contractors used a Ross Laboratories

**Table 2.1.** Data types and characteristics. The 2005 imagery was added for comparison of on-line public imagery against our acquired imagery so no ground measurements are available. A greater range of ground depths was measured but some were washed away or in shadow at the time of image capture. Ground measurements of depth data are not available for 2005, and there are no sonar measurements for 2005 or 2008. The RMSE for the georectification of 2007 imagery to digital orthophotoquads was 1.05 m, which affects accuracy of matching of image-derived depths to sonar. Error in spatial location of the 2005 and 2008 imagery does not affect results because either no ground data were available (2005) or ground targets were used (2008).

| Data | 2005 | 2007 | 2008 |
|---|---|---|---|
| **Spatial resolution** | 0.5 m | 0.1 m | 0.5 m |
| **Radiometric resolution** | 8-bit | 10-bit | 8-bit |
| **Number of target measurements** | 0 | 0 | 23 |
| **Depth ranges** | N.A. | N.A. | 0.24-2.23 m |
| **Sonar measurements** | N.A. | 5,624 | N.A. |

825B single beam echo sounder, Trimble R8 RTK GPS, Trimble HPB450 radio transmitter, DigiBar Pro sound velocity probe, and HP Laptop to acquire the data. Rover RTK data were sent via serial cable to Hypack Survey software to provide both horizontal and vertical control to the survey vessel (Global Remote Sensing, 2008) and were input directly in real-time in Hypack 6.2b. The contractors recorded mobilization parameters and offsets for the SBES and the RTK antenna and applied them during data processing. Radio communication between the RTK base station and the survey vessel rover (fixed atop transducer pole mount) provided horizontal and vertical positioning. When calibrated, the sounder achieves an overall accuracy of approximately 0.06 m up to 3 m depth (Ross, 2009, personal communication). We utilized the sonar data to the spatial extent of our acquired imagery below the Walterville Canal tailrace.

**Table 2.2.** Discharge at the U.S. Geological Survey gauges used in the McKenzie River on the dates of image and sonar acquisition. Only the Walterville gage was needed to run HAB on the Hendricks bridge image used to compare results from 2005, 2007 and 2008.

| | **Discharge (cms) at time of data acquisition** | | | |
|---|---|---|---|---|
| **Data acquisition** | **Leaburg USGS gage 14163150** | **Leaburg canal EWEB gage** | **Walterville USGS gage 14163900** | **Walterville canal EWEB gage** |
| **Station number** | 14163150 | - - - | 14163900 | - - - |
| **Q at time of sonar 9/20/07-9/30/07** | 28.3 | 39.6 | 29.7 | 63.3 |
| **Q at time of 10 cm imagery, 10/28/2007** | 55.5 | 44.3 | 34.8 | 67.5 |
| **% change between dates of ground and aerial data** | 96% | 12% | 17% | 7% |
| | | | | |
| **Q at time of 0.5 m imagery, 9/26/2008** | 54.1 | 42.6 | 31.1 | 53.5 |
| **Q at time of 0.5 m DOQ 8/4/2005** | - - - | - - - | 32.3 | - - - |

Logistical constraints prevented the flight company from collecting imagery at the same time as the sonar surveys. The discharge at the time of flight in late October was higher than when the sonar data were collected throughout September (table 2.2).

### *4.2. Data acquisition 2008*

The 2008 0.5 m resolution, three-band (red, green, blue), film-based aerial photographs were acquired on September 26, 2008. The imagery covered two large extents of the study area: one on the upper portion at Leaburg, the other extending from Hendricks Bridge and along the Walterville canal (figure 2.1*c*). Conditions were sunny and mostly clear at the time of acquisition. The company, 3DiWest, located in Eugene, Oregon, orthorectified the 2008 imagery.

The day before and the morning of the flight, we set 23 weighted targets in the water attached to buoys for identification and retrieval and measured their depths (figure 2.2). Seven of the targets were lost due to being flipped over or moved by the current or by being in portions of the image where HAB could not be run because of shadows or riffles. Measured depths ranged from 0.2-2.0 m, all in the main channel. The targets were set on the day prior to and on the day of the flight. Discharge was similar on these days and the river depth did not change (table 2.2).

**figure 2.2.** Setting targets from the McKenzie Fire and Rescue jet boat on river before the flight. The targets are cement discs painted white for visibility in the image.

### *4.3. HAB-2 model implementation*

The HAB-2 model requires: the digital number (*DN*) values for the river channel, the number of pixels and the length of a cross-section of the river in the image, the $DN_0$ value (value of the pixel at the just wetted surface), the slope of the river at that reach, and the

discharge ($Q$) of the river from the nearest gauging station. We extracted the Digital Number ($DN$) values of each of the pixels from a cross-section of the river on each of the geo-referenced images using ArcMap 9.3 licensed with 3D analyst (ESRI, 2009), measured the length of the cross-sections, and obtained the $DN_0$ values. These values were then entered into the HAB-2 spreadsheet, along with the discharge at the time of the flight and slope and roughness values for that portion of the river. A value of 1.0 is first entered for the extinction coefficient $\beta$, which is then recalculated through iterations of the model.

After running HAB-2 to calculate the extinction coefficient $\beta$ and determine equation (3), we used the raster calculator in ArcMap to apply equation (3) to the image. We added the 2007 sonar points as a layer to the map file (.mxd) and extracted the intersecting points (sonar and HAB-2 depths) using Spatial Analyst. We exported the resulting layer containing a table of the two sets of depths as a data base file (.dbf). We graphed the HAB-2 modelled points and the sonar points longitudinally by the Easting coordinate (the river runs East-West) to visually examine the fit.

### *4.4. Evaluation of HAB results*

We regressed the overlapping HAB-2 and 2007 sonar depths for the entire image, as well as for only those areas without shadow. Due to the speckling in the 2007 imagery (figure 2.3), we filtered the red band on the image at Hendricks Bridge to remove local spectral variance that might have affected the regression results. We used several ranges of low-pass filtering (3x3, 5x5, 7x7, 9x9) as well as an Olympic filter (3x3, 9x9) in which the highest and lowest "scores" (*DN* values) within the window are dropped. We focused the

analysis of 2007 data on the river near Hendricks Bridge (figure 2.1*c*), an area that possessed a range of river characteristics, including riffles and pools, shadowed and shadow free areas, and a variety of depths (figure 2.4).

For the 2008 imagery, as with the 2007 imagery, we regressed the measured and modelled depths at the ground targets (no sonar data were available in 2008). The stronger spectral returns from the 0.5 m resolution 2008 imagery suggested that we might detect signals from greater depths than with the 2007, 0.10 m resolution imagery.

Because green light penetrates to greater depths than red light (Campbell, 2007), we tested the effectiveness of the HAB model using the green band as well as the red bands for the sunlit Hendricks Bridge image. On the same Hendricks Bridge reach, we also qualitatively evaluated how riffles and shadows affect HAB-2 results by comparing depths in nearby areas that were affected by those features.

**figure 2.3.** True colour image at the river's edge zoomed-in 13X relative to figure 2.4 to illustrate image speckle and granularity. The white objects in the river are ground targets placed in the water at varying depths. Pixel resolution is approximately 10 cm.

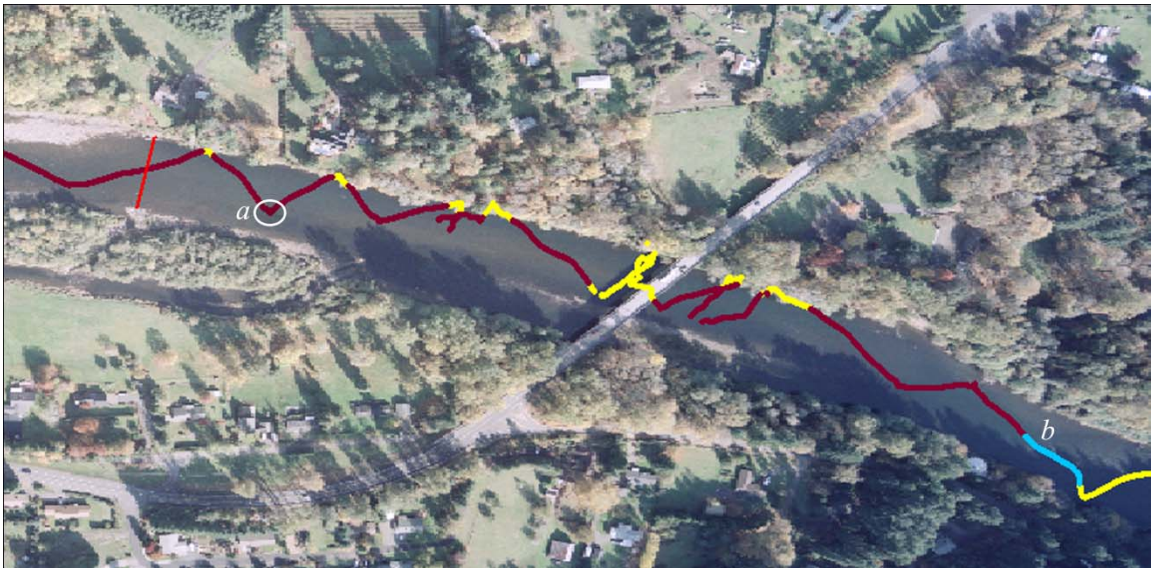


**figure 2.4.** True colour image and sonar depth points near Hendricks Bridge. Sonar depth points are displayed in red, except those that were clipped owing to their location in shadow, under over hanging trees, or on the bridge, which are displayed in yellow. The bright red line is the location of the cross-section used in figure 2.10. Locations (*a*) and (*b*) are sites where we believe ground validation data are incorrect (sonar depths greater than 3 m are shown in blue), as discussed in section 6.1.1. This image portrays just a small portion of the river area covered by sonar and imagery (figure 2.1c). Downstream is to the left.

Finally, in the interest of testing the utility of the model on historical imagery for which no ground validation depths are available, we ran the model on a free, publicly accessible 2005 high-resolution (0.5 m) digital orthophotoquad (DOQ) (OIE, 2008). We qualitatively evaluated the resultant cross-section at a relatively stable section of the river near Hendricks Bridge and compared it with the 2007 and 2008 results.

## 5. Results

### *5.1. HAB-2 results, 2007*

Figure 2.5 compares modelled and sonar depths for a representative subset of the 2007 data with obstructions and shadows removed. Figure 2.5 only displays a spatial subset of

the total data near Hendricks Bridge (2,151 points) because the image becomes too cluttered for interpretation when all 5,624 plus sonar data and equal number of HAB data in the image are included. A regression of all of the sonar depths and HAB-2 depths for the Hendricks Bridge image resulted in an $R^2$ value of 0.52 (figure 2.6*a*, table 2.3). The fit of the regression line between the HAB-2 and the sonar depths after clipping the shadows, bridge, trees overlapping the water, and shadows (less 320 points) decreased to an $R^2$ value of 0.40 (figure 2.6*b*, table 2.3). The low pass and Olympic filters did not substantially improve the fit of modelled to sonar depths, when using the data for which all obstructions and shadows were removed ($R^2$ values range from 0.40 to 0.48, table 2.3).

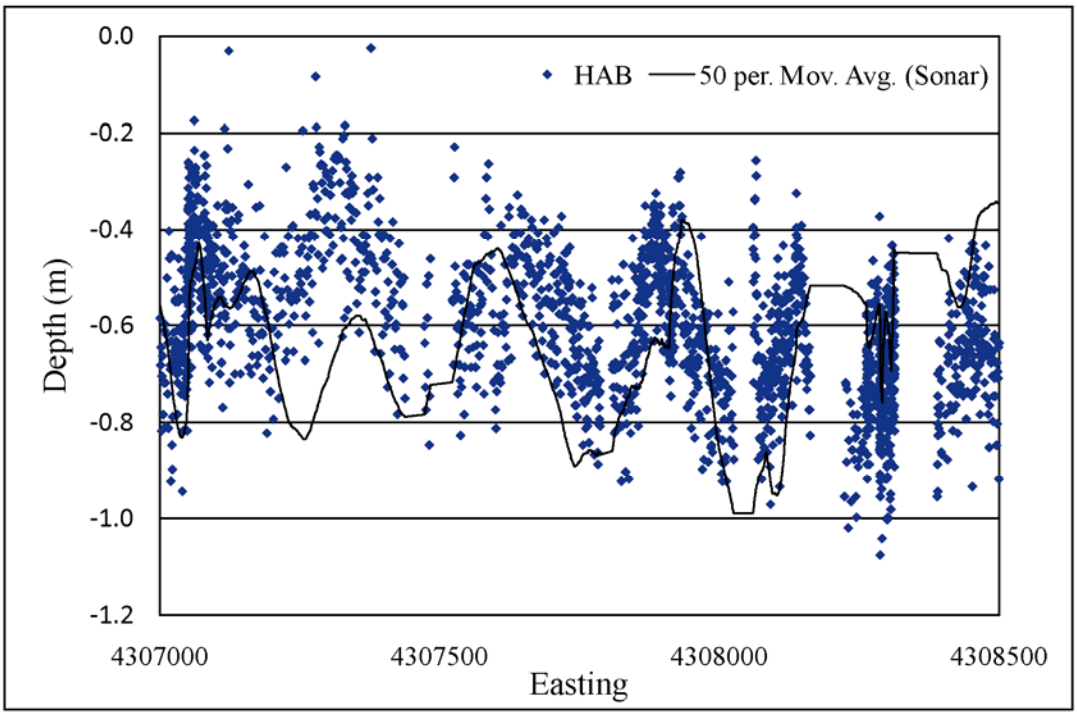


**figure 2.5.** Longitudinal trend of HAB modelled depths (points) and a moving average of the sonar depths (black line) without obstructions/shadows. The moving average for the sonar data is used rather than the sonar data path to enable visual comparison.

**Table 2.3.** HAB results of all comparisons made on the imagery. $DN_0$ values vary because of differences in radiometric resolution of film (Table 2.1).

| Data | Ground truth | Processing | Resolution (m) | Band | $DN_0$ | Beta | $R^2$-value | Description |
|---|---|---|---|---|---|---|---|---|
| **2007** | sonar-all points | raw | 0.1 | Red | 559 | 0.55370 | 0.52 | extremely variable modelled depths < 2 m |
| | sonar-no obstructions | raw | 0.1 | Red | 559 | 0.55370 | 0.40 | extremely variable model depths between 0.5 and 1.5 m |
| | sonar | 3x3 filter | 0.3 | Red | 540 | 0.36608 | 0.40 | |
| | sonar | 5x5 filter | 0.5 | Red | 548 | 0.34879 | 0.41 | |
| | sonar | 7x7 filter | 0.7 | Red | 540 | 0.45518 | 0.40 | |
| | sonar | 9x9 filter | 0.9 | Red | 546 | 0.41753 | 0.41 | |
| | sonar | Olympic filter | 0.3 | Red | 166 | 0.58807 | 0.48 | |
| | sonar | Olympic filter x2 | 0.9 | Red | 166 | 0.52515 | 0.48 | |
| **2008** | targets | raw | 0.5 | Red | 115 | 0.77613 | 0.89 | model values fit up to just over 1.5 m |
| | targets | raw | 0.5 | Green | 114 | 0.72859 | 0.25 | model values only fit between 0.5 and 1.5 m |
| | | part shadow | 0.5 | Red | Qualitative evaluation of resultant cross-section | | | shadow modelled as deep water |
| | | shadowed HAB xs | 0.5 | Red | Qualitative evaluation of resultant cross-section | | | same shape as 2008 Red but deeper |
| | | riffle xs | 0.5 | Red | Qualitative evaluation of resultant cross-section | | | white riffles modelled as out of water |
| **2005** | NA | OIE DOQ raw | 0.5 | Red | 120 | 0.51434 | NA | same shape as 2008 Red imagery used in this study |

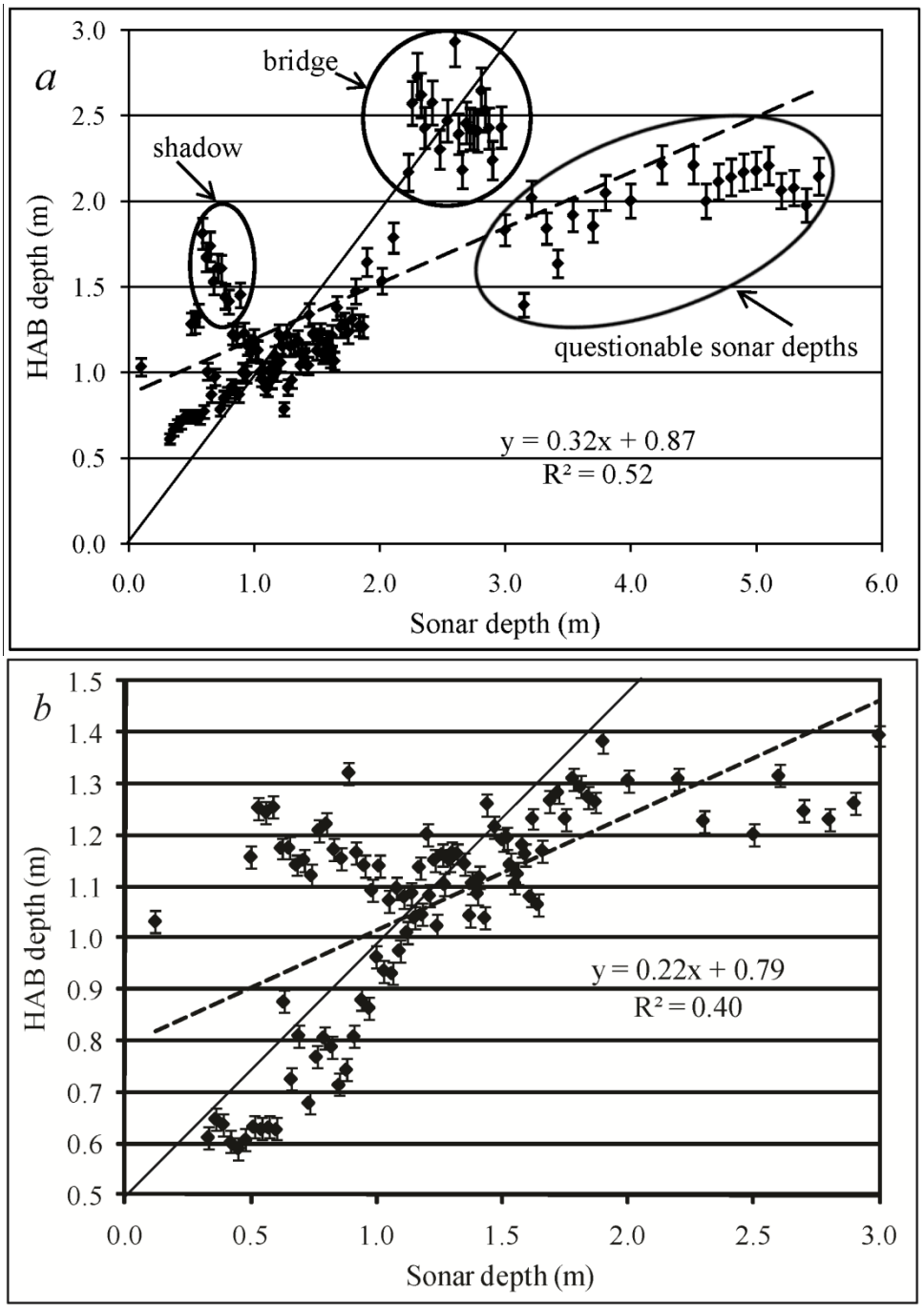


**figure 2.6.** The 2007 red band imagery HAB modelled depths vs. averaged sonar depths resulted in an $R^2$ value of (*a*) 0.52 for all data points and (*b*) 0.40 with obstructions and shadows removed (trendlines are dashed). The zero-intercept is included in both graphs to show where the results diverge from an exact fit. Points in shadow and at the bridge are identified in (*b*), as is an area of questionable sonar depths (also in blue in figure 2.4).

### *5.2. HAB-2 results, 2008*

The regression of modelled and measured target depths from the 2008 imagery resulted in an $R^2$ value of 0.89 (figure 2.7, table 2.3). Use of the green band with the HAB-2 modelled to a poorer fit, with an $R^2$ value of 0.25 (table 2.3).

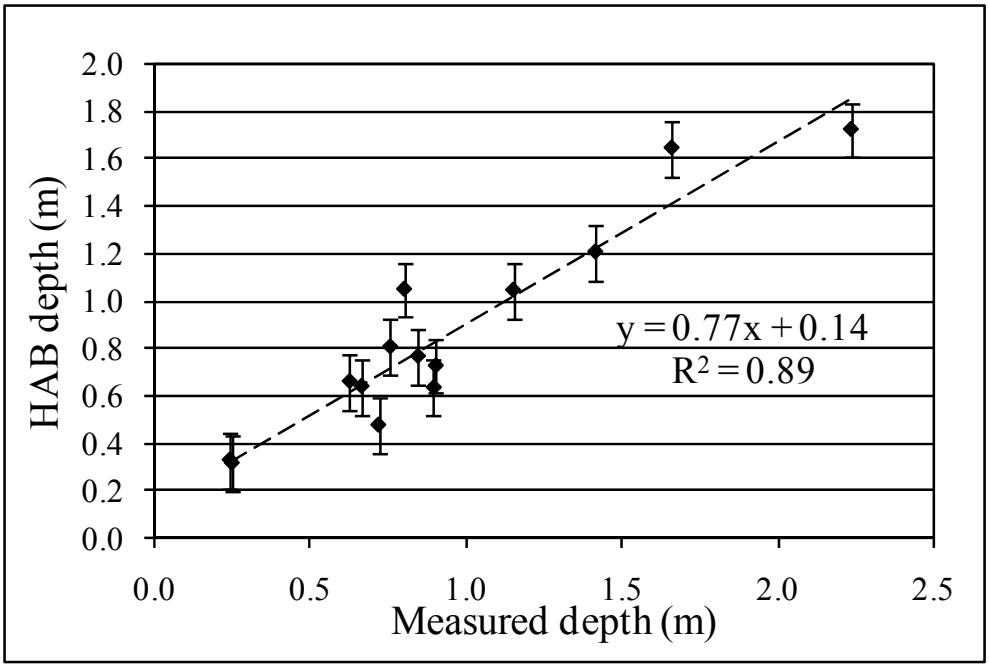


**figure 2.7**. The red band HAB modelled depths vs. ground measured target depths for the 2008 imagery.

The turbulent parts of riffles are much lighter (i.e. are white water) than immediately adjacent portions of the river with approximately the same depth. The white water portions of the riffle units are portrayed by HAB-2 models as being shallower or above the water surface (figure 2.8).

Conversely, shadow creates a darker than normal surface on the river, which HAB-2 models as deeper. On the modelled cross-section of the river, the depths in the

shadowed half of the river are modelled as becoming progressively deeper near the bank, despite the fact that the river shallows towards the bank (figure 2.9).

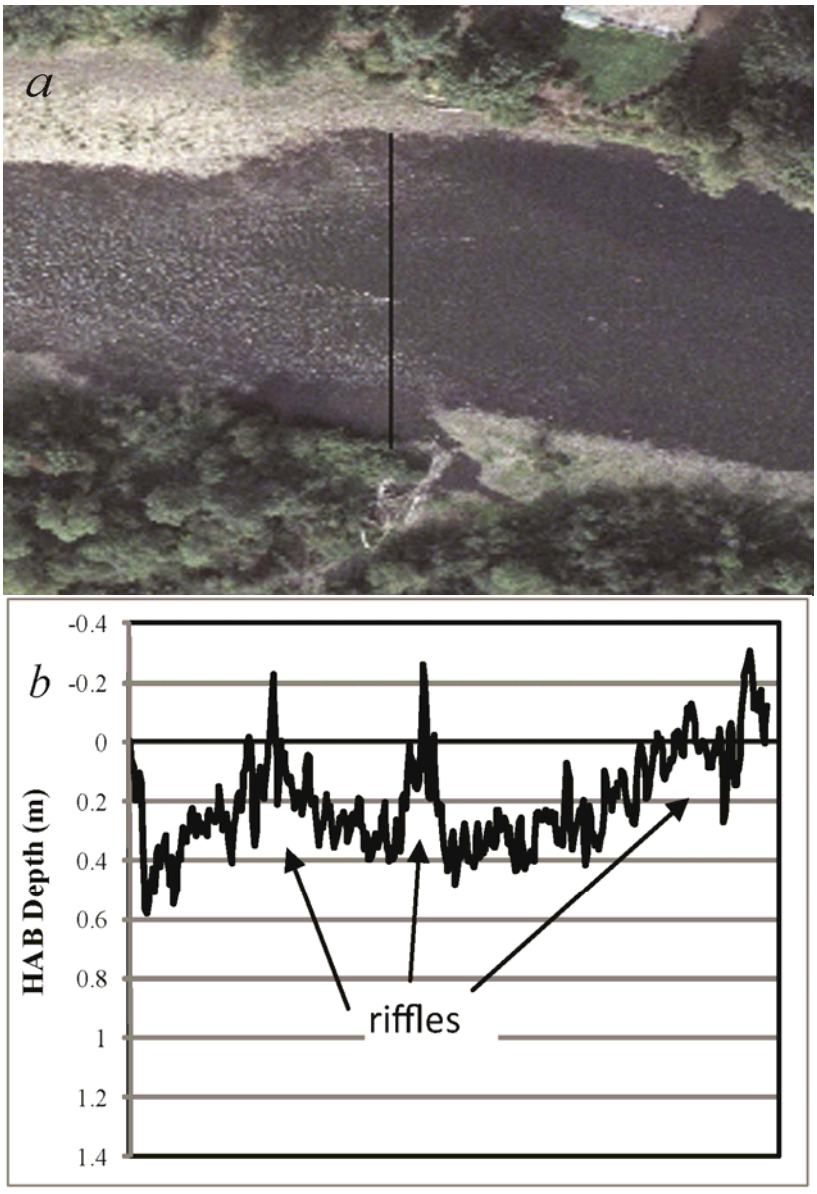


**figure 2.8.** Photograph with cross-section drawn across the river (*a*) and the HAB modelled cross-section (*b*) of the channel at the beginning of a riffle (the dark line at zero denotes what should be the water surface), a few hundred meters downstream of Hendricks Bridge. Note that the riffles visible in (*a*) are modelled as "out of the water" (above the water surface at zero).

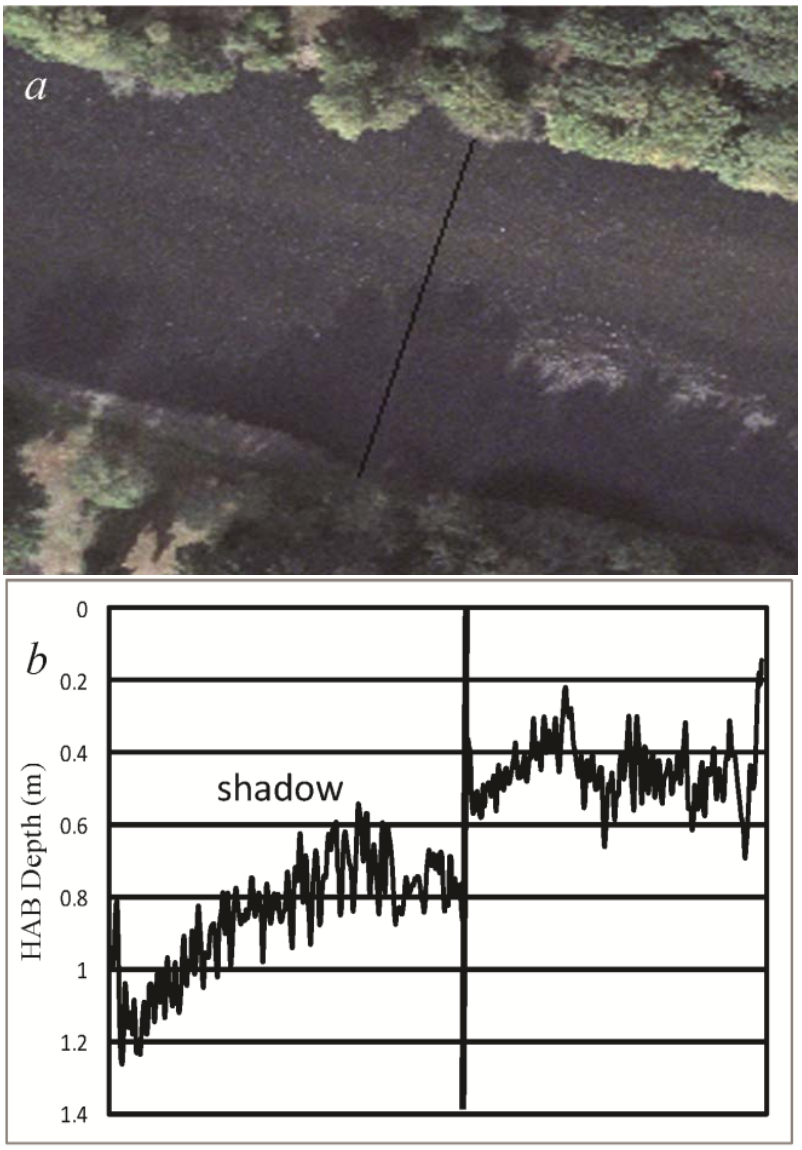


**figure 2.9.** Photograph (a) and HAB modelled cross-section (*b*) of the channel half covered by shadow (left of line), downstream of Hendricks Bridge. Note that the shadow in (*b*) is modelled as far deeper than the rest of the channel.

### *5.3. Comparison of 2005 DOQ to 2007 and 2008 HAB results*

We ran HAB-2 on a 2005 DOQ to generate a cross-section (visible in figure 2.4) for a relatively stable river reach (figure 2.10*a*) that can be compared to HAB-2 cross-sections for 2007 (figure 2.10*b*) and 2008 (figure 2.10*c*) at the same location. Discharges on these

three dates differed by less than 10% relative to the 2005 discharge (table 2.2). The cross-section shapes are similar for the three dates, although the depths in the deepest part of the thalweg differ by about 0.3 m. These variations could be the result of channel infilling, although the relative effects of channel change or imagery differences are unknown.

## 6. Discussion

In the following sections, we first discuss the general model performance for the two years. Subsequent sections discuss possible reasons for differences in the model performance between 2007 and 2008, including: (1) issues with ground validation data (location and depths); (2) issues with film and scanning; (3) surface turbulence; and (4) shadows and obstructions.

### *6.1. General model performance*

The model and sonar depth profiles in 2007 follow a broadly similar longitudinal pattern, but with some significant discrepancies (figure 2.5). The modelled depths diverge from sonar depths where there are shadows or obstructions such as Hendricks Bridge or overhanging trees; areas that sonar can capture, but aerial imagery cannot (figure 2.6a). The model and sonar depth profiles follow a relatively similar longitudinal pattern after clipping out the shadow, bridge, and trees (figure 2.6b), although the $R^2$ value decreases (table 2.3). This probably happens because the high depth values in the data with all shadows and obstructions included biases the regression to the high values producing a false "better fit". Filtering the imagery did little to reduce the pixel-scale local spectral

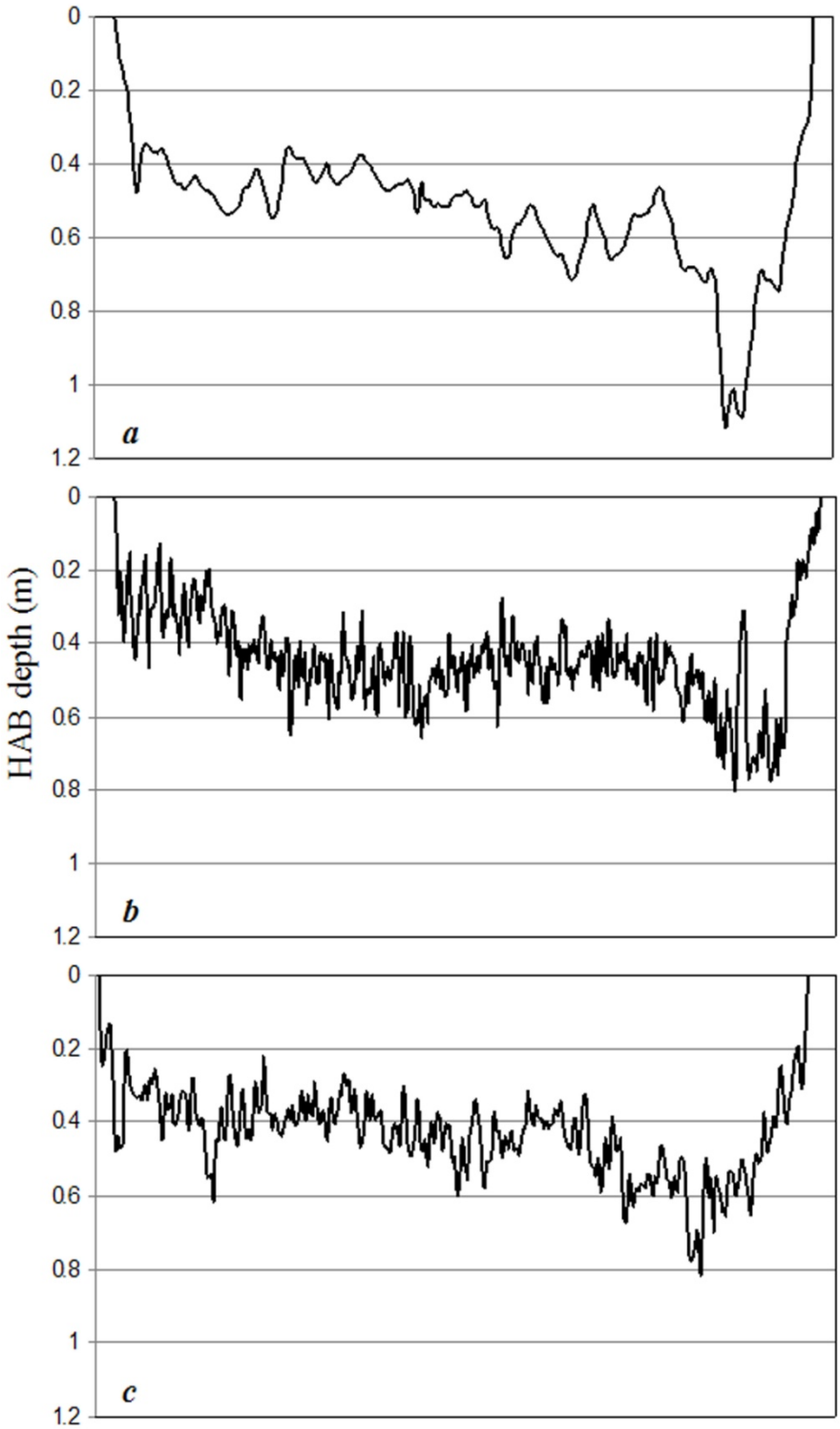


**figure 2.10.** HAB modelled depths on the same cross-section at Hendricks Bridge from the (*a*) 2005 DOQ 0.5 m imagery, (*b*) 2007 true colour 10 cm imagery, and (*c*) 2008 true colour 0.5 m imagery.

variation that affected the HAB-2 modelling. Traditional low-pass filtering at multiple scales produced no change or negligible improvement of fit for the 3x3, 7x7, 5x5 and 9x9 window sizes (table 2.3). The 'Olympic' filtering improved the fit by 0.08 at both scales. The slightly greater improvement by the 'Olympic' filtering, in which the lowest and highest *DN* values (scores) are dropped, probably results from the reduction in the local noise exhibited in the imagery across very small distances (figure 2.3).

The higher $R^2$ value (0.89) for the comparison of ground measurements and HAB depths for the 2008 data (table 2.3, figure 2.7) probably result from a number of factors. In 2008, the ground measurements were taken on the day before and the day of the flight, so discharge and associated depths were more comparable than in 2007 (table 2.2). The 0.5 m resolution imagery also reduced the image granularity and potential effects associated with cobble-scale variations in bottom reflectance due to different coloured rocks and substrate (figure 2.11). Many of the river characteristics, such as bed colour and texture and interstitial spaces between cobbles, can be adjusted for by using a band ratio (Legleiter et al. 2004, 2009), which we could not use in this case but can easily be used with digital imagery. This issue emphasizes the importance of requesting non colour-adjusted imagery.

The red band absorbs more strongly than green light with depth, so it is often thought that the green band will perform better at greater depths. However, the test result of a lower $R^2$ value (0.25) for the green band suggests that factors such as increased backscatter may generate lower accuracy readings, which is consistent with theoretical arguments recently presented by Legleiter et al. (2009).

**figure 2.11.** Photograph of a representative colour and size variation of the substrate in the river.

Visual inspection suggests that the best HAB-2 modelled depth estimate results for both 2007 and 2008 range between 0.25-1.5 m depths. Depths under 0.25 m are so shallow as to be within the typical error range of the model (±15 cm; Fonstad and Marcus, 2005). At depths over approximately 1.5 m scattering and absorption lead to light returning to the sensor that is not entirely a function of depth (Legleiter et al., 2004). Depths greater than 1.5 m appear to reach the limit of light penetration to the river bottom and 1.5 m is a standard maximum depth estimate in clear water rivers (Marcus et al., 2003).

The $R^2$ value of the obstruction free regression from the 2007 imagery is lower than the test of the HAB-2 model where Fonstad and Marcus (2005) obtained $R^2$ value of 0.77 on the Brazos River, Texas, using 1 m resolution digital aerial imagery, but higher than their $R^2$ value of 0.26 for the Lamar River, Wyoming, using 1 m resolution, 128-band hyperspectral imagery. The $R^2$ value from the 2008 imagery in this study is highest of all the tests. Regardless, the model approximates the overall trend of the sonar depths

well and cross section profiles are consistent with the river configuration (figure 2.10). $R^2$ values also incorporate error due to problems with ground data and the spectral variations in the scanned film, as is discussed in following sections. This highlights the need to qualitatively compare results on a visual basis as well as use statistical accuracy assessment techniques, something often noted in remote sensing of rivers (Marcus and Fonstad, 2008).

### *6.1.1. Ground validation data*

Each technique for gathering ground data (2007-sonar, 2008-field measured targets) carries its own inherent errors, which in turn affects the match of model and ground data. For example, there is a drop off downstream of a gravel bar that is visible in the imagery but it is not observed in the sonar data (see location (*a)* in figure 2.4). Even more notable is a concentrated area of sonar depths ranging from 3 to 6 m, depths that are not likely to exist in this site in the McKenzie River (see area (*b)* highlighted in blue in figure 2.4, also figure 2.6a). Sonar data in these segments are probably in error, meaning that we are probably fitting the model to erroneous data. Likewise, even though the fit of target and HAB data in 2008 was much closer, some of the mismatch may be due to difficulties in accurately measuring water depths in fast flowing rivers (see section 4.2). The error of the orthophotos together with the errors of the sonar data lead to discrepancies, especially in areas of rapid changes. This is because of the nature of the two types of data: the sonar is point data that essentially captures the top surface on which it falls (top of cobbles, between them, etc.), while the HAB-2 model, using pixels, captures the average depth of the substrate within the pixel. The targets, though similar, cover a larger area on the river

bottom and therefore may approximate the average depth more similarly to the model. The sonar data thus illustrates the general spatial association between trends in the two data sets and identifies possible problem areas in the application of the model rather than providing a precise point-to-point validation data set.

### *6.1.2. Film and scanning*

All our imagery consisted of scanned colour negatives, which affected the pixel values (figure 2.3) and the HAB-2 results. Even with a professional grade photogrammetric scanner (a Leica DSW 500 was used), the optical response of film was not of the same consistency and quality as digital photography. Moreover, the scanner operates with a fixed camera and light source bracketing a moving film stage, so each scan is a grid of individual tiles that are stitched together to form the final image. Each tile is captured three times, filtered for red, green, and blue. Often, in areas of little tonal variance (particularly large bodies of water), the seams between the tiles are darker and the grid becomes visible. When the software disregards the outer edges of the tile, the effect is minimized. This, however, reduces the effective size of the tile and results in a greater number of tiles per image (Gray, 2009, personal communication).

In addition to the stitching and blending functions highlighted above, radiometric calibration files operate in the background. This can increase green band *DN* values and also means that we are not running HAB-2 on the original pixel values. Therefore, we also could not use the ratio-based technique that can partially normalize for variations in bottom albedo.

Finally, Newton Rings, caused by the interaction of film base and glass (Gray, 2009, personal communication), often appeared on the images. These rings of darker and lighter colour values affect the HAB model.

The film based imagery thus is not ideal for HAB-2 modelling. However, using film-based imagery provides an indication of the accuracy of HAB-2 with historical images, many of which are film-based. Because these issues do not occur with digital imagery, it is likely that modern digital imagers will yield higher model accuracies than those reported in this article.

### *6.1.3. Turbulence*

Riffles on the water surface affect the pixel *DN* value and therefore the HAB-2 modelled depths. Within riffles on the river, the white and lighter coloured portions are modelled in HAB-2 as being above the water surface (figure 2.8). This would occur for any highly reflective variation on the surface of the water. We were unable to test HAB-2 against the sonar data, because the sonar sounder was removed from the water before crossing riffles where it might have been damaged. These areas could be avoided using automatic detection and riffles could even be corrected by using a filter to find and delete values above the water surface and connect valid depths across the bottom.

### *6.1.4. Shadows and obstructions*

Shadows make the water surface darker than normal and are therefore modelled in HAB-2 as deeper than actual depths. The shadows are darkest closest to their source, which in the case of the McKenzie River are usually trees on the river bank. The edge of the

shadowed channel therefore is modelled as the deepest water, with depths shallowing as the shadow gets lighter farther away from the tree (figure 2.9). Other obstructions, such as bridges, also alter the surface pixel value and therefore cannot be modelled accurately by HAB-2 (figure 2.4). Minimizing shadows should be taken in consideration as much as possible in planning imagery acquisition.

### *6.2. Utility of historical imagery*

The HAB-2 modelled cross-sections for the 2005, 2007, and 2008 imagery were similar in overall shape. The cross sections are all generally shallowest on the left bank, then gradually deepen across the channel until they drop off into the narrow thalweg near the right bank (figure 2.10). The width of the thalweg in the 2005 and 2007 images (figure 2.10*a* and *b*) are similar, and narrower than that of the thalweg in 2008 (figure 2.10*c*), which appears to be almost twice as wide with the deepest part shifted slightly away from the right bank. The differences in the shapes of the channels (not smoothed here) could be useful in monitoring in-channel changes. The differences in the imagery resolution and type are apparent in the variability exhibited in the cross-section figures, with the most data points and therefore the most variability in depth shown in the finest scale imagery (2007, figure 2.10*b*). The depth values range between 0.4 and 0.6 m for all the images to the left to the thalweg, and in the thalweg, the depth values range between 0.75 and 1.1 m. The comparability of cross-sections indicates that the HAB-2 model can be used to generate relatively accurate cross-sections with historic imagery where no ground validation data are available.

### *6.3. Management applications*

The McKenzie River is a significant water supply and fisheries river, being the sole water source for the Eugene area (EWEB, 2007). Salmon also populate the McKenzie, though in declining numbers (USGS, 2005; NOAA, 2005), which has led to its inclusion in the Endangered Species Act Recovery Plan for Chinook and Steelhead (NOAA, 2005). Because water depth and substrate play a role in salmon spawning habitat (Stewart *et al.* 2002), mapping the channel bathymetry downstream of the dams and canals provides important information on habitat and alterations to sediment movement (Magilligan *et al.* 2007; Smith, 2002). Moreover, in 2006, EWEB began development of watershed and flow routing models for estimating pollution loads, contaminant runoff and transport, water balance, rainfall runoff and other objectives.

The bathymetric data collected for this project will likely be used by EWEB to develop timely and more detailed databases for their channel routing models. The utility of the model in management ultimately depends on the users' needs. The model provides more realistic channel forms flow modelling relative to the trapezoidal cross sections presently being used in the MIKE-11 models. However, depths at any one point are likely to be less accurate than those derived from ground measurements. Whether or not to use HAB is thus dependent on whether local accuracy is more important than having global coverage for the whole river that is approximately accurate. In the case of the McKenzie models, the management agencies are presently planning to combine both ground-based and HAB measurements to characterize the system. In addition, the HAB depth maps can be used to identify possible habitat areas for a variety of species, and comparisons of

channel shapes over time, but the accuracy of the modelled depths could not be used for engineering purposes.

The results from the 2005 DOQ suggest even broader potential applications. While direct comparison of depth of the river channel are not possible over different years at different discharges, qualitative analysis of differences in channel form over of time is possible and can be used in various applications. The availability of on-line, aerial photos is becoming more prevalent in many parts of the world. This makes it possible for catchment councils, students, land-use planners, habitat monitors, restoration specialists, and others to apply the HAB-2 model to gain information about in-channel depths, habitats, and change.

## 7. Summary and conclusions

This study evaluates HAB-2 model depth estimates developed from aerial, high resolution, film-based, true colour imagery from 2007 and 2008 in the McKenzie River, Oregon. Over 5,000 sonar data depths from 2007 as well as limited ground-base targets in 2008 enable the most rigorous test of the HAB model to date. The $R^2$ value for comparison of sonar and HAB depths was 0.52 with all points included. The overall trend of HAB and sonar depths in 2007 is similar, except where shadows, riffles, or obstructions alter the spectral reflectance (figures 2.5 and 2.6).

The $R^2$ value for 2008 imagery was 0.89, an improvement that probably resulted from the coarser spatial resolution (0.10 m in 2007, 0.5 m in 2008), which decreased variations in modelled depth resulting from local cobbles and boulders and substrate colour (figure 2.11). Furthermore, error owing to differences in river discharge between

the time of flight and of sonar measurements was eliminated in the 2008 when both ground and aerial data were obtained within a day of one another (table 2.2). The best depth estimate results for the HAB-2 model range between 0.25-1.5 m depths.

Shadows, riffles, and obstructions all lead to inaccurate model results and must be eliminated from the imagery or corrected for in order to use HAB throughout an entire river. Furthermore, the type of imagery is important. With true-colour film-based imagery, the photo must be scanned without colour balancing. Moreover, the granularity of the film (figure 2.3) creates false variations in depth. The use of low pass filters to reduce the granularity did not improve results (table 2.3), although an Olympic filter increased the results slightly. Imagery collected with a digital camera is preferable to film.

Despite these limitations, the HAB-2 model provides a useful tool for creating continuous depth maps that can be used for modelling and identifying river habitats. Additionally, the HAB-2 model can be utilised with historical aerial imagery. The HAB-2 model can fill the gap in important river information using information (aerial imagery) that is likely already part of the larger data acquisition and can powerfully inform further research.

Research presented in this chapter evaluates the accuracy and utility of the HAB-2 model. In the next chapter, I investigate the impacts of a small dam and two diversion canals on sediment movement. A key component of this investigation is the modeling of critical discharge needed to move the median grain sizes on the river bars and what the results mean for river management.

# CHAPTER III

# EVALUATION OF THE IMPACTS OF A RUN-OF-RIVER DAM AND TWO DIVERSION CANALS ON GRAVEL DISTRIBUTION AND MOVEMENT ON THE MCKENZIE RIVER, OREGON

This chapter is to be submitted to *River Research and Applications*. This chapter includes material that will be published as a coauthored article with Patricia F. McDowell, who provided editorial assistance.

## INTRODUCTION

Understanding the relationship between sediment movement and stream characteristics has been at the foundation of engineering, restoration, and geomorphic river research. The rates of movement or transport are necessary to estimate and predict erosion, deposition, and channel change in river channels. With the majority of U.S. river channels altered either directly or indirectly (Downs and Gregory, 2004), it is important to understand the effects of the alteration on sediment movement in the river. In order to predict and prepare for the effects of changes in development and climate change on water supply and quality and to minimize negative impacts on aquatic life and habitats, a greater understanding of the impacts of river regulation is needed. This is central to the EPA National Water Program Research Strategy 2009-2014 (EPA, 2009), for example. River regulation can include dams, water diversion or removal, or some combination of

both, which in turn affect longitudinal sediment movement through either reduced flow or sediment supply (Graf, 2006; Gregory, 2006). While dam removal has increased in both discourse and application (O'Connor et al., 2008; Grant, 2001), many dams exist for hydropower and water supply and a majority of them will not be removed. Additionally, canals divert and sometimes return water for a variety of purposes. Assessing the impacts of these flow regulations on the sediment mobility can improve river management, engineering and environmental applications, and designs where possible, and can inform future project development.

In order to investigate the effects of a run-of-river dam and two diversion canals on sediment movement, we characterize grain size distributions and model the post-dam discharge needed to mobilize the bar gravels on a large, relatively low gradient portion of a regulated gravel-bedded river: the lower McKenzie River, Oregon. We use field sampling and modeling to investigate the following research questions:

- How do the dam and canals affect grain size distribution in the vicinity of the structures?
- How do the effects differ between the dam and canals?
- How frequently are the mean size gravels mobilized under current flows?
- What do the sedimentary effects of the river management mean for environmental flow design for improved salmon habitat?

Water carrying almost no sediment load flows from the dam and is returned to the river at the canal tailraces. We hypothesize that this flow makes bar gravels sampled below each of these features coarser.

Sediment grain size has long been used in calculating river competency and transport (Shields, 1936; Parker and Klingeman, 1982; Wilcock, 2001; Rubin and Topping, 2001) and in estimating the magnitude and frequency of discharge events capable of moving the sediment in a channel (Buffington and Montgomery, 1999a, 1999b). One way to investigate the impacts of regulation is to analyze differences in grain size distribution. Grain size distribution has been used in studying fluvial processes and channel form (Montgomery and Buffington, 1997; Wohl and Merritt, 2005), initiation of grain motion (Buffington and Montgomery, 1997; Kaufmann et al., 2008), bedload transport and deposition (Church and Hassan, 2002), and habitat suitability for salmonid spawning and rearing (Kondolf, 2000). Quantifying the threshold of bedload grain motion is considered of major importance in bedload transport applications (Bathurst et al., 1987), environmental flushing flows design (Kondolf and Wilcock, 1996), and assessment of aquatic habitat (Montgomery et al., 1996; Buffington and Montgomery, 1997).

The critical threshold sediment entrainment provides the lower bound of discharge that moves sediment, an important characteristic of consideration in river management. Grain size distribution and bed mobility are also the most notable characteristics for ecological response to changes in flow (Cronin et al., 2007) that strongly influence habitat suitability for aquatic species (Kondolf and Wolman, 1993). Variability in the combination of bed material characteristics (i.e., size variability, shape, density) and bed packing produces a large range of critical threshold conditions (Lorang and Hauer, 2003). The transport of sediment through the river system depends on the supply of sediment (size and quantity) and the river's ability to transport it. While the scale of the channel and the rate of energy expenditure are determined by discharge and gradient, the

morphology of the river is determined by the size and quantity of sediment input into the system. The quantity of sediment supply is important in channel structure and character. Therefore, research often focuses on the response of the channel to changes in sediment supply by observing changes in bed-surface character and distribution. These changes are rapid, first-order responses that may be the most effective means of monitoring the sediment supply changes over shorter timescales (Buffington and Montgomery, 1999b; Lisle and Hilton, 1992). Reduced sediment supply can result in increased surface grain size and decreased sediment mobility and transport rates (Gran et al., 2006; Topping et al., 2000), whereas increased sediment supply increases or decreases grain size, depending on the input (Knighton, 1991; Jackson and Beschta, 1984). Grain size and sediment supply are strongly linked to erosion and incision, as low supply removes protective alluvial cover, allowing abrasion of bedrock by the (fewer) grains being transported (Sklar and Dietrich, 1998; 2001).

A relatively new approach to dam management, particularly for salmon in the Pacific Northwest, is the use of environmental flows -- the management of dam releases to restore some elements of the pre-dam hydrograph to improve habitat (Risley et al., 2010). Understanding the flow magnitude needed to move sediment on the river is instrumental in reaching the goals of environmental flows. This paper presents the results of the modeled critical discharge needed to move the $D_{50}$ grain size on approximately three gravel bars above and below each alteration. We use field data, hydraulic modeling, and long-term and 1996 flood stream flow records to discuss the results with respect their importance in environmental flow considerations.

STUDY SITE

The McKenzie River is a sixth-order, 138 km (86 mi.) long, westward flowing tributary of the Willamette River in western Oregon (Figure 3.1). The river originates in the Cascade Range and is regulated by three large dams (Blue River, Cougar, and Carmen-Smith) in the mountainous, upper one-third of the watershed and a smaller, 22 ft. high run-of-river dam and two canals in the middle one-third of the watershed. The river flows through the western Cascade Mountains, exhibiting an upwardly concave longitudinal profile. The study area is located in that middle one-third of the watershed where the river

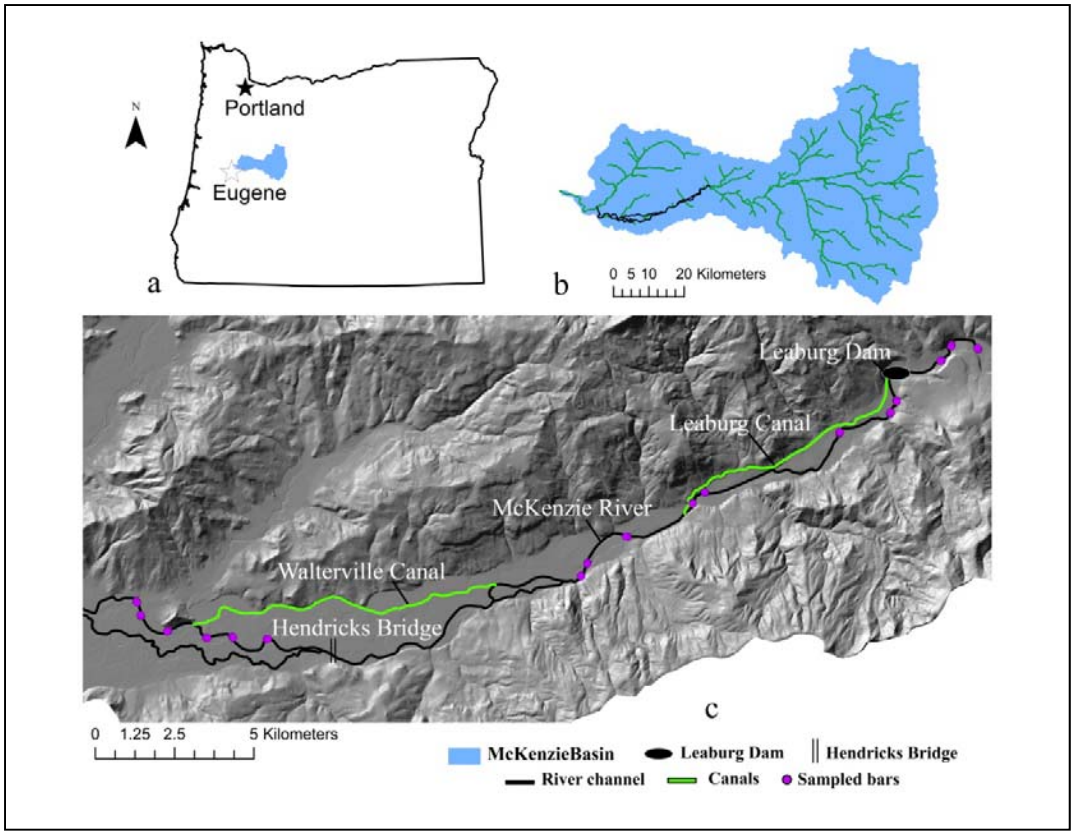


Figure 3.1. Study area clockwise from top left: (*a*) Location of the McKenzie River catchment in central western Oregon, (*b*) McKenzie River catchment with major streams and study reach outlined in green and black, respectively, and (*c*) the study area between Leaburg dam and the tailrace of Walterville canal with the sampled gravel bar sites.

channel is mostly unconfined and the valley widens with distance downstream. Though there are local variations, the river throughout the study site is characterized by a slope of approximately 0.002 (Figure 3.2). The river has a single channel and long, relatively straight reaches with occasional large amplitude bends, mid-channel bars and islands that locally give the river a multithreaded character. The sediment transport capacity is typically high relative to sediment supply, so the channel bed is predominantly cobble and boulders (EA Engineering, Science, and Technology, 1991). The river is the sole source of water for the city of Eugene, Oregon, and the source of the Leaburg-Walterville Hydroelectric Project. This project, on the lower McKenzie, includes one dam and two diversion canals diverting water for two off-river hydropower plants, all of

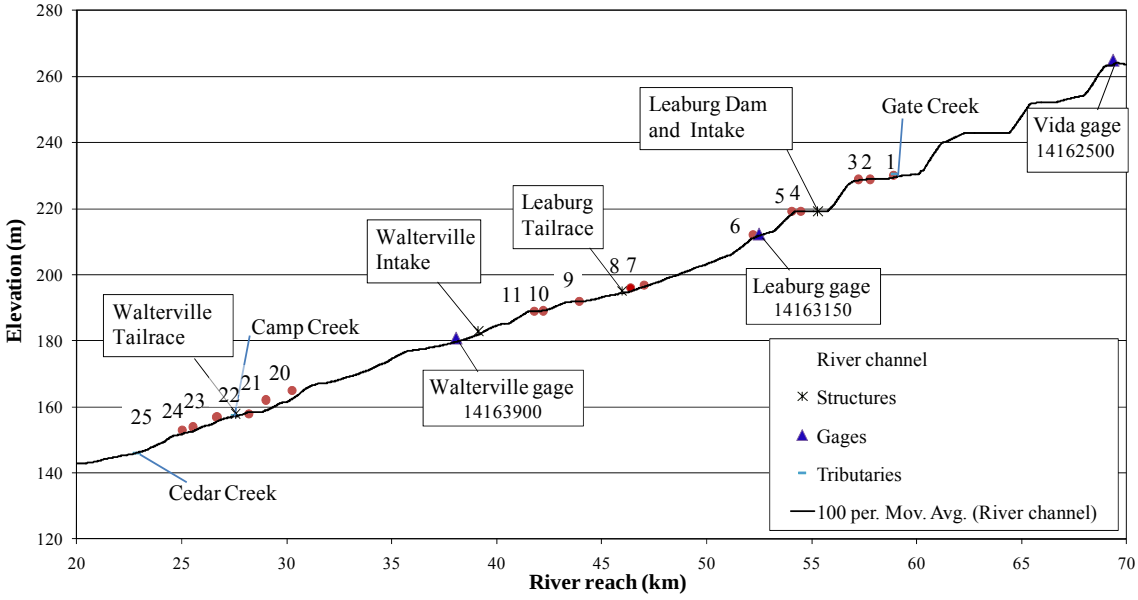


Figure 3.2. Longitudinal profile of the study reach extending from ~5 km above Leaburg dam to ~3 km below the Walterville tailrace. The dam and both canal intakes and tailraces are shown along with bar sampling sites, gaging stations used, and major tributaries along the reach. The 100 per. Mov. Avg. (River channel) is a line created from the 100 point moving average of thousands of LiDAR data points along the river flow line to depict the river channel.

which are owned by the Eugene Water and Electric Board (EWEB) (EWEB, 2007). Both hydroelectric projects were relicensed by the Federal Energy Regulatory Commission (FERC) in 1997, lasting through 2037. The relicensing resulted in the implementation of minimum stream flows of approximately 28 cms (1,000 cfs) in the reaches of the river where EWEB diverts as much as 71 cms (2,500 cfs) for its Leaburg power canal and 73 cms (2,577 cfs) for its Walterville power canal (Risley et al., 2010). The flows in the canals exceed the flows in the main stem at certain times of the year, but remain near 100% or equal to that of the main stem for most of the year (Table 3.1).

The purpose of the Leaburg run-of-river dam is to divert flow into the Leaburg canal. The Leaburg dam and canal intake are located at approximately river km 55 (34 mi) (Figures 3.1 and 3.2, Table 3.2). The canal runs ~9 km (~5.5 mi) downstream to the power plant, where the water is released back to the river at the tailrace located at approximately river km 46 (28.5 mi). Water is diverted into the Walterville canal intake via a series of chevrons placed to increase the head of the river at the diversion, which is located at river km 39 (24 mi) and runs almost 12 km (7.5 mi) downstream. The Walterville canal return flow, or tailrace, is located at approximately river km 27 (17 mi). The study area extends from ~0.5 km above Leaburg dam to ~-.5 km below the Walterville tailrace (Figures 3.1*c* and 3.2) and focuses on three sites: Leaburg dam,

Table 3.1. Canal flow as a percentage of flow in the main channel of the McKenzie River in Water Year 2009 from USGS gage data (USGS, 2010).

| Canal | Fall | Winter | Spring | Summer | Annual range |
|---|---|---|---|---|---|
| Leaburg | 117 | 115 | 100 | 129 | 1-246 |
| Walterville | 137 | 108 | 71 | 119 | 0-252 |

Leaburg canal tailrace, and Walterville canal tailrace. We selected these three features because we hypothesize that the flow of "hungry" water below each feature will have an effect on the downstream grain sizes. We expect to see coarser grain sizes on the bars downstream of each feature than those upstream. We were unable to include the Walterville diversion (or intake) because channel bathymetric data were not available below the intake. In this study we present an evaluation of the impact of the study reach canals and dam using river bar sediment grain size analysis, critical shear stress, critical stage height, and flow exceedance differences above and below the structures.

Table 3.2. Study feature location and year completed on the study area reach of the McKenzie. The dams in the upper McKenzie were completed in 1963 (Carmen-Smith diversion and dam, Trail bridge dam, Cougar dam) and 1969 (Blue River dam).

| Feature | Year completed | River km (mi) | Location |
|---|---|---|---|
| Leaburg Dam & Intake | 1930 | 55.3 (34.4) | river channel & right bank |
| Leaburg Tailrace | 1930 | 46.0 (28.6) | right bank |
| Walterville Tailrace | 1910 | 27.6 (17.1) | right bank |

## METHODS

### *Field sampling*

In large rivers that are not wadeable, the options for gravel sampling are limited. Channel bars represent storage of traction load that is moved sporadically by high flows and are a reflection of sediment supply conditions and macroscale channel processes (Knighton, 1998), including regulation impacts. True stability does not exist in natural rivers, but even they can be influenced externally and become relatively stable with characteristic equilibrium forms (Howard, 1981). Regulated rivers, however, often experience a smaller range of flows than the natural (pre-regulation) range and can

become (often purposefully) less dynamic, thereby reducing habitat quality or diversity. An understanding of bars and their response to channel flow is necessary in characterizing overall morphology of river channels at the reach scale (Lanzoni and Tubino, 1999). Furthermore, in a regulated river where flow releases, or environmental flows, are being considered to improve habitat for salmon downstream, sampling on bars is important, as bars generally mobilize only at higher flows and could be a monitor of the effectiveness of the flow releases. The status of salmon habitat is particularly important for FERC (Federal Energy Regulatory Commission) dam relicensing and for biological opinions submitted by NOAA (National Oceanic and Atmospheric Administration) Fisheries on the operation of the dam for species listed under the Endangered Species Act.

We sampled grain size on bar surfaces instead of cross-sections in the channel because: 1) the majority of the McKenzie River is not wadeable and we needed to be able to measure at sites within range of the canals and dam and 2) we were evaluating sediment mobility and therefore needed to sample the potentially mobile gravels on the surface. We selected the bars based on their proximity to the Leaburg dam and the Leaburg and Walterville canals (Figure 3.1, Table 3.2), accessibility by boat (input locations), and accessibility for safe sampling along the bar at low flow conditions (Kondolf, 1997; Fassnacht et al., 2003). We sampled virtually all of the bars in the study reach. Bar surface grain sizes can be considered a minimum, as they tend to be finer than the reach-average bed-material size (Bunte and Abt, 2001). The McKenzie bar sampling took place in September 2008 and August 2009, months when flow is usually at annual low flow conditions. Between these dates, three events with durations of 2, 18, and 10

days were of a magnitude large enough to possibly mobilize of the $D_{50}$ or smaller grain sizes on bars 9, 20, and 23 (based on our modeled results), respectively. At bars 20 and 23, there was one four-day storm event that may have potentially changed the grain size distribution. However, distribution sizes are not compared between years and long-term gage data (~20 years) were used in analysis. To minimize variability between samplers we used a gravelometer consisting of a template with square holes of sieve sizes (<2 to 180 mm) to classify grains into size classes in the field (Potyondy and Bunte, 2002). Small grains were binned into a <2 mm category (Fassnacht et al., 2003), as they comprised a very small portion of the sampling. We sampled based on the pebble count techniques of Bunte and Abt (2001) using systematic sampling at 1 m intervals along a tape measure grid of 100 grains (Wolman, 1954). While Rice and Church (1996) recommended 400 particles to improve estimates of percentiles within one tenth of a phi unit for 95% confidence limits, our research focus was on differences upstream and downstream of the feature of interest, not differences between each individual bar. Therefore, we analyzed differences between the pooled samples of the bars above and below each feature, forming pooled sample sizes of ~200 - ~350 grains for each group.

*Grain size and flow analysis*

The analysis of grain size distribution is commonly used to assess dam impacts (AWRC, 2007; Sennatt et al., 2006). We plotted the cumulative grain size distribution to determine $D_5$, $D_{16}$, $D_{50}$, $D_{84}$, and $D_{95}$ sizes for use in calculating sorting and in evaluating overall differences in sediment distribution on bars above and below the dam and

diversion canal outlets. We calculated sorting using the geometric (modified) Folk and Ward (1957) graphical measures equation of standard deviation (Blott and Pye, 2001):

$$\sigma = \exp [(\ln D_{16} - \ln D_{84})/4 + (\ln D_5 - D_{95})/6.6] \qquad (3.1)$$

where $D_i$ is the grain size diameter in mm of the ith percentile. To test for difference between the means upstream and downstream, we pooled all the gravels upstream and downstream and calculated the mean from each. Then we used a Kolmogorov-Smirnov test to whether the two distributions were different.

A common method for evaluating threshold entrainment is using estimates of shear stress to estimate flow (Duncan et al., 1999). Bed shear stress and sediment bed characteristics are key properties in entrainment (Coleman and Nikora, 2008). We identified the threshold of incipient motion using critical stage height. (Parker et al., 1982; Recking, 2009). We calculated the critical shear stress ($N/m^2$), or entrainment threshold, for the $D_{50}$ grain size using the Shields' equation (Shields, 1936):

$$\tau_{cr} = \theta_{cr} g d (\rho_s - \rho) \qquad (3.2)$$

where $\theta_{cr}$ is the Shield's parameter (0.045), g is gravity (9.82 $m/s^2$), d is the grain diameter (m), $\rho_s$ is the grain density (2650 $kg/m^3$), and $\rho$ is the density of water (1000 $kg/m^3$). The value chosen for Shield's parameter is considered to be well suited for gravel deposits of uniform sizes (Komar, 1987; Mao et al., 2008) and lies in the transition zone between hydraulically rough and smooth flow conditions (Gordon et al., 2004).

We determined the critical stage (water depth) needed to mobilize the $D_{50}$ grain size at each sampling site by solving for D using the Du Boys' equation adapted by Bradley et al. (1972) for alluvial channels, assuming that flow was approximately uniform and that the energy slope could be approximated by the local water surface slope:

$$\tau_{cr} = \rho g D S \quad (3.3)$$

where ρ is fluid density (kg/m$^3$), g is gravity (m/s$^2$), D is depth of flow (m), and *S* is slope (m/m). Baker and Ritter (1975) also suggest that D is a close approximation to R when considering streams transporting bed-load material. We used water surface slopes determined from LiDAR, except at one bar location (3) in the backwater of the dam where we used the lowest alluvial surface.

To estimate the discharge corresponding to the calculated critical $D_{50}$ stage for each gravel bar, we used WinXSPRO 3.0 (Hardy et al., 2005), which uses numerical integration to solve Manning's equation in channel cross-sections. WinXSPRO requires the input of channel topography, longitudinal slope of the water, and an estimate of hydraulic roughness. WinXSPRO iterates Manning's equation with flow increasing in depth until the predicted cross-sectional discharge equals that of the stage-discharge regression equation. The cross-section at each bar was constructed from existing sonar data within the wetted channel merged with existing airborne-LiDAR-derived elevation data on dry land, with the exception of bars 1 and 2. The sonar data on the McKenzie River were obtained for modeling purposes (Walther et al. in press) and the LiDAR data were obtained in 2009 from EWEB, a member of the Oregon Lidar Consortium (OLC ) maintained through the Oregon Department of Geology and Mineral Industries (DOGAMI, 2009). No sonar was available upstream of bar 3, so we estimated cross-sectional bed topography for bars 1 and 2 from aerial imagery using the HAB-2 model (Walther et al., in press; Fonstad and Marcus, 2005). We used the method of Arcement and Schneider (1989) to estimate Manning's roughness coefficients for the channel and floodplain.

A sensitivity analysis of the Shields parameter ($\theta_{cr}$) and slope with regard to the critical shear stress and critical stage height show that both can contribute to variation in the results to differing degrees. The sensitivity of critical stage height to slope was highest (almost 50%) as compared to the Shields parameter (~10%). For this reason, we choose the Shields' value of 0.045 to represent average conditions for the entire study area. We used slopes measured at each bar to represent the local variations in river slope.

Given estimates of the discharge at the critical $D_{50}$ stage for each bar, we wanted to know the frequency of mobilization, or the recurrence interval, which is important in environmental management and environmental flows planning for habitat maintenance and restoration. To determine the recurrence interval for this discharge we used USGS gage data (Table 3.3) in the PeakFQ model (Flynn, 2006a, 2006b), which estimates instantaneous peak flows for a range of recurrence intervals by fitting the Pearson Type III frequency distribution to the logarithms of instantaneous annual peak flows following Bulletin 17B guidelines (IACWD, 1982). We compared the calculated discharge to the 2-, 5-, and 10-year post-dam recurrence intervals and also to the peak flow of the well-documented Pacific Northwest Flood of 1996 which had an ~100 year recurrence interval and was the largest food on the system since 1964 (Johnson et al., 1996, 2000).

It is assumed that the entrainment and transport of the median (or smaller) grain sizes occur when the critical discharge (calculated from critical stage height) is equaled or exceeded. Therefore, the results represent only median grain motion, without accounting for other hydraulic conditions (turbulence, etc.) and sediment characteristics that also affect entrainment (Andrews, 1984; Komar, 1987; Pohl, 2004). Full bed mobilization would require a much higher discharge than that based on the $D_{84}$ grain size, due to

channel characteristics such as form and location, and sediment characteristics such as grain angles, exposure, and packing (Knighton, 1991).

Finally, to explain their relative hydrologic and geomorphic contributions to the river channel, we used the GIS program ArcMap 9.3 (ESRI, 2009) and the ArcHydro extension (Maidment, 2006) to quantify the drainage area and used the LiDAR-derived elevation data to calculate the slope of each of the small tributaries nearest the bars in the upstream direction.

Table 3.3. U.S. Geological Survey streamflow-gaging stations used in the study (USGS, 2010).

| Station No. | Streamflow-gaging station name | Drainage area ($km^2$) | River km (mi) | Period of record (water years) |
|---|---|---|---|---|
| 14162500 | McKenzie River near Vida | 2408 | 69.4 (43.1) | 1925-2009 |
| 14163150 | McKenzie River below Leaburg Dam, near Leaburg | 2667 | 52.5 (32.6) | 1990-2009 |
| 14163900 | McKenzie River near Walterville | 2799 | 38.1 (23.7) | 1990-2009 |

## RESULTS

### *Grain size distribution characteristics*

*Cumulative frequency curves and downstream trends.* The cumulative frequency curves for each bar show the variability above and below Leaburg dam (Figure 3.3), Leaburg tailrace (Figure 3.4), and Walterville tailrace (Figure 3.5). At Leaburg dam, the grain sizes for the three bars upstream of the dam and the three bars downstream of the dam vary within each group and some overlap occurs between bars 1, 3, 4, and 6 below the 40th percentile (Figure 3.3). More generally, the gravels below the dam are coarser and include much larger grain sizes in the upper quartile of the curve than those above the

dam. The canals, however, exhibit a different pattern. At the Leaburg canal tailrace, the curves of the grain sizes between the bars upstream of the tailrace and those downstream of the tailrace are more similar in overall shape and show less variation than those of the Leaburg dam groups (Figure 3.4). Overall, the gravels are finer below the Leaburg canal tailrace. At the Walterville canal tailrace, the gravels above and below the dam exhibit a large amount of overlap in the distribution curves (Figure 3.5). The grain sizes of the bars upstream and downstream of the Walterville tailrace show slightly greater variation and more overlap than those of the Leaburg canal bars. Only the curves from bars 21 and 24 are distinct for at least half of the curve. Sorting values show that all of the bars are very well-sorted ($\sigma < 1.2$ from Folk and Ward, 1957) (Table 3.4).

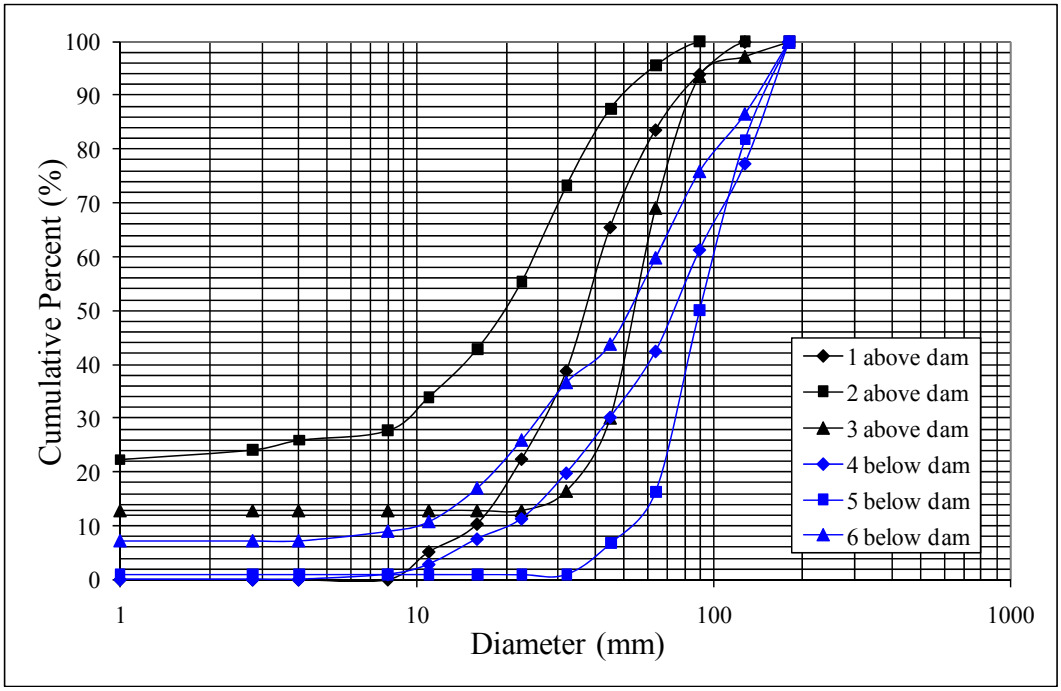

Figure 3.3. Cumulative percent finer frequency curves for sediment bars sampled above and below Leaburg Dam.

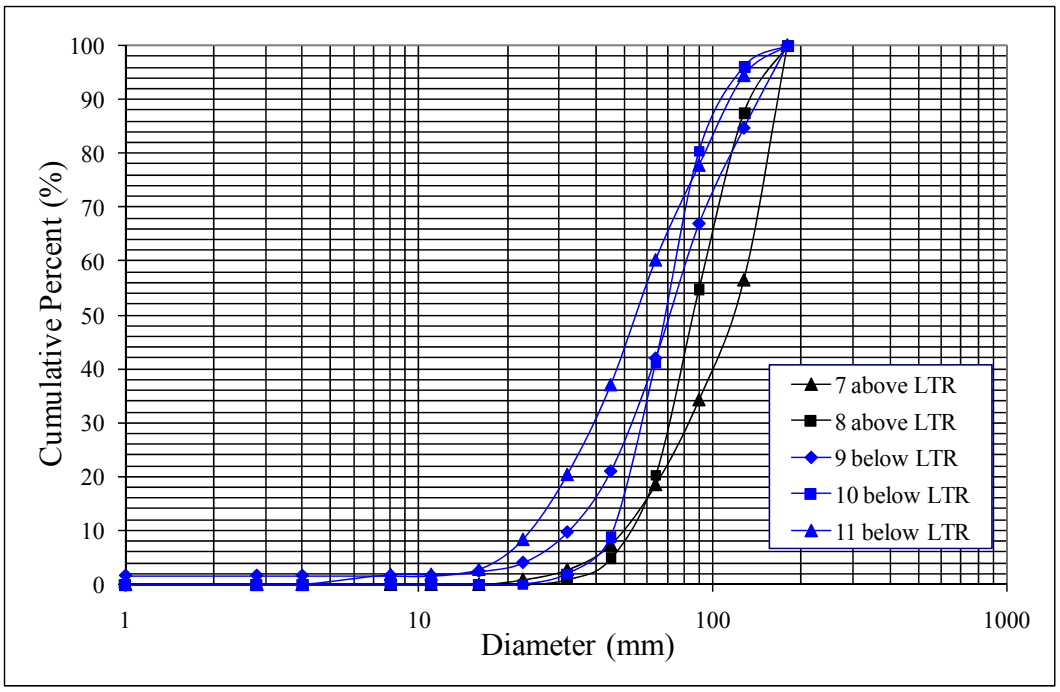


Figure 3.4. Cumulative percent finer frequency curves for sediment bars sampled above and below Leaburg canal tailrace.

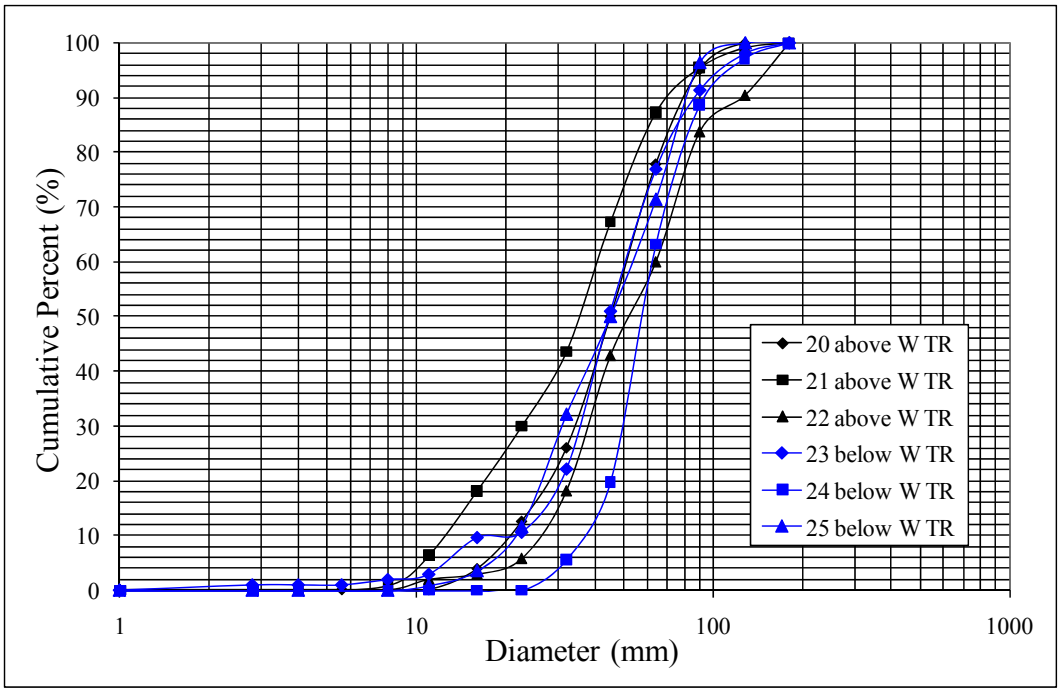


Figure 3.5. Cumulative percent finer frequency curves for sediment bars sampled above and below Walterville canal tailrace.

It is well known that the median surface grain size of gravel-bed rivers decreases exponentially with downstream distance at the largest spatial scales (e.g., Robinson and Slingerland, 1998; Morris and Williams, 1999; Hoey and Bluck, 1999). The pattern of grain size fining with distance downstream is not statistically significant at the scale of this reach of the lower McKenzie (Figure 3.6). Instead, there are lower grain size values ($D_{50}$) at the beginning of the reach above Leaburg dam, and higher values in the segment of the river between the Leaburg dam (and diversion canal) and the Leaburg tailrace (Figure 3.6a). The data exhibit no fining trend. The residuals illustrate the variability of the grain size (Figure 3.6b).

Table 3.4. River number, location (km and bank side), and grain sizes (mm) for the 5th, 16th, 50th, 84th, and 95th percentiles. Lines separate each group of bars above and below the dam or canals.

| Bar | River km (mi) | Location (bank) | $D_5$ | $D_{16}$ | $D_{50}$ | $D_{84}$ | $D_{95}$ | Sorting ($\sigma$) |
|---|---|---|---|---|---|---|---|---|
| 1 | 58.9 (36.6) | above dam (right) | 11 | 19 | 37 | 64 | 96 | 0.53 |
| 2 | 57.8 (35.9) | above dam (left) | <2 | <2 | 20 | 41 | 61 | 0.21 |
| 3 | 57.2 (35.6) | above dam (left) | <2 | 34 | 54 | 78 | 95 | 0.40 |
| 4 | 54.5 (33.9) | below dam (left) | 14 | 27 | 72 | 150 | 170 | 0.45 |
| 5 | 54.0 (33.6) | below dam (left) | 32 | 64 | 89 | 130 | 165 | 0.65 |
| 6 | 52.2 (32.4) | below dam (left) | <2 | 16 | 52 | 125 | 160 | 0.28 |
| 7 | 47.0 (29.2) | above L tailrace (left) | 40 | 60 | 115 | 160 | 175 | 0.63 |
| 8 | 46.4 (28.8) | above L tailrace (right) | 45 | 60 | 86 | 125 | 160 | 0.69 |
| 9 | 43.9 (27.3) | below L tailrace (left) | 24 | 40 | 70 | 128 | 130 | 0.58 |
| 10 | 42.2 (26.2) | below L tailrace (left) | 40 | 50 | 68 | 94 | 125 | 0.72 |
| 11 | 41.8 (26.0) | below L tailrace (right) | 19 | 28 | 55 | 100 | 130 | 0.54 |
| 20 | 30.2 (18.8) | above W tailrace (left) | 17 | 26 | 45 | 70 | 128 | 0.57 |
| 21 | 29.0 (18.0) | above W tailrace (right) | 11 | 16 | 36 | 59 | 90 | 0.52 |
| 22 | 28.2 (17.5) | above W tailrace (left) | 22 | 30 | 52 | 90 | 160 | 0.56 |
| 23 | 26.7 (16.6) | below W tailrace (right) | 14 | 28 | 45 | 73 | 95 | 0.59 |
| 24 | 25.5 (15.9) | below W tailrace (left) | 31 | 43 | 58 | 82 | 125 | 0.69 |
| 25 | 25.0 (15.5) | below W tailrace (right) | 16 | 25 | 45 | 74 | 87 | 0.59 |

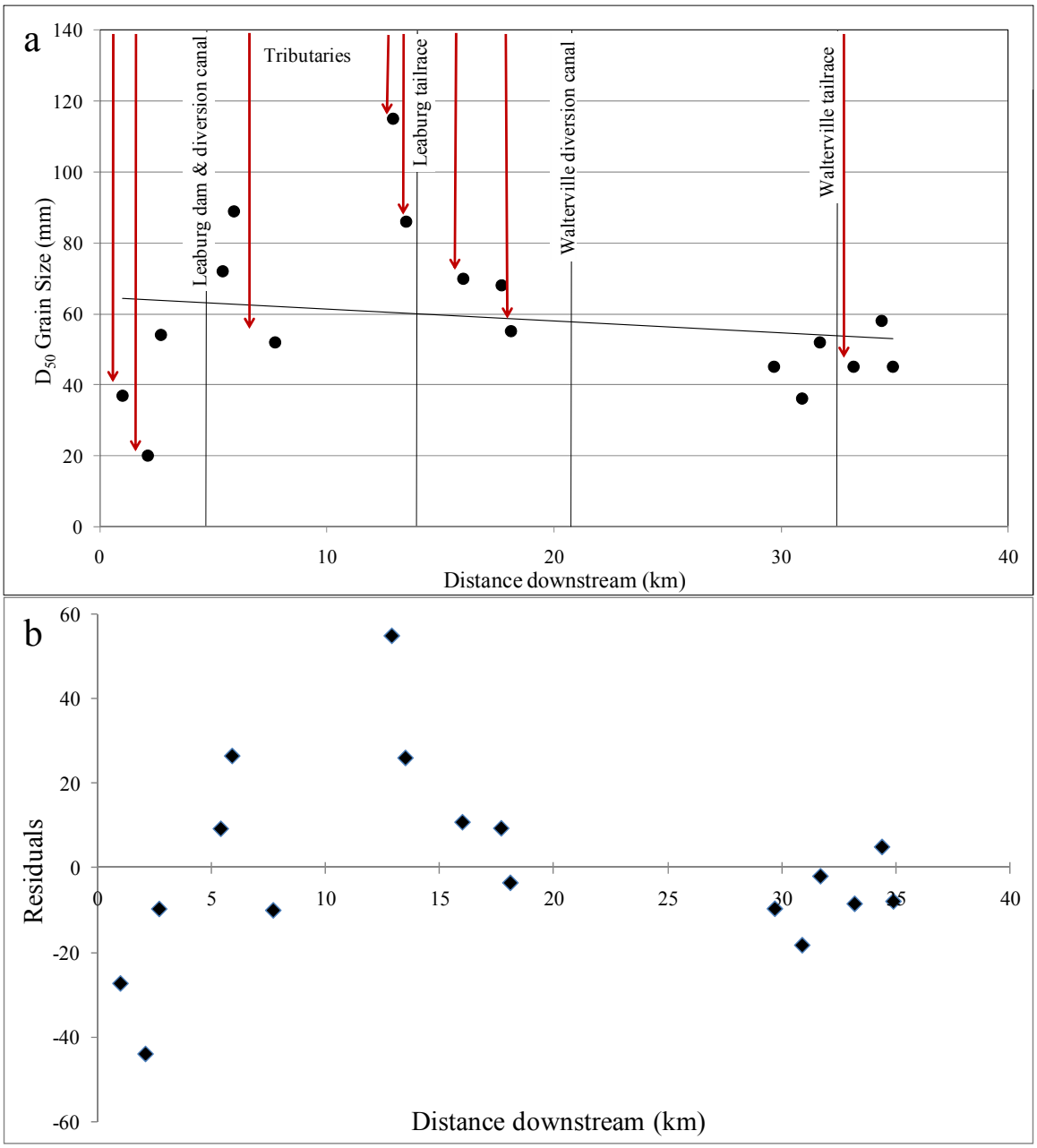


Figure 3.6. (a) $D_{50}$ grain size values with distance downstream graphed with the Leaburg dam and canal diversion, Leaburg tailrace, Walterville diversion, Walterville tailrace, tributaries (red arrows) along the reach. A regression line fitted to the data is shown. (b) Residuals of the $D_{50}$ grain size values with distance downstream. The $R^2$ value ($R^2$=0.03) and P-value (P>0.05) show no significant relationship between grain size and downstream distance.

*Pooled grain size statistics.* We pooled the grain size data from the 2-3 bars above the feature of interest into one group and 3 bars below the feature into another group. Both the pooled $D_{50}$ and $D_{84}$ grain sizes of the bars downstream of the dam are larger than those of the bars upstream of the dam. Conversely, both the pooled $D_{50}$ and $D_{84}$ sediment sizes were smaller for the bars downstream of the Leaburg canal tailrace than those above the tailrace. The differences of the pooled grain sizes of the bars above and below the Walterville canal tailrace are small. Both the pooled $D_{50}$ and $D_{84}$ are slightly larger below the tailrace than above it (Table 3.5). The Kolmogorov-Smirnov test (Zar, 1999) showed a statistically significant difference in the shape of the distribution of the pooled samples above and below all three sites.

Table 3.5. Pooled grain size $D_{50}$ and $D_{84}$ (mm) and results of Kolmogorov-Smirnov Test for each site. Paired pooled grain size distributions were tested against the null hypothesis that the distributions are the same at the 0.05 significance level.

| Location | $D_{50}$ | $D_{84}$ | Kolmogorov-Smirnov test results |
|---|---|---|---|
| Above dam | 37 | 62 | $D(0.4632) > D_{0.05,\,326}$ (0.0755) |
| Below dam | 77 | 104 | $p<0.01$ differ |
| Above LT | 97 | 107 | $D(0.3302) > D_{0.05,\,212}$ (0.0933) |
| Below LT | 69 | 100 | $p<0.01$ differ |
| Above WT | 43 | 75 | $D(0.1321) > D_{0.05,\,318}$ (0.0762) |
| Below WT | 50 | 76 | $p<0.01$ differ |

*Modeled critical discharge and flow frequency*

The critical shear stress for the $D_{50}$ at each bar ranges from 14.6 -83.9 $N/m^2$ (Table 3.6). The calculated stage height needed to entrain the $D_{50}$ of the bar gravels and the estimated discharge to reach that stage at each bar ranges from 0.8 to 4.7 m and 144 to 2,476 cms, respectively (Table 3.6). The lowest discharge values are at bars located

above the dam, while the higher values are dispersed throughout the rest of the study reach. Except for bar 3, the modeled critical discharge of each of the bars was met or exceeded during the documented 1996 flood (Table 3.6). When plotted with the post-dam 2-, 5-, and 10-year flood return intervals ($Q_2$, $Q_5$, $Q_{10}$), 13 of the 17 bars have critical discharge values hovering around or below the $Q_2$ value and four of the bar values are hovering around or below the $Q_5$ value (Figure 3.7).

Table 3.6. Slope, calculated critical shear stress and critical stage height above the bar surface needed to entrain the $D_{50}$ of each bar, numbered upstream to downstream, WinXSPRO modeled channel discharge (Q) for each, and whether the critical discharge was exceeded in the flood of 1996.

| Bar | Slope | Critical shear stress ($N/m^2$) | Critical Stage Height (m) | $Q_{Stage}$ (cms) | Exceeded in 1996 Flood |
|---|---|---|---|---|---|
| 1 | 0.0035 | 27.0 | 0.8 | 144 | Y |
| 2 | 0.0016 | 14.6 | 1.0 | 190 | Y |
| 3 | 0.0008 | 39.4 | 4.7 | 2476 | N |
| 4 | 0.0035 | 52.5 | 1.5 | 387 | Y |
| 5 | 0.0024 | 64.9 | 2.7 | 436 | Y |
| 6 | 0.0035 | 37.9 | 1.1 | 494 | Y |
| 7 | 0.0035 | 83.9 | 2.5 | 611 | Y |
| 8 | 0.0019 | 62.7 | 3.3 | 827 | Y |
| 9 | 0.0030 | 51.0 | 1.7 | 529 | Y |
| 10 | 0.0035 | 49.6 | 1.4 | 553 | Y |
| 11 | 0.0013 | 40.1 | 3.1 | 711 | Y |
| 20 | 0.0032 | 32.8 | 1.0 | 254 | Y |
| 21 | 0.0018 | 26.2 | 1.5 | 264 | Y |
| 22 | 0.0024 | 37.9 | 1.6 | 699 | Y |
| 23 | 0.0014 | 32.8 | 2.4 | 512 | Y |
| 24 | 0.0023 | 42.3 | 1.9 | 565 | Y |
| 25 | 0.0020 | 32.8 | 1.7 | 554 | Y |

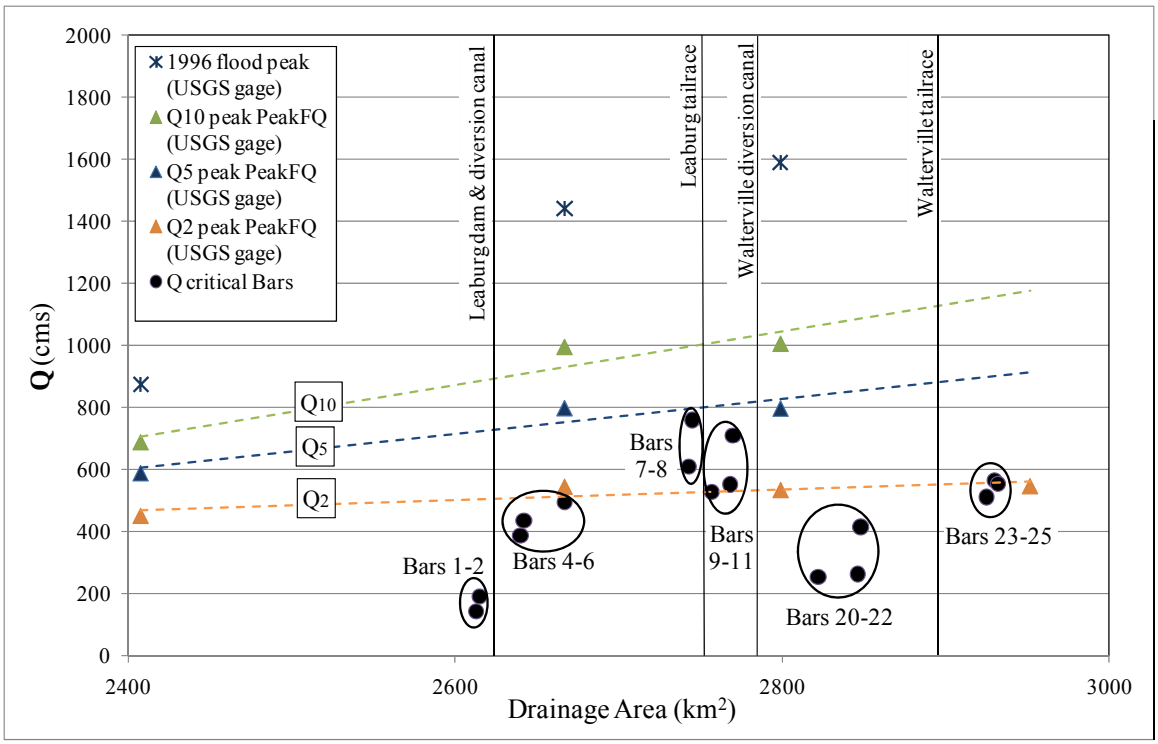


Figure 3.7. The calculated discharge at three different return intervals (2-, 5-, and 10-year) and the modeled discharge needed to move the $D_{50}$ of the gravels at each bar plotted against drainage area. The locations of the Leaburg dam and diversion, the Walterville diversion, and both the Leaburg canal and Walterville canal tailraces are shown. The bars above and below each feature are circled for visual comparison. The modeled discharge for bar 3 is excluded because it is anomalously large due to its location at Leaburg Lake.

## DISCUSSION

In the following sections, we first discuss the differences observed in the grain-size distributions in terms of the cumulative frequency and the pooled $D_{50}$ and $D_{84}$, as well as possible reasons for the differences. The key influences on grain size distribution that are discussed include sediment disconnection, hungry water, dewatering of the main channel for the canals, and tributary inputs into the channel. Subsequent sections discuss the modeled entrainment discharge and how the results compare to calculated post-dam flood frequencies. Lastly, we discuss other evidence and possible reasons for the modeled

discharge results, including canal information and geomorphic channel changes, and model limitations.

*Grain size distribution characteristics*

*Dams.* Unaltered, natural streams typically show a decrease in median ($D_{50}$) and coarse ($D_{84}$) grain sizes with distance downstream (Graf, 1980; Chien, 1985; Knighton, 1987). However, in dammed rivers, coarsening can often occur downstream of the dam (Collier et al., 1997). Though the scale of the response of a river to a dam is variable, an increase in median grain size is a typical sedimentary response for two possible reasons, disconnection from the upstream sediment supply and sediment-starved water flowing from the dam (Ward and Stanford, 1979; Kondolf, 1997; Buffington and Montgomery, 1999b). The upper McKenzie (above Leaburg dam) is also considered coarse sediment supply limited relative to transport capacity a result of the larger dams upstream (Stillwater Sciences, 2006).

On the McKenzie River at Leaburg dam, the below-dam bars have far fewer of the small grain sizes compared to the above-dam bars. The difference between the pooled sample distributions above and below the dam is statistically significant ($p<0.01$). Additionally, both the pooled $D_{50}$ and $D_{84}$ grain size percentiles increase over 50% below the dam. Thus, gravel coarsening on the bars below Leaburg dam is exhibited in both the cumulative frequency curve and the pooled grain sizes. The dam acts as a barrier to downstream sediment delivery, resulting in gravel coarsening below the dam.

*Canals.* There are three potential canal effects on grain size distribution on the bars in the main channel. These include: 1) the canal return flow "hungry water" effect, 2) the

dewatering of the main channel, and 3) the tributary inputs in the main channel. Studies on canal return flow effects on grain size distribution primarily focus on controlling sediment and pesticide inputs from irrigation canals (Weston et al., 2004; Brown et al., 1981; Brown et al., 1974) and within canal sediment transport (Petit et al., 1996). On the McKenzie River, essentially no sediment is introduced into the canal at the intake and very little sediment transport occurs within the canals, primarily the occasional sediment introduced from the slope along the canal that is then moved down-canal, where it is trapped until removed by EWEB. The canal tailraces add "hungry water" to the main stem--sometimes more than is in the channel. Despite this, the gravels on the bars above and below the canals show far less variation than those above and below the dam.

Below the Leaburg tailrace, all three bars exhibit a greater percentage of smaller grain sizes than the bars above the tailrace. The distributions of the two pooled samples are significantly different ($p<0.01$). This is reflected in the diameters of the $D_{50}$ and $D_{84}$ percentiles, which decrease below the tailrace by ~ 30% and ~7%, respectively.

At the Walterville tailrace, the difference between the bars above and below the return flow is less clear. In fact, five of the six cumulative frequency curves overlap for much of the curves. Still, the distributions of the pooled samples are significantly different ($p<0.01$). The diameters of both the $D_{50}$ and $D_{84}$ percentiles are higher at the bars below the return flow, but the difference is small--14 and 1%, respectively.

This fining below the Leaburg tailrace and slight coarsening of the gravels below the Walterville tailrace are contrary to the concept of coarsening with the addition of sediment-starved water. However, a second effect of the canals is the dewatering of the main channel for the length of the canal, and reduction of competency may further

diminish the sediment delivery already limited by the upstream dams (EWEB, 1991). Thus, not only is the sediment supply reduced at the dam, but the large percentage of water that is removed from the channel into the canals (greater than or equal to the amount of water remaining in the channel for the majority of the year-see Table 3.1) also reduces the competency of the river between the diversion and the tailrace, further limiting the movement of sediment downstream in the channel. The distribution of sediment, and the frequency with which sediment is added or removed from channel locations, reflects the degree to which sediment transport in the river system is connected or disconnected (Harvey, 2002; Hooke, 2003). Any factor that impedes sediment conveyance constrains sediment delivery downstream (Fryirs et al., 2007). Thus, between the diversion and tailrace, the sediment size in the channel may be partly determined by sediment introduced from local sources in this reach. The result could be fining or coarsening, depending on the size of local sediment introduced. For example, bars 7 and 8, above the Leaburg tailrace, have generally higher $D_{50}$ and $D_{84}$ grain size values than the bars below the tailrace. This might reflect input of coarser grain sizes from local sources, and limited mobilization of these inputs above the tailrace. Ultimately, the reduced volume of water above the tailrace may play a greater role in disconnecting and reducing sediment delivery than the increased volume of water below the tailrace plays in mobilizing sediment downstream. Disconnecting sediment along a channel can result in erosion and river incision, and therefore the increased importance of external sources of replacement sediment.

In sediment-starved rivers, tributary inputs are a key source of sediment replacement into the main channel. Within the study area, the combination of the upstream dams, rip-

rapping of banks, and encroachment of vegetation on point bars has reduced the major sources of sediment, so that the tributaries, whose hydrologic contribution are relatively small, may have become the primary sources of sediment (EA Engineering, Science, and Technology, 1991). Sediment recruitment at tributary confluences can alter the typical longitudinal sediment pattern of downstream fining, reducing the decline or even increasing average grain sizes in a variably shaped saw-tooth pattern (Church and Kellerhals, 1978; Knighton, 1980). The grain size increases reflect the influx of sediment of sufficient volume or size to redefine the grain size characteristics of the channel (Rice et al. 2001). At spatial scales of ~1 km or less, a stochastic pattern is often produced (Rice et al. 2001). In our study, the generally observed downstream fining pattern (Knighton, 1998) is affected by small $D_{50}$ values above the dam and large $D_{50}$ values in the dewatered portion of the river between the Leaburg dam and the Leaburg tailrace (Figure 3.6a).

Sedimentary inputs from a number of small tributaries along the study reach appear to influence median grain sizes on the bar below the confluences, but the influence varies. The potential combined hydrologic and sedimentary influences of the dam and canals and the tributaries are illustrated in Figure 3.6 where the $D_{50}$ grain size pattern (Figure 3.6a) is shown above the residuals of the $D_{50}$ values (Figure 3.6b) along the same x-axis of distance downstream.

Along the study reach of the relatively coarse grained gravel-bedded McKenzie, the majority of the tributaries (selected for location above a sampled bar) appear to contribute to a decrease in median grain size at the proximate downstream bar (Figure 3.6a). The tributaries above the dam appear to decrease the $D_{50}$ values. Similarly, the $D_{50}$ value is

relatively low on bar 6 below the first tributary below the dam, in contrast to the coarser values for bars 4 and 5 below the dam (but upstream of bar 6). Though still large, the $D_{50}$ value decreases at bar 8, just below a different tributary. Below tributaries, the $D_{50}$ values at bars 9 and 11 also decrease. Finally, just below Walterville tailrace, the tributary inputs may slightly decrease the $D_{50}$ value at bar 23.

This possible influence is also observed in the pooled $D_{50}$ and $D_{84}$ grain size values. The pooled grain size values below Leaburg tailrace are larger than those below Walterville tailrace, in line with a general decrease in grain size with distance downstream. However, the expected increase in grain size does not occur below the Leaburg tailrace and though it does occur below the Walterville tailrace, it is very small. The tributary inputs may be the reason for this. The influx of sediment from Camp Creek, located less than 75 m below Walterville tailrace and ~400 m above the next sampled bar, appears to decrease the median grain size value at bar 23, dampening the increase in the pooled grain size values. The increase in finer sediment than what is in the channel could buffer the coarsening despite the increased discharge at the tailrace, thereby reducing the amount of difference between the pooled grain size values on the bars above and below the tailrace.

Bar 7 could provide an example of a tributary increasing the grain size immediately downstream of its input, as the $D_{50}$ value and residual are the largest respective values on the study reach. The tributary upstream of bar 7 is located ~6 km downstream from the previous sampled bar so it is not immediately clear what the relative effect is on the grain size. However, Stallman et al. (2005) posited that several tributary inputs increase the mean grain size in the upper McKenzie River (above the study area) where a higher than

reference sediment yield from Deer Creek appeared to compensate for upstream sediment trapping. The tributary at bar 7 has the smallest drainage area and the steepest slope (an order of magnitude or more greater than the slopes of the other tributaries) of all tributaries (Table 3.7). This suggests that this tributary could be delivering sediment to the channel via a debris flow mechanism or a fluvial process transporting coarser sediment. Since this input occurs in a dewatered section of the main channel, the tributary sediment input may increase the grain size values at a point where the river is less competent and therefore unable to move the larger grains.

Table 3.7. Drainage area and slope of selected tributaries near sampled gravel bars.

| Creek | Distance (km) | Drainage area (km2) | Slope | Location |
|---|---|---|---|---|
| Gate | 0.9 | 124.2 | 0.010 | upstream of bar 1 |
| Indian | 1.6 | 16.2 | 0.050 | upstream of bar 2 |
| Trout | 6.2 | 9.6 | 0.053 | upstream of bar 6 |
| Unnamed | 12.8 | 2.5 | 0.215 | upstream of bar 7 |
| Fish return | 13.5 | -- | -- | upstream of bar 8 |
| Holden | 15.9 | 11.0 | 0.043 | upstream of bar 9 |
| Haagen | 17.8 | 13.0 | 0.053 | upstream of bar 11 |
| Camp | 32.4 | 68.1 | 0.004 | upstream of bar 23 |

*Modeled critical discharge and flow frequency*

The balance of sediment supply and river's capability to transport it influences the channel structure and pattern, thereby creating physical habitats. The calculated critical stage height, and therefore critical discharge values, vary among the bar cross-sections, without regard for longitudinal location or lateral in-channel location (Table 3.6, figure 3.7).

*Leaburg dam.* Bar 3 has the largest critical stage height (over four times greater than at bars 1 and 2) and discharge for the study sites (Table 3.6). This is the closest bar to Leaburg Lake, and it appears to be influenced by a backwater effect from the lake, because its slope is half of the nearby bars. Compared to bars 1 and 2, bar 3 has more fines but is coarser at the 15th-90th percentiles. The critical stage height values are generally higher below the dam than above the dam (excepting bar 3), and therefore the critical discharges are also higher. All of the critical discharge values of the bars located upstream and immediately downstream of Leaburg Dam (bars 1-6) are below the post-dam 2-year return flow ($Q_2$) estimates from the nearby gage (Vida) (Figure 3.7). Below the dam, the critical discharge values are greater than those above the dam, with the largest value occurring at bar 6.

*Leaburg canal tailrace.* The stage height values needed to move the median grain sizes are generally greater at the bars above the tailrace than below, but there is little difference in the critical Q (Table 3.6). The critical discharge values of the bars above the tailrace fall between the post-dam $Q_2$ and $Q_5$ estimates from the Leaburg gage. The critical discharge value at bar 8 is greater than that of bar 7. One reason for this is that bar 8 has a much lower slope and a greater critical stage height than bar 7, so a higher discharge is needed to move the gravels. At bar 8, the low slope is observable in the LiDAR measurements and a large portion of the channel appears shallower in both the cross-section and in the orthophotograph of the site. This, despite similar or lower grain size percentile values, results in a higher critical discharge. The textural coarsening in the dewatered section of the river just above the Leaburg canal tailrace results in rougher surfaces, increasing critical shear stresses at the bed and thereby reducing transport

capacity (Buffington and Montgomery 1999a), especially when the channel slope decreases as it does at bar 8.

Below the tailrace, all of the critical discharge values fall on or between the post-dam $Q_2$ and $Q_5$ estimates (Figure 3.7). Bar 11 has higher critical Q and stage height than bars 9 and 10. Bar 11 has finer sediment than the other two (Table 3.4), so the difference is due to lower slope at bar 11 (Table 3.6).

*Walterville canal tailrace.* Calculated stage heights and critical discharges are slightly lower at the bars upstream of the tailrace than those downstream (Table 3.6). Critical discharge values of the bars above the tailrace fall well below the post-dam $Q_2$ trendline, while those of the bars below the tailrace are clustered around it.

*Geomorphic channel changes*

While we have presented some of the relative differences in the effects of the dams and canals on grain size and mobilization of sediment, the combined effects of the regulation on the river is geomorphically apparent in a number of other channel characteristics. In terms of flow changes that could influence geomorphology, regulation from the upstream dams has slightly increased the minimum flows from ~36 to 38 cms (1,260 to 1,350 cfs) and reduced the two-year discharge by more than half from ~1825 to 850 cms (64,400 to 30,000 cfs), as recorded at the Vida gage (EWEB, 1991).

Risley et al. (2010), using historical orthophotographs on the same portion of the lower McKenzie River as our study, have show that between 1939 and 2005, all measured channel characteristics decreased, suggesting a less dynamic river (Table 3.8). For over 72 river reaches, Graf (2006) found these to be common changes that

collectively reduce the geomorphic complexity of the river. Specifically, with respect to bars, Risley et al. (2010) found that, between 1939 and 2005, the area of active gravel bars in three reaches (labeled reaches 8, 9, and 10) within our study area decreased by 20, 100, and 25%, respectively. This is indicative of a less active river channel overall. Furthermore, more than 13% of the river banks have been stabilized using rip-rap (Runyon, 2000). This figure is a minimum as it only represents U.S. Army Corps of Engineers projects. More private stabilization exists and continues to be implemented on the river.

Table 3.8. Summary of changes in channel characteristics on the Leaburg and Walterville reaches (numbered 8, 9, and 10 in Risley et al., 2010) of the McKenzie between 1939 and 2005 (from Risley et al., 2010).

| **Characteristic** | **Change** |
|---|---|
| Grain size ($D_{50}$ & $D_{84}$) | Decrease |
| Avulsions | Decrease |
| Lateral migration | Decrease |
| Area of active gravel bars | Decrease |
| Length of secondary channel features | Slight decrease |
| Length of primary channel | Equal or decrease |

*Salmonid habitat*

Restoration of endangered species, particularly salmonids in the Pacific Northwest, is a major element of river regulation and dam research and policy. Substrate and river landforms are important aspects of habitat needs of salmon. Our research affirms that geomorphology is key to these issues (Graf, 2005). Even small changes in flow can induce measurable changes in the ecosystem (Poff and Ward, 1989). Because substrate is such key habitat characteristic, bed mobility is used as a distinguishing threshold for ecological response to a change in flow (Biggs and Close, 1999). Dam flood releases

have been effective at flushing sediments to improve salmon habitat (May et al., 2009) and at incorporating terrestrial material and nutrients for salmon diet (Eberle and Stanford, 2010), but also at disrupting river metabolism (Cronin et al., 2007). In the McKenzie River, the limited supply of sediment, reduced area of suitable depositional conditions for finer materials, and decreased bar dynamics have likely resulted in coarser bar gravels than in the pre-dam period. The $D_{50}$ grain sizes of the bars on much of the river are large, many of them already too coarse for salmon spawning (EA Engineering, Science, and Technology, 1991).

Grain size characteristics of a river play a dual role in salmonid success: food production and reproduction. The link between sediment and biomass of benthic organisms has been established (Hynes, 1970; Minshall, 1984), and the abundance of fish corresponds to biomass of available food in the form of detritus, periphyton, and invertebrates (Osmundson et al., 2002). Furthermore, grain size is one of the important habitat requirements for spawning and varies depending on species and size of fish. Some key species in the McKenzie River include spring Chinook salmon, steelhead, and cutthroat trout. The substrate size criteria for spawning areas for these species varies between 6-102 mm (Table 3.9), with $D_{50}$ values ranging between 20-45 and 15-30 mm for Chinook and steelhead, respectively (Kondolf and Wolman, 1993). Our $D_{50}$ values exceed the Chinook range at 11 of the 17 bars and the steelhead range at all but one bar (Figure 3.8). The $D_{84}$ values of six bars exceed the maximum of 102 mm, with the highest values found on the bars from Leaburg dam to below Leaburg tailrace (4-11).

Together with the decrease in geomorphic complexity in the river corridor noted above, our measured grain size characteristics suggest that habitat in an almost 30 km

section of the river is only partially suitable, and we hypothesize that the dam and canal effects play a role in causing this to occur.

Table 3.9. Substrate size criteria for spawning areas of key anadromous fish in the McKenzie River. Larger species generally range between 13-102 mm and smaller species range between 6 to 52 or 76 mm, depending on the size of fish (Bjorn and Reiser, 1991).

| Species | Substrate size (mm) | Source |
|---|---|---|
| Spring Chinook Salmon | 20-45[a] ($D_{50}$) | Buffington et al., 2004; Graf, 1996 |
| | 13-102[b] | Bjorn and Reiser, 1991 |
| Steelhead | 15-30[a] ($D_{50}$) | Buffington et al., 2004; Graf, 1996 |
| | 6-102[c] | Bjorn and Reiser, 1991 |
| Cutthroat Trout | 6-102[c] | Bjorn and Reiser, 1991 |

[a] Kondolf and Wolman, 1993
[b] Bell, 1986
[c] Hunter, 1973

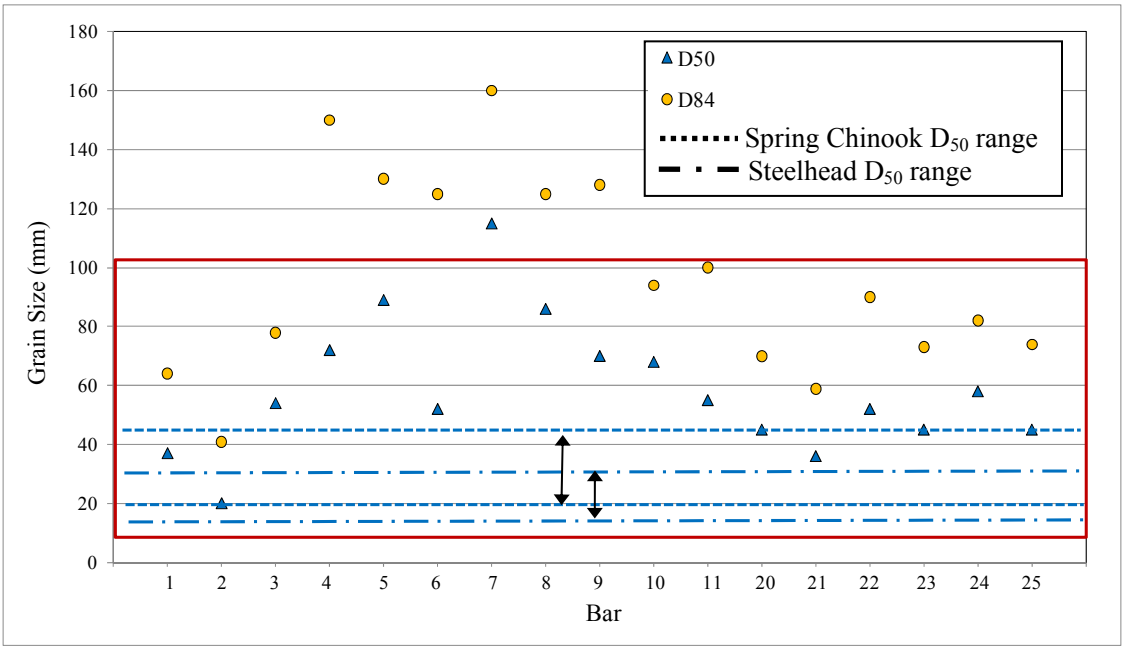


Figure 3.8. Bar $D_{50}$ and $D_{84}$ grain size values shown with the overall substrate size ranges for spawning for Spring Chinook, Steelhead and Cutthroat Trout (red box) and the $D_{50}$ substrate size ranges for spawning Spring Chinook and Steelhead (blue lines).

*Equation and model limitations*

Sediment transport involves complex interactions between flow and the grain sizes in transport, all with characteristic time scales of supply (Howard and Dolan, 1981). These complexities in river systems pose many challenges to sediment transport analysis and human impact assessment. Some of the problems with incipient motion calculations include an inability to account for turbulence, the change in grain size distribution with velocity, variability in mobility from bed break-up, or the variability of the processes involved at different parts of the river or for different river characteristics (Lorang and Hauer, 2003; Parker and Klingeman, 1982). Furthermore, incipient motion calculations, calibrated to specific to grain size characteristics (e.g. specific ranges of grains, uniform grain sizes and shapes), assume specific flow conditions (steady, uniform) and channel shapes (rectangular, trapezoidal). Additionally, sediment functions rely on hydraulic geometry relationships that often include roughness values that are difficult to estimate (Yen, 1992). These equations are subsequently used in other equations, propagating the error of each calculation. When based on time-averaged bed shear stress, incipient motion calculations may under predict sediment transport (Papanicolaou et al., 2002). Despite all the developments and the research done, some of the classic works (Leopold and Maddock, 1953; DuBoys, 1879) remain standards against which comparisons are made and models are based. The dynamic nature of rivers includes inherent variability and natural feedbacks that the equations cannot account for (e.g. vegetation, floodplain interactions, etc.) and more research is needed to improve estimates of the non-measurable parameters (e.g. roughness).

The joining of sonar measurements and LiDAR measurements also incur error to create the channel cross-sections that may omit or smooth some of the channel variability. The WinXSPRO model essentially fills the cross-section and smoothing may increase the modeled critical discharge value. While these issues affect the critical discharge calculations, and anomalies should be noted, the functions can be useful in determining a range of possible geomorphic responses to an applied mean force and for comparison against other similar systems (Lorang and Hauer, 2003).

*Implications for management*

This study serves to highlight the importance of sediment size and mobility in the fluvial system, especially with respect to management using environmental flows. Environmental flow is the flow needed in a river to maintain a healthy ecosystem and an environmental flow prescription defines the necessary seasonal and inter-annual variation in low flows, high flows, and floods to support ecosystem species and ecological functions (Richter et al. 2006). Restoration projects are beginning to focus on restoring environmental flow regimes in rivers that have been regulated by damming for water supply, hydropower, flood control, and other purposes. In order to implement environmental flows on a river, specific recommendations must be made. The process of developing environmental flow recommendations results in a range of recommended flow discharges for low flows and high flows throughout the year, and inter-annually targeted floods (Richter et al. 2006). It is understood that river ecosystem health deteriorates when the movement of water, sediments and organic materials through a river system are disrupted or altered by human activities (Poff et al. 1997; Richter et al.

2003). Therefore, environmental flows are implemented with the aim of more closely mimicking the natural flow regime of the river, and thus, the movement of sediments. For this reason, knowledge of sediment characteristics and mobility of the river is necessary in determining environmental flows for habitat restoration.

Though it remains to be seen if the future implementation of environmental flows on the McKenzie will result in improved salmon habitat, our modeled critical discharge values suggest that flows above the 2-year return frequency are capable of moving the $D_{50}$ on the majority of the bars, and flows around the 5-year return frequency can move the $D_{50}$ on all of the bars except bar 3 (due to a local backwater control). These results are promising for the implementation of environmental flows on the McKenzie River, as increased discharge on the river would primarily increase flow in the "reduced water" sections of the river and mobilize the larger sediment located in those reaches. However, environmental flows do not address the issue of sediment supply.

The McKenzie is a sediment-starved system with high grain size values relative to the identified ecological needs. Thus, the environmental flow prescription must incorporate flows that will flush larger gravels without coarsening the system overall, a difficult prospect (Kondolf and Wilcock, 1996). Though increased flow pulses have the potential to incorporate bank sediments and thereby increase the local sediment supply (Gregory et al. 2007), the overall contribution of bank sediments into the river is unknown and the presence of revetments throughout the study reach minimizes the potential supply from banks. The grain size distribution of the tributary inputs is also unknown. Our study suggests that the tributaries may be contributing sediment that is primarily finer than the gravels on the bars within the channel. Thus, implementation of seasonal or inter-annual

flushing flows may be able to mobilize the large gravels, particularly those located within the reduced water segments of the river. The periodic mobilization of large gravels and the continued contribution of finer than in-channel sediment could alter the overall grain size distribution and result in the desired decrease in the $D_{50}$ and $D_{84}$ grain size values (with respect to salmon habitat). To determine if this is the case, measures of both bank and tributary contributions (volume and grain size) are needed to determine the flow volume, timing, and frequency. The implementation of the recommended flows must then be followed by monitoring of both channel changes and grain size distributions over time. In the absence of a decrease in grain size values following the implementation and monitoring of the environmental flows, the question of whether sediment augmentation is needed arises. This question is valid, but given that sediment augmentation is costly and must be maintained, we recommend that sediment augmentation be re-visited only after the previous steps are taken and are proven unsuccessful first.

## CONCLUSIONS

River regulation has varying impacts on a river channel characteristics. The type of regulation, together with localized characteristics, affects the ability of the river to move sediment downstream. While the mean grain sizes above and below the small run-of-river Leaburg dam show the classic coarsening pattern, coarsening to the same degree is not observed below the tailraces. The pooled $D_{50}$ and $D_{84}$ grain size percentiles increase below Leaburg dam as expected from theory and previous studies. The “hungry water” effect predicts that sediment will coarsen below the canal tailraces. While there is a slight coarsening below the Walterville tailrace, sediment fines below the Leaburg

tailrace. It is possible that fining below the Leaburg tailrace is a result of the input of sediment from tributaries. At the Walterville canal tailrace, the coarsening effect appears to be dampened by fine sediment input from Camp Creek located below the tailrace and above the bars. A degree of decrease in mean grain size is observed on the majority of bars immediately downstream of a tributary, indicating that the main effect of tributaries in the study area on sediment in the main channel bars is fining. Thus, despite the fact that the canals return an approximately equal amount of sediment-starved flow back to the main channel, a clear coarsening effect is not observed.

The critical discharge is at or below the 2-year return frequency for 12 of the 17 bars, at or below the 5-year return frequency for four of the remaining bars. The estimated critical discharge does not occur for at bar three, which is attributed to a Leaburg Lake backwater effect. During the 1996 flood, the critical discharge was exceeded for all of the bars except bar three. Though the results show no dominant pattern of sedimentary impacts from the canal return flow, they point to the possible importance of tributary sediment contributions, particularly in segments of the river with reduced flow. Both decreased in-channel complexity and large gravel sizes suggest that the quality of anadromous fish habitat has been reduced over time on a large segment of the river.

Sediment storage behind small dams, together with assessments of the effects of canal water diversions, in-channel reductions in flow, and sedimentary inputs from the tributaries are needed to better understand the impacts of the variety of types of river regulation beyond large dams. The differences in pooled grain sizes above and below the McKenzie River dam and canals are representative of a channel response to altered sediment and water supply as characterized on the bars, but also include the influence of

the tributaries near the sampled bar. The dam and canal impacts on grain size distribution could be more broadly quantified with further studies of grain size distribution at other in-channel features (pools, riffles, etc.), within the canals and tributaries, and from the subsurface (for estimating possible armouring ratio). Quantifying the size and volume of the longitudinal and lateral sedimentary inputs would enhance understanding of the relative impacts of the dam and canals on the channel sediment. Furthermore, on a disconnected, sediment-starved river, such as the McKenzie, the importance of the tributary sedimentary inputs is increased and could play a key role in habitat development and maintenance.

One step in improving river management has been the focus on developing environmental flow regimes. Understanding past and current management effects on a river is an important part of that development (Brown and Bauer, 2010). Though it remains to be seen if the future implementation of environmental flows on the McKenzie will result in improved salmon habitat, our modeled critical discharge values suggest that flows above the 2-year return frequency can move the $D_{50}$ on the majority of the bars and flows around the 5-year return frequency can move the $D_{50}$ on all of the bars except one. These results are promising for the implementation of environmental flows on the McKenzie River, as increased discharge on the river would primarily increase flow in the "reduced water" sections of the river and mobilize the larger sediment located in those reaches. Even so, the reduction of the supply of sediment needs to be further investigated and may require other steps beyond environmental flows, such as gravel augmentation.

This study highlights the need to include knowledge of geomorphic processes in any hydrologic alteration planning. Though Poff et al. (2010) included geomorphic features in

river classification for establishing regional environmental flow standards, geomorphology has typically been left out of much of the development of environmental flow recommendations (Richter et al., 2006) and ESA Recovery Planning (NOAA, 2005). The geomorphic, hydrologic, and ecologic characteristics of a river are important in refining the limitations of management in a system to achieve desired outcomes (Null et al., 2010). Our work further highlights the importance of continued collaboration with EWEB, the USGS, and the USACE on environmental flows regulations to incorporate the geomorphic component. Salmonid fish depend on this complex combination of considerations to improve habitat on regulated rivers.

The research presented in this chapter documents the impacts of the dam and canals on the lower McKenzie River, Oregon, and discusses the importance of sediment movement for habitat and river management using environmental flows. In the next chapter, I map the distribution of small dams in Oregon and discuss the issues associated with the available data sets and in assessing the geomorphic impacts of the dams.

# CHAPTER IV

# DOCUMENTING THE DISTRIBUTION AND GEOMORPHIC EFFECTS OF SMALL DAMS (<30 FT) IN OREGON: FINDINGS AND METHODOLOGICAL LIMITATIONS

This chapter is to be submitted to *Geomorphology*. This chapter includes material that will be published as a coauthored article with W. Andrew Marcus, who provided editorial assistance.

## 1. Introduction

The period of major dam construction in the U.S. has passed. The focus of dam research has now shifted to understanding their hydrologic, geomorphic, and ecological impacts on river dynamics (Collier et al., 1996; Graf, 2006; 2005; 1999; Petts and Gurnell, 2005; Salant et al. 2006; Smith, 2002) and investigating management strategies to reduce these impacts (Bach, 2008; Gregory et al. 2007; Magilligan et al. 2007). Yet almost all the research has focused on large dams, even though there are many more low-head dams on rivers. Chin et al. (2008) identify ~97% of the dams in Texas as small or medium sized. Although they impound less total water volume than large dams, small dams fragment the river landscape, disrupting ecological and sedimentary channel connectivity (Chin et al., 2008; Csiki and Rhoads, 2008, 2010).

Connectivity, the exchange of matter, energy, and biota via fluid flow, plays a large role in creating river landscapes (Ward et al. 2002; Wipfli et al. 2007). Large dams disrupt flow and sediment transport (Graf, 2006; Ward and Stanford, 1983) which results

in a wide range of changes in the hydrologic regime and stream morphology. Over time, streams adjust to dam closure and reductions in sediment supply through a combination of bank erosion, bed erosion, substrate coarsening, and changes in channel planform (Chin et al. 2002; Wohl and Rathburn, 2003). In turn, these changes drive downstream habitat changes (Nilsson and Berggren, 2000) that can degrade ecosystem function and contribute to the decline of certain species (Hall et al. 2007).

While not of the same magnitude of large dams, small dams still have the potential to longitudinally disconnect the stream. The much larger number of small dams suggests that their cumulative impacts could be significant and, at a minimum, are deserving of more study than they have received. An understanding of the distribution and impacts of smaller dams is needed to understand their overall and cumulative effects on streams and develop potential mitigation strategies. To address this need, this study:

- Compares methods for mapping small dams in Oregon using publicly available imagery and data,
- Documents and examines reasons for variations in the geographic distribution of small dams between different ecosystems of Oregon, and
- Evaluates the potential for using optical imagery to remotely map small dam impacts on river morphology and discusses the major limitations of this approach.

2. Regional setting

This study examines small dams throughout Oregon. Several publicly available datasets for Oregon waterways document small dam locations and attributes, often to evaluate their effects on fish passage, particularly Pacific salmon. Moreover, Oregon rivers are rich in their diversity, providing a wide range of river types and settings for comparison. The range of physiography and climate in Oregon is extensive. The elevation varies from sea-level on the Coast to almost 3500 m in the Cascades (Loy et al. 2001). Climate and vegetation range from a temperate rainforest (up to 508 cm precipitation) in the Coast Range to high alpine volcanic mountains (114-356 cm precipitation) in the Cascades to high desert steppe (15-114 cm precipitation) of the Northern Basin and Range and (18-64 cm precipitation) Columbia Plateau (Thorson et al. 2003). Oregon hosts very large rivers with high winter precipitation and spring snowmelt flows West of the Cascades, as well as ephemeral rivers with flashy responses to storms and salt pans in the East (Loy et al. 2001).

To evaluate differences in small dam distributions and their potential impacts across this wide range of settings, we characterize small dam distributions at the ecoregion extent. Ecoregions classify the landscape into areas of generally similar vegetation, topography, and climate. In this study, we document dam distributions with respect to Oregon's nine Level III ecoregions (Thorson et al. 2003) which include the Coast Range, Willamette Valley, Cascades, Eastern Cascades Slopes and Foothills, Columbia Plateau, Blue Mountains, Snake River Plain, Klamath Mountains, and Northern Basin and Range (Figure 4.1).

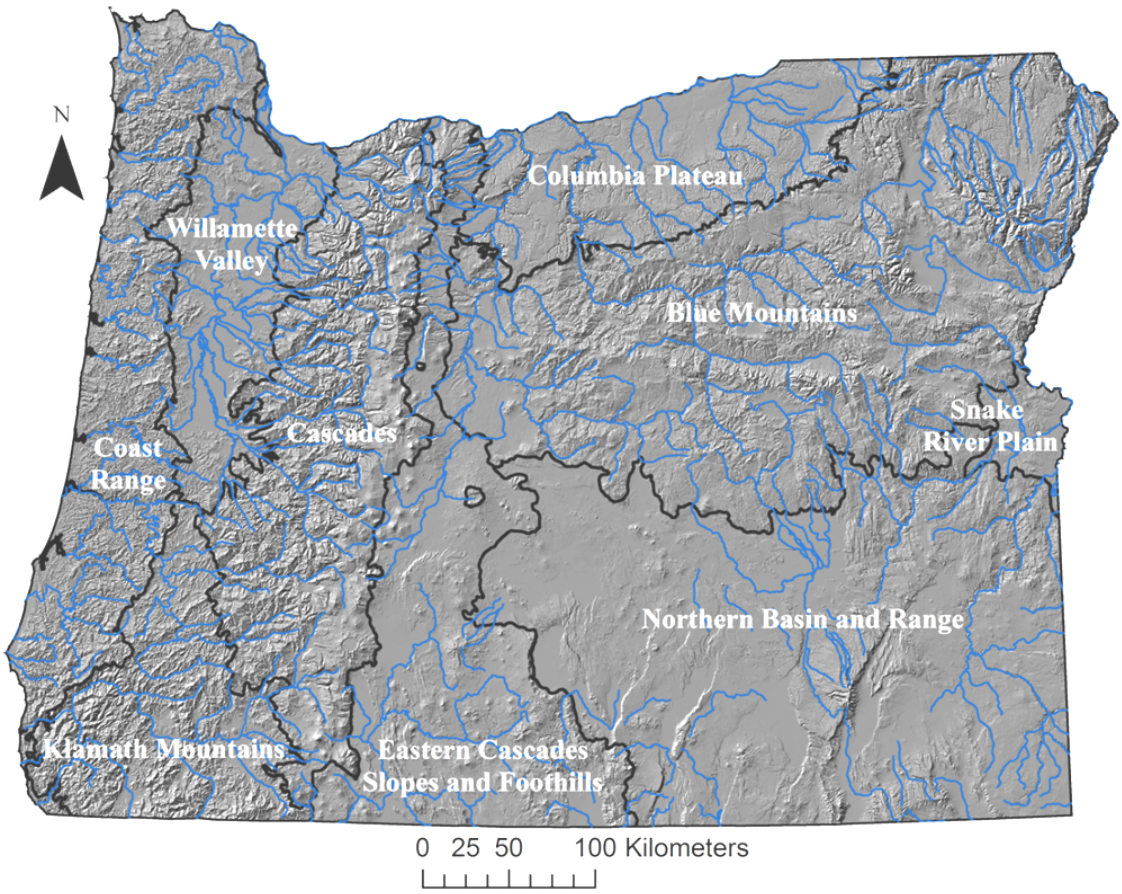


**Figure 4.1.** State of Oregon showing the nine Level III ecoregions (Thorson et al. 2003) and major stream systems.

3. Data and methods

The goals of this study are to compare data sets for mapping small dams in Oregon, use those data to document geographic variations in small dam distributions between different ecoregions, and evaluate the potential for remote mapping of dam impacts in these settings. To accomplish this, we: 1) assessed the potential to map small dam distributions and attributes using Google and Oregon Imagery Explorer (OIE) imagery, as well as on-line data sets from the Oregon Water Resources Department (OWRD) dam data and Oregon Department of Fish and Wildlife (ODFW) fish passage

barrier data, 2) mapped small dam locations and attributes throughout Oregon using the OWRD and ODFW data sets, and 3) evaluated the potential to map geomorphic impacts of small dams across a range of sites using Google or OIE imagery.

### 3.1. Imagery and data sets for mapping small dams in Oregon

We chose imagery that was widely available, free, and had spatial resolutions that potentially displayed small dams. Imagery that met these criteria included true colour, ~1 m satellite imagery on Google Earth (2010) and 0.5 m resolution true colour Oregon Imagery Explorer aerial photographs (OIE, 2005). The publically available online GIS data sets that we evaluated were the OWRD (2009) dam data set and the ODFW (2009) fish passage barrier dataset (ODFW, 2009).

Google Imagery has the advantages of being available for all parts of the world, being free to the public, and being readily available to most users with internet connectivity. To test the ability of the imagery to locate small/low-head dams we "flew" along streams in Google Earth and attempted to visually locate the small/low-head dams. We also used a .kml file developed using the OWRD data set (described below) to identify known dam locations on rivers and compare those to what could be seen visually on the computer screen.

OIE Imagery is available for all of Oregon and is freely available on-line. We did the same with the OIE Imagery streamed into ArcMap with the dam data sets added as layers to identify visible dams compared against known dam locations.

The OWRD dataset is available on-line and includes dams that are greater than or equal to 10 ft. in height and store greater than or equal to 9.2 acre-feet of water behind

them. The dataset contains 1264 dams, first located to the nearest second of latitude and longitude on USGS 1:24,000-scale quadrangle maps, and updated in 2009. The dataset attributes include: dam name, dam height, storage, river, basin, county, and township and range location down to the quarter section, latitude, longitude, and permit and inspection information.

The ODFW fish passage barrier dataset is also available on-line (ODFW, 2009). It contains data on natural and artificial barriers to fish passage in Oregon, including features such as bridges, cascades, culverts, dams, debris jams, fords, natural falls, tide gates, and weirs. The dataset contains nearly 18,000 barrier features from three primary sources: the Oregon Department of Fish and Wildlife (ODFW), the Oregon Department of Transportation (ODOT) and the US Bureau of Land Management (BLM). The fish passage barrier data were obtained from the various data originators in 2008 and 2009 and compiled to remove duplicate features. The dataset attributes include fish passage status, feature type and subtype, name, height, width, year, stream name, latitude, longitude, and owner/operator information. The dataset is still considered a work in progress, with the intent to make the database comprehensive and accurate (ODFW, 2009).

Differences in the two datasets reflect the different priorities of the agencies that contributed to the data. The focus of the OWRD dams dataset is on water resources and dams greater than or equal to 10 ft. in height. The aim of the ODFW fish passage barrier dataset is to "establish and maintain a statewide inventory of artificial obstructions in order to prioritize enforcement actions" (ODFW, 2009). The different methods of data

collection resulted in different numbers and types of dams being included, as is discussed further in the Results section.

We mapped both the OWRD and ODFW data in ArcMap 9.3 (ESRI, 2009) onto a 10 m DEM of the state with a NAD 1983 datum in the HARN Oregon Statewide Lambert projection (Gesch, 2007; Gesch et al. 2002).

### 3.2. Mapping the distribution of small dams and variations between ecoregions

We focused our study on dams less than 30 ft. in height that were located in permanent, in-channel locations, or within flow paths near unchannelized headwater areas. Although the OWRD dataset included storage as an attribute and many studies use storage to characterize the potential for dam impacts (Graf, 1999; Chin et al. 2008), the only attributes common to both datasets were height and location, which is why we classified dams by height. A 30 ft dam can be a relatively large dam in some settings, but has relatively little storage in the mountainous Coast Range and Cascade ecoregions of Oregon. We removed animal feed lot water ponds, seasonal dams, off-channel dams, waste lagoons, dairy waste ponds, effluent waste ponds, and industrial waste ponds from the OWRD data, and other types of fish passage barriers such as culverts and cascades from the ODFW data. After culling the data sets, we compared the number of dams, their locations, and their heights within each ecoregion.

To determine the total number of small in-channel, permanent dams in each Oregon ecoregion, we removed overlapping dams between the datasets by: (1) applying a 1 km buffer to minimize any projection differences between the data sets; and (2) manually checking the lists for dams with the same names or locations. This was done by

running down the two lists alphabetically to match dams by name and then spatially confirming any remaining dams with different names in the data sets. The manual check was needed because of frequent variations in dam name and slight differences in spatial location. Variations in dam name included differences in; (1) the order of proper names (e.g. Ben Odell dam vs. Odell, Ben dam), (2) descriptors (e.g. Clear Creek Res.-West Fork vs. W. Fk. Clear Creek Res. Dam, or Bates Pond Dam vs. Bates Reservoir), or (3) the use of historical names in one data set (e.g. previous owner or a pioneer era description) and a modern name in the other. Dams with the same or similar names but slight differences (within 1 km) in location were checked in ArcMap to confirm that they were the same dam. This created an "overlap" data set of dams that are found in both data sets.

We stratified the data by level III ecoregions to determine if there are patterns in small dam distributions related to landscape-scale variations. Ecoregions are areas of with broadly similar environments as defined through an analysis of biotic and abiotic variables (Omernik, 1995; Bailey, 1995; Omernik and Bailey, 1997; Thorson et al. 2003). There are nine level III ecoregions in Oregon (Figure 4.1).

Next, to assess the relation between small dam distributions and ecoregion, we documented the number, size and basin areas of dams within each ecoregion. To classify the dams by size we stratified the dams into 2.5 ft increments up to 29.5 ft, with one final group of dams 30 ft. in height. We did this for each data set and for the overlap set, which was based on the ODFW data because sometimes the data sets showed different dam heights for the same dam. Next, we divided ecoregion area by number of dams in the

ecoregion (based on the total from each data set less the overlap value so as not to double count dams in both data sets) to calculate the dam density in each ecoregion.

We determined the drainage area above each of the over 1000 dams using the ArcHydro extension (Maidment, 2009) in ArcGIS (ESRI, 2009). In order to do this, we first resampled the original DEM from 10 m to 30 m to reduce the processing time. Next, we added the river and streams layer from the Oregon Geospatial Data Library (ODFW, 1997) and dams from the two dam data sets. We reconditioned the DEM (stream buffer: 5 m, drop in z units: 10 m) by "burning" the streams into the DEM (lowering the DEM elevation on cells spatially contiguous with the stream layer) to marry the imagery and the data, filled topographic sinks (often relics of DEM creation) in preparation for the hydrographic analyses of flow direction and flow accumulation. We snapped dam locations to the cells of greater flow accumulation (snap distance: 30 m) for both dam data sets to reduce errors from any slight offset of the dams and streams. We extracted the flow accumulation values at that point (dam). After adding one cell count for the point the dam occupies to the total to get the complete sum of cells contributing flow to each dam and multiplying that by the pixel area, we joined the resultant drainage area value to the original FID number to attach the drainage basin area value to the dam.

### 3.3. Geomorphic analysis

The initial assessment of Google imagery (discussed further in the Results section) indicated that the satellite imagery was too coarse to detect small dams or adequately see variations in the small streams where many small dams are located. We therefore turned to Oregon Imagery Explorer (OIE, 2005) 0.5 m, colour aerial imagery

that is available free on-line. We were able to stream the imagery in ArcMap 9.3 (ESRI, 2009), then overlay the small dam datasets on the imagery to select dams for analysis.

We initially focused on small dams in the Willamette Valley ecoregion which contained the most dams of all the ecoregions. Our goal was to document differences in geomorphic variables that could be remotely measured above and below the dams to evaluate dam impacts. We selected geomorphic variables that could be readily measured by remote means and that are widely used in geomorphic analysis. These variable included: channel planform, width, sinuosity, functional surfaces (e.g. active or vegetated bars), standard active area, and geomorphic complexity (Graf, 2001; 2006), as well as depth in clear water streams (Fonstad and Marcus, 2005) and the amount of large wood. The plan was to extend this analysis longitudinally 1 km up and down stream of the dam. As is presented later in the Results and the Discussion sections, a series of issues prevented accurate and consistent remote measurement of these variables in small dam settings.

## 4. Results

### 4.1. Comparison of data sets and methods for mapping small dams

The process of "flying" along watercourses to visually location small dams generally failed, with only the only the well-known, larger dams showing up on the imagery. The use of the .kml file built using locations of small dams listed in the OWRD data allowed us to zoom in to known dam locations. This process further confirmed that visual inspection using Google imagery missed the large majority of small dams listed in the OWRD data set because of the low resolution of the imagery (Figure 4.2a) and

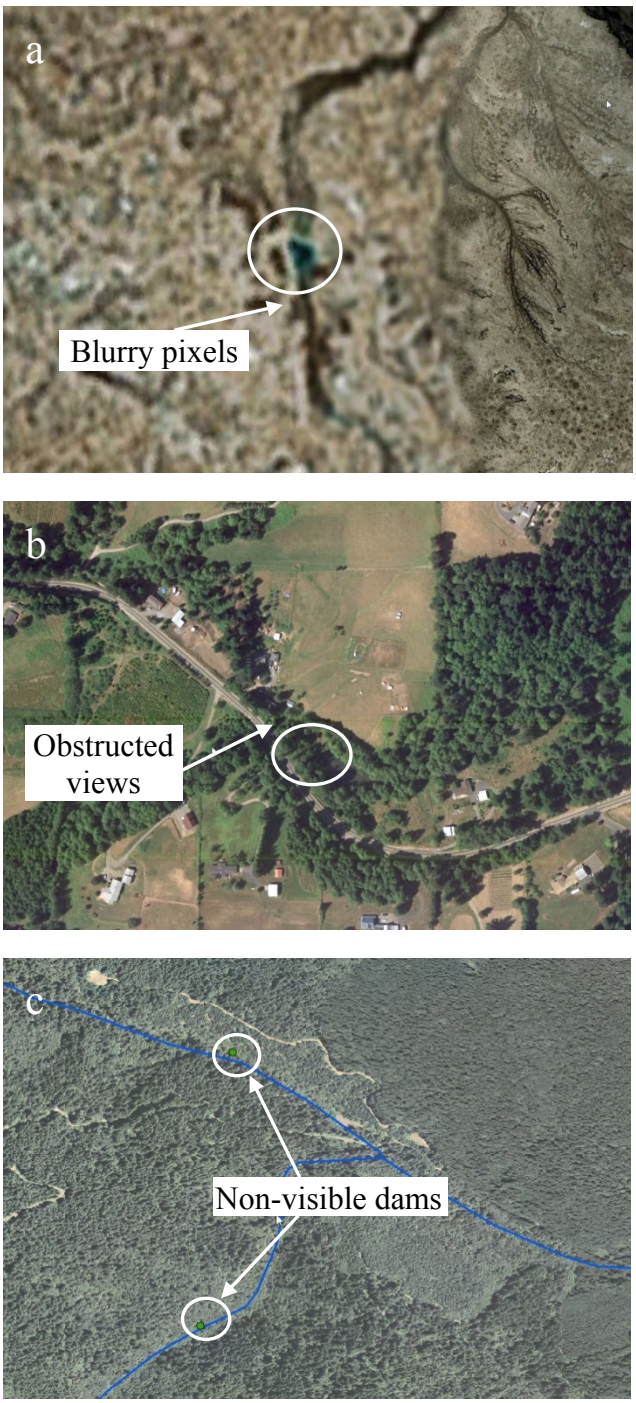


**Figure 4.2.** Google Earth and OIE aerial imagery depicting the difficulties in mapping small dams, which are often not visible. In Google Earth this occurred either due to areas of low resolution imagery (a) or obstructions to the dam or channel (b). In the OIE imagery known dams were frequently not visible, either from partial or completely blocked views of the river containing the dam in densely forested areas such as this one in the Willamette Valley ecoregion (c) (dam locations are circled).

obstructed views of the dam or channel (Figure 4.2b). We attempted the process with the OIE imagery, but it also failed to provide consistent results that could be used for a systematic inventory. In some cases the dams were visible on OIE imagery and in others they were not (Figure 4.2c). This was not a simple function of dam size (i.e., that larger dams were more visible), but also depended on the look angle of the aircraft, vegetation, shadow, and image quality. In addition, the nature of the dams made them hard to detect in many cases, as small dams were often submerged (e.g. flow diversion dams), very narrow in width, and/or were constructed with stream bed material that did not show up well in the imagery. We therefore turned to the existing on-line GIS data sets to document small dam locations throughout Oregon.

The OWRD dam dataset identifies 798 permanent dams that are 30 ft in height or less, while the ODFW fish passage barrier dataset lists 832 such dams (Table 4.1, Figure 4.3). Three hundred eighteen of the dams are in both data sets, leading to 1,312 total dams. There are no dams listed under 10 ft. in height in the OWRD data even though some of the overlap dams are listed as less than 10 ft. in the ODFW data, with some having height values of zero. Differences in dam heights for the same dam are greatest in dams under 10 ft., though disparities exist across the range of heights from 0-30 ft. (Figure 4.4). The data sets not only contain discrepancies in dam heights, but they are also difficult to compare and impossible to join without extensive manual editing due to differences in the names used for identifying the dams (Table 4.2). This speaks to the accuracy of data sets and the need for improvement in the dam attribute data.

**Table 4.1.** Number of dams in different size classes in the OWRD and ODFW data sets. The OWRD and ODFW data rows list the number of dams found solely in each data set. The overlap row enumerates the locations where a dam is listed in both data sets. The dam sizes in the overlap category were determined using the ODFW data in situations where the data sets showed different dam heights for the same dam.

| | | **Height range (ft)** | | | | | | | | | | | | | |
|---|---|---|---|---|---|---|---|---|---|---|---|---|---|---|---|
| | | 0 - 2.4 | 2.5- 4.9 | 5.0- 7.4 | 7.5- 9.9 | 10.0- 12.4 | 12.5- 14.9 | 15.0- 17.4 | 17.5- 19.9 | 20.0- 22.4 | 22.5- 24.9 | 25.0- 27.4 | 27.5- 29.9 | 30 | Total |
| **Number of dams** | OWRD data | 0 | 0 | 0 | 0 | 157 | 84 | 145 | 67 | 134 | 52 | 98 | 36 | 25 | 798 |
| | ODFW data | 213 | 81 | 87 | 48 | 75 | 32 | 52 | 30 | 65 | 39 | 61 | 27 | 22 | 832 |
| | Overlap | 11 | 1 | 2 | 3 | 35 | 24 | 41 | 22 | 50 | 32 | 54 | 25 | 18 | 318 |
| | Total | 202 | 80 | 85 | 45 | 197 | 92 | 156 | 75 | 149 | 59 | 105 | 38 | 29 | 1312 |

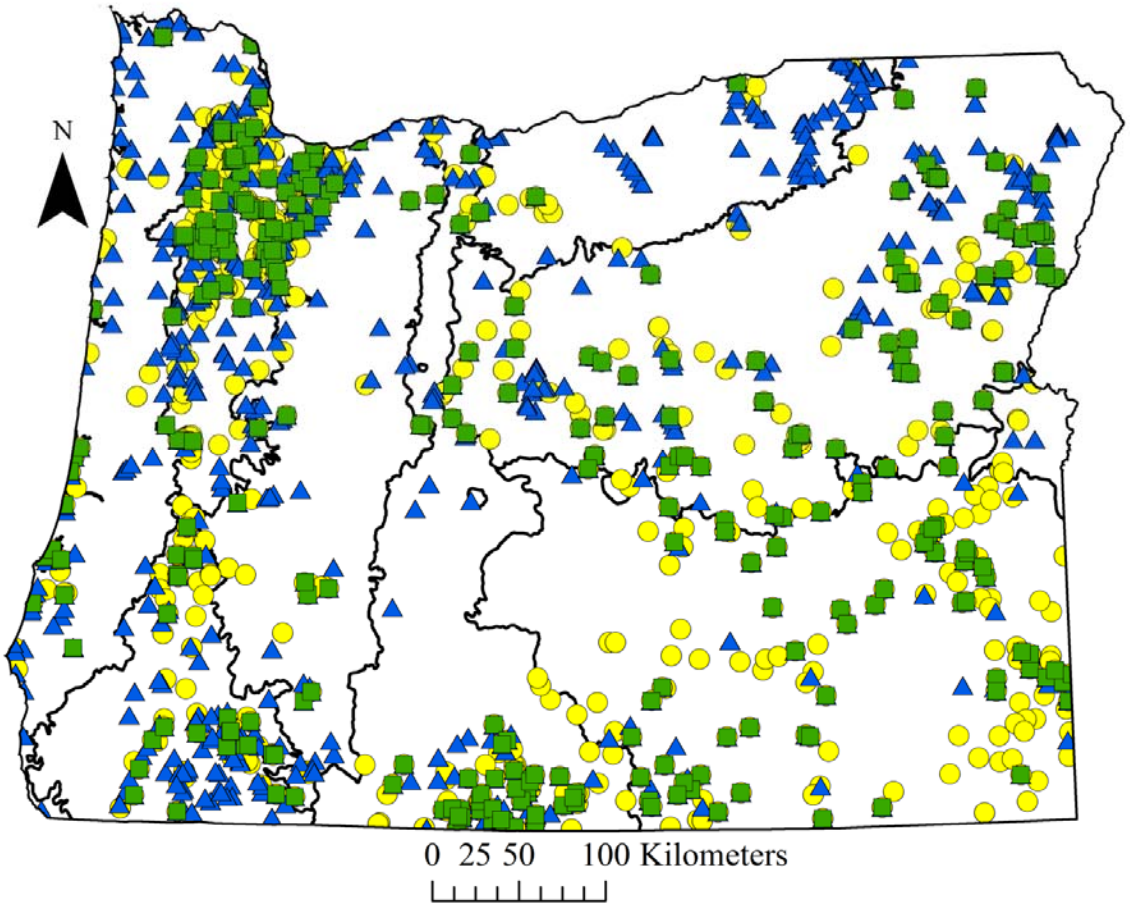


**Figure 4.3.** The distribution of permanent dams 30 ft. or less in height in Oregon. The locations of dams found only in the ODFW fish passage barrier data (832) are shown in blue. Dam locations listed only in the OWRD dam data (798) are shown in yellow. Areas of overlap where each data set contains the same dams (318) are shown in green (c).

A large number of dams, across all size categories, are only listed in one data set but not the other (Table 4.1). There are many more smaller dams in the ODFW data set (464 dams 10 ft. in height and under) than in the OWRD data set (71 dams 10 ft. in height) (Figure 4.5). There are more dams in the OWRD data set in the >10-20 ft. and >20-30 ft. ranges (440 and 287, respectively) than in the ODFW data set in those ranges

(183 and 185, respectively). Overall, the majority of dams (~76%) are only captured in one data set (Table 4.1).

**Table 4.2.** Example of differences in naming convention and dam heights (ft.) in the overlapping dams in the OWRD fish passage barrier (left) and ODFW dam (right) data sets.

| **ODFW fish passage barrier name** | **ODFW dam height** | **OWRD dam name** | **OWRD dam height** |
|---|---|---|---|
| Abbeloos Reservoir Dam | 17 | Abbeloos Res | 17 |
| Albertsons Reservoir Dam | 30 | Albertson Reservoir (Lake) | 28 |
| Altnow Reservoir Dam | 23 | Altnow Res. | 20 |
| Anderson - Roy Reservoir Dam (Dobbes Lake Dam) | 26 | Anderson - Roy Res. | 25 |
| Antelope Reservoir (Klamath) Dam | 18 | Antelope Dam | 16 |
| Arkansas Dam | 18 | Arkansas Dam | 16 |
| Arntz Dam | 22 | Arntz Dam | 20 |
| Arritola Reservoir Dam | 18 | Arritola Res | 18 |
| Art McKay Dam | 17 | McKay Acres Dam | 15 |
| Badger Lake Dam | 23 | Badger Lake (Hood River) | 22 |
| Bailey Reservoir Dam | 12 | Jenkins | 12 |
| Barry, Nick Reservoir Dam | 29 | Barry , Nick Res | 27 |
| Bates Pond Dam | 26 | Bates Res | 26 |
| Becker Reservoir Dam | 10 | Becker | 10 |
| Beede North Dam | 12 | Beede North | 12 |
| Beede South Dam | 22 | Beede South | 22 |
| Beer's Reservoir Dam | 14 | Beer s Res. | 11 |
| Belchers Dam | 28 | Peyralans Res. | 23 |
| Ben Odell Dam | 16 | Odell, Ben | 14 |
| Bend Pacific Power Dam | 14 | Bend Hydro (MirrorPond) | 16 |

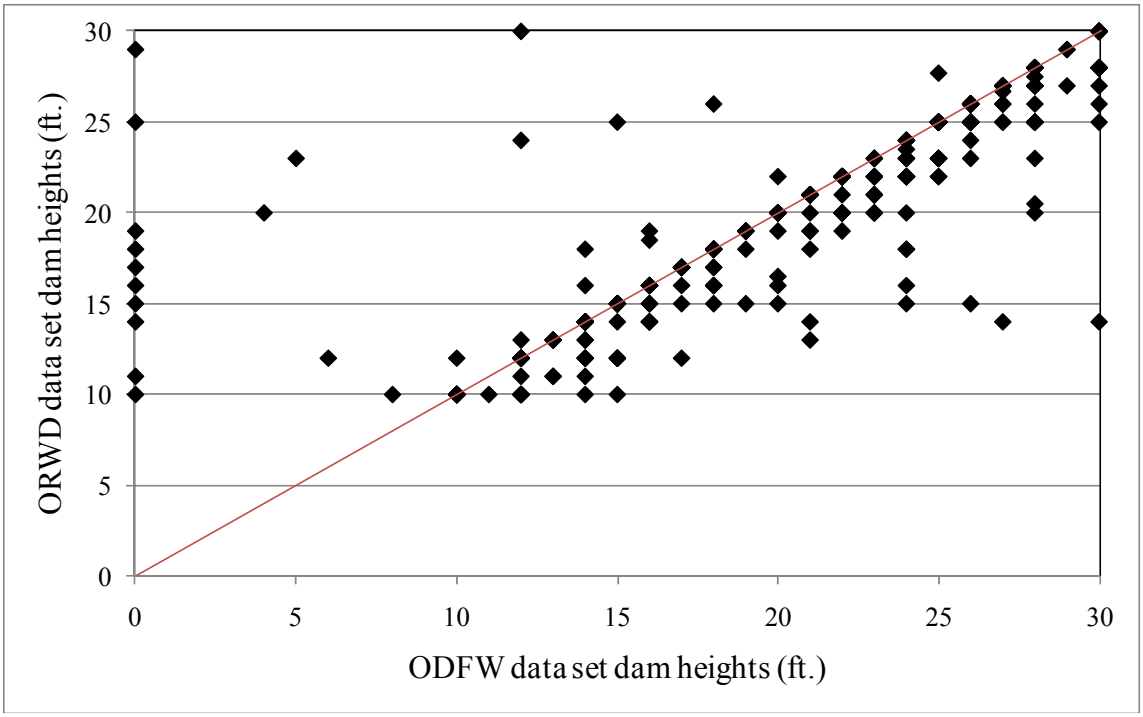


**Figure 4.4.** Differences in dam heights between the overlapping dams in each data set. The line of one to one correspondence is drawn in red.

4.2. Distribution of small dams

The greatest number of dams in both datasets is located in the Willamette Valley ecoregion (Table 4.3). The Willamette valley also has the greatest density of small dams per square kilometer by an order of magnitude, followed by the Klamath Mountains. The overall dam density for the whole state is the same for both data sets (0.003), although densities between the two data sets vary by a factor of two to three for most ecoregions and by a factor of four for the Columbia Plateau (Table 4.3).

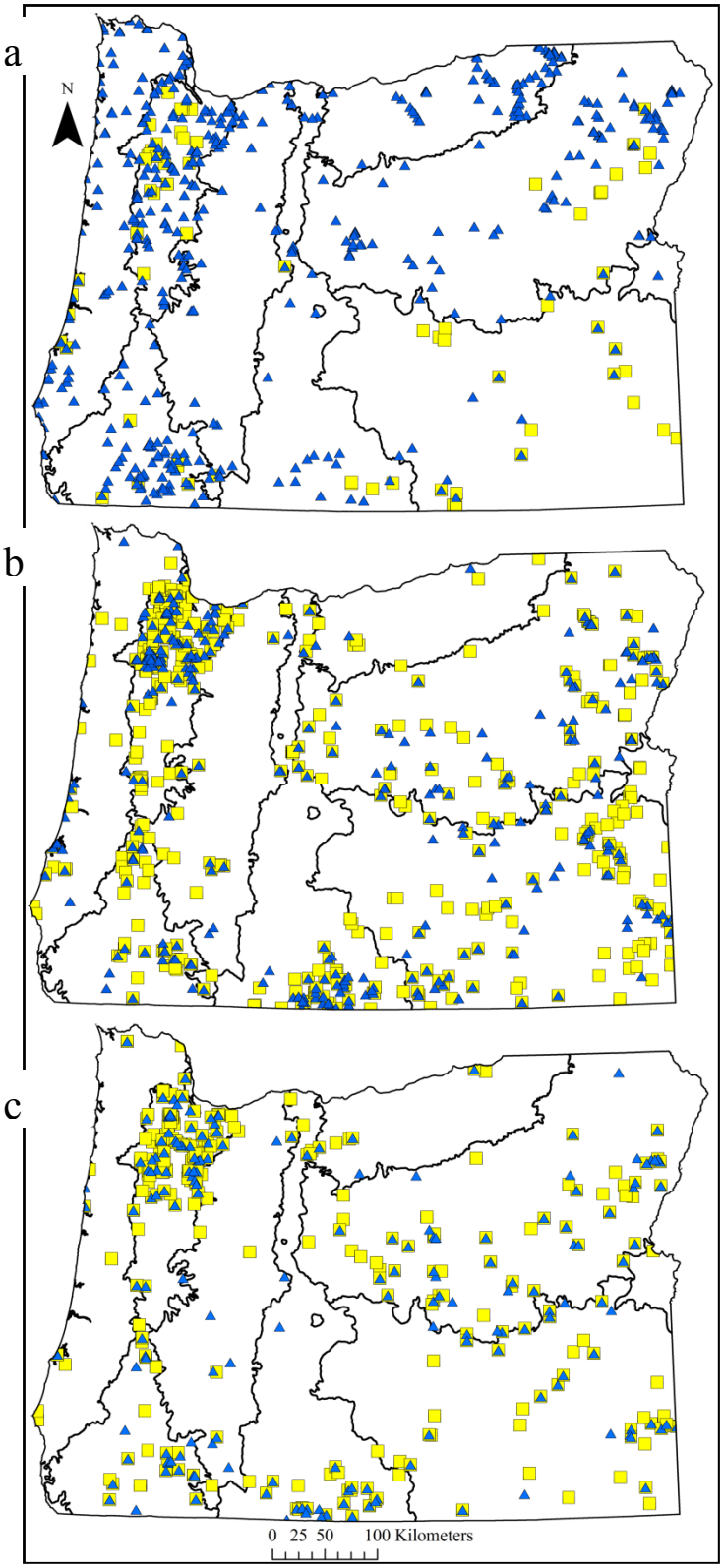


**Figure 4.5.** Differences in ODFW fish passage barrier data (blue) and OWRD dam data (yellow) by size groups of 0-10 ft. (a), >10-20 ft. (b), and >20-30 ft. (c).

**Table 4.3.** Distribution of dams and dam density in each ecoregion in OWRD fish passage barrier (left) and ODFW dam (right) data sets.

| Ecoregion | Area ($km^2$) | OWRD | | ODFW | |
|---|---|---|---|---|---|
| | | Number | Dams/$km^2$ | Number | Dams/$km^2$ |
| Blue Mountains | 61,958 | 139 | 0.002 | 169 | 0.003 |
| Cascades | 29,016 | 30 | 0.001 | 57 | 0.002 |
| Coast Range | 23,481 | 33 | 0.001 | 92 | 0.004 |
| Columbia Plateau | 17,589 | 17 | 0.001 | 73 | 0.004 |
| Eastern Cascades | 27,418 | 72 | 0.003 | 70 | 0.003 |
| Klamath Mountains | 15,664 | 67 | 0.004 | 97 | 0.006 |
| Northern Basin & Range | 59,642 | 143 | 0.002 | 85 | 0.001 |
| Snake River Plain | 2,559 | 6 | 0.002 | 4 | 0.002 |
| Willamette Valley | 13,802 | 291 | 0.021 | 185 | 0.013 |
| Total | 251,128 | 798 | 0.003 | 832 | 0.003 |

The 1,312 total dams from both data sets vary in both dam height and contributing drainage area between ecoregions. The Columbia Plateau and Coast Range ecoregions have the smallest median dam heights (~4 ft. and ~7 ft., respectively), while the median small dam height in other regions is ~15 ft (Figure 4.6, Table 4.4). Every ecoregion contains at least one dam with a recorded height of zero and all of the ecoregions, except for the Snake River Plain (maximum height = 25ft.), contain at least one dam with a height of 30 ft. The mean dam height of small Oregon dams from both data sets is 15 ft.

The Columbia Plateau has the largest median contributing drainage area by an order of magnitude (222 $km^2$), followed by the Cascades (14 $km^2$), with the median areas for the other ecoregions varying between 2 and 9 $km^2$ (Figure 4.7, Table 4.5). The Coast

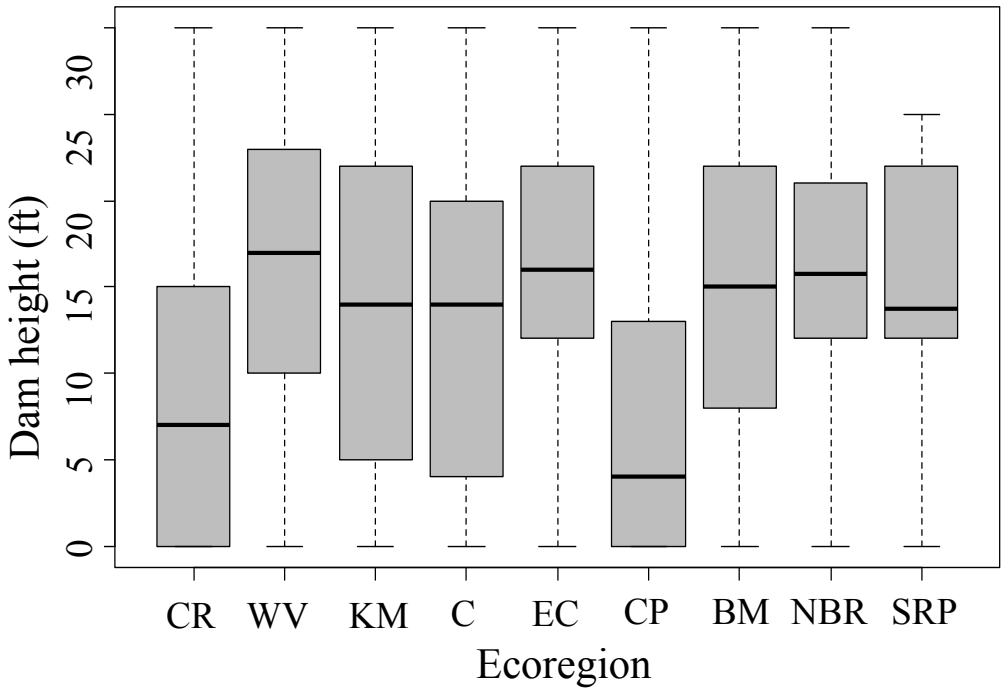


**Figure 4.6.** Range of dam heights for all dams of 30 ft or less in height in the nine Oregon ecoregions using all 1,312 dams. Ecoregions are abbreviated as: CR=Coast Range, WV=Willamette Valley, KM= Klamath Mountains, C=Cascades, EC=Eastern Cascades Slopes and Foothills, CP=Columbia Plateau, BM=Blue Mountains, NBR=Northern Basin and Range, and SRP=Snake River Plain. See Table 4 for quartile values.

Range, Willamette Valley, Klamath Mountains, and Snake River Plain ecoregions have the lowest median drainage area (Figure 4.7b), although basin areas above dams span a large range of values for in all of the ecoregions, excepting the Coast Range and the very small Snake River Plain (Figure 4.7a). The total percentage of catchment area above one or more small dams in each ecoregion ranges from 15% in the Coast

**Table 4.4.** Percentiles of dam heights (ft.) in each ecoregion for small dams of 30 ft. or less in height. The percentiles are broken down into the minimum, 25th percentile, median, 75th percentile, and maximum values of dam heights in each ecoregion and in Oregon as a whole. Every ecoregion contains at least one dam with a recorded height of zero and all of the ecoregions, except for the Snake River Plain, contain at least one dam with a height of 30 ft. The mean dam height of small Oregon dams is 15 ft.

| Ecoregion | Min | 25th | 50th | 75th | Max |
|---|---|---|---|---|---|
| Blue Mountains | 0 | 8 | 15 | 22 | 30 |
| Cascades | 0 | 4 | 14 | 20 | 30 |
| Coast Range | 0 | 0 | 7 | 15 | 30 |
| Columbia Plateau | 0 | 0 | 4 | 13 | 30 |
| Eastern Cascades | 0 | 12 | 16 | 22 | 30 |
| Klamath Mountains | 0 | 5 | 14 | 22 | 30 |
| Northern Basin & Range | 0 | 12 | 16 | 21 | 30 |
| Snake River Plain | 0 | 12 | 14 | 21 | 25 |
| Willamette Valley | 0 | 10 | 17 | 23 | 30 |
| Oregon | 0 | 8 | 15 | 22 | 30 |

Ranges to 89% in the Cascades (Table 4.6). Sixty one percent of all drainage area in Oregon is above at least one small dam (Table 4.6).

Small dams tend to be located in areas where changes in slope occur, particularly at the edges of elevation changes, or foothills (Figure 4.8). Many of the small dams outline the edges of the valleys, such as those in the Willamette Valley (Willamette Valley ecoregion) and Applegate Valley (Klamath Mountain ecoregion) (Figure 4.9a-4.9b). Many also outline the base of ridges, such as the ridges jutting out into the Deschutes river valley (western Blue Mountains ecoregion) (Figure 4.9c). Exceptions to this pattern occur in areas of high density population, such as the greater Portland metropolitan area, and in very large valleys, such as the Harney Basin.

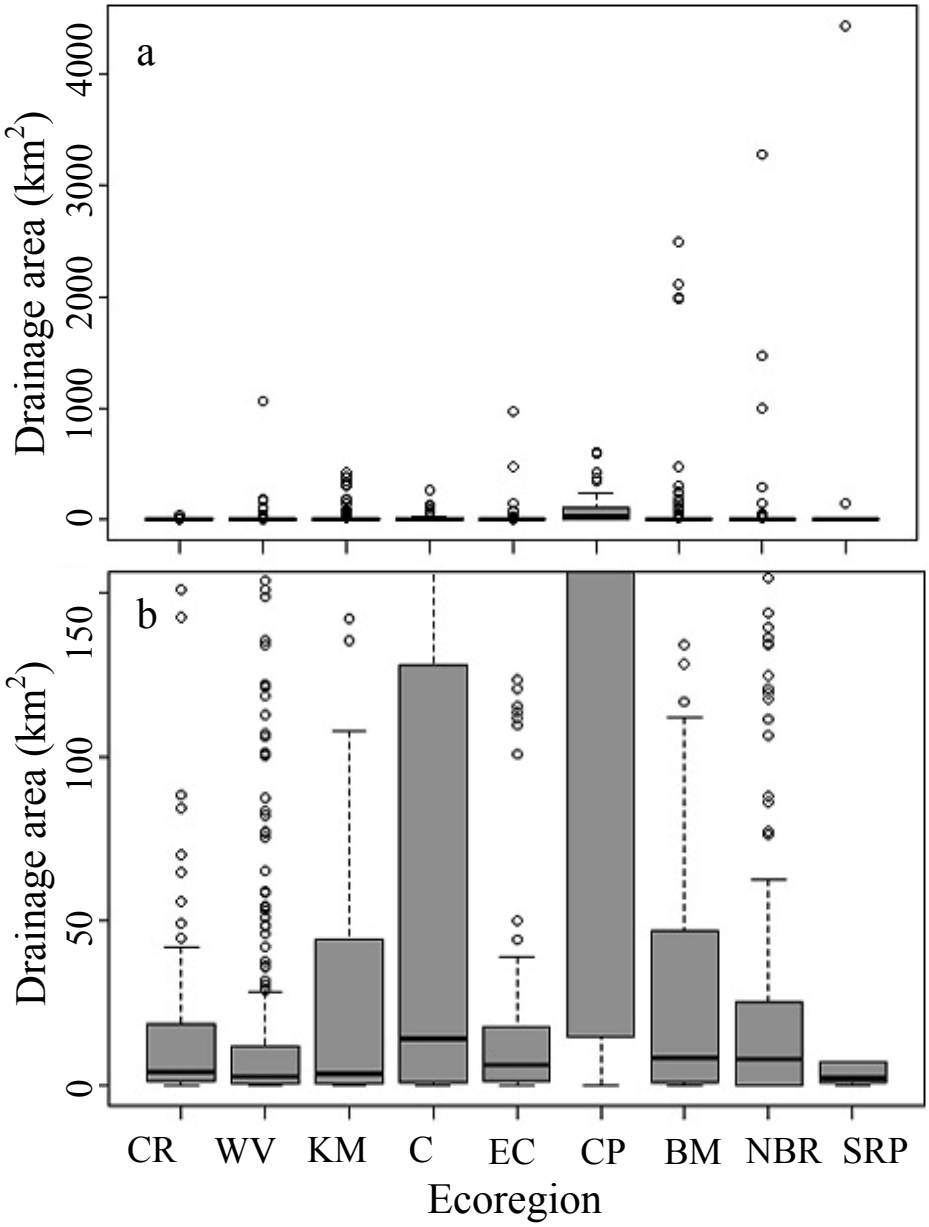


**Figure 4.7.** Drainage area of dams in each ecoregion shown with the full-range (a) and scaled to show only the 0-150 km$^2$ range in order to better visualize variations between ecoregions outside the Columbia Plateau (b). Ecoregions are abbreviated as in Figure 4.4. See Table 4.5 for quartile values.

**Table 4.5.** Percentiles of contributing drainage area ($km^2$) of the dams in each ecoregion for dams of 30 ft. or less in height. The percentiles are broken down into the minimum, 25th percentile, median, 75th percentile, and maximum values of drainage areas in each ecoregion and in Oregon as a whole. The mean drainage area of Oregon dams is 333 $km^2$.

| Ecoregion | Min | 25th | 50th | 75th | Max |
|---|---|---|---|---|---|
| Blue Mountains | 0.002 | 1.00 | 8.60 | 47.03 | 24,870 |
| Cascades | 0.004 | 1.04 | 14.2 | 126.60 | 2,683 |
| Coast Range | 0.010 | 1.25 | 3.99 | 17.69 | 459 |
| Columbia Plateau | 0.008 | 16.40 | 222.3 | 1118.80 | 6,003 |
| Eastern Cascades | 0.004 | 1.33 | 6.27 | 17.54 | 9,761 |
| Klamath Mountains | 0.004 | 0.59 | 3.64 | 43.63 | 4,225 |
| Northern Basin & Range | 0.002 | 0.16 | 7.99 | 25.27 | 32,800 |
| Snake River Plain | 0.014 | 1.02 | 2.09 | 6.11 | 44,380 |
| Willamette Valley | 0.001 | 0.63 | 2.73 | 11.86 | 10,654 |
| Oregon | 0.002 | 0.77 | 5.15 | 33.11 | 44380 |

**Table 4.6.** Total catchment area and percentage of catchment area above one or more small dams in each ecoregion.

| Ecoregion | Total Area ($km^2$) | Total Catchment Area ($km^2$) | Total Catchment Area above one or more small dams (%) |
|---|---|---|---|
| Blue Mountains | 62,119 | 30,763 | 49.5 |
| Cascades | 29,011 | 25,887 | 89.2 |
| Coast Range | 23,296 | 3,446 | 14.8 |
| Columbia Plateau | 17,351 | 8,580 | 49.4 |
| Eastern Cascades | 27,335 | 20,042 | 73.3 |
| Klamath Mountains | 15,645 | 8,074 | 51.6 |
| Northern Basin & Range | 57,510 | 45,345 | 78.8 |
| Snake River Plain | 2,547 | 1,313 | 51.6 |
| Willamette Valley | 13,746 | 8,148 | 59.3 |
| Oregon | 250,854 | 153,362 | 61.1 |

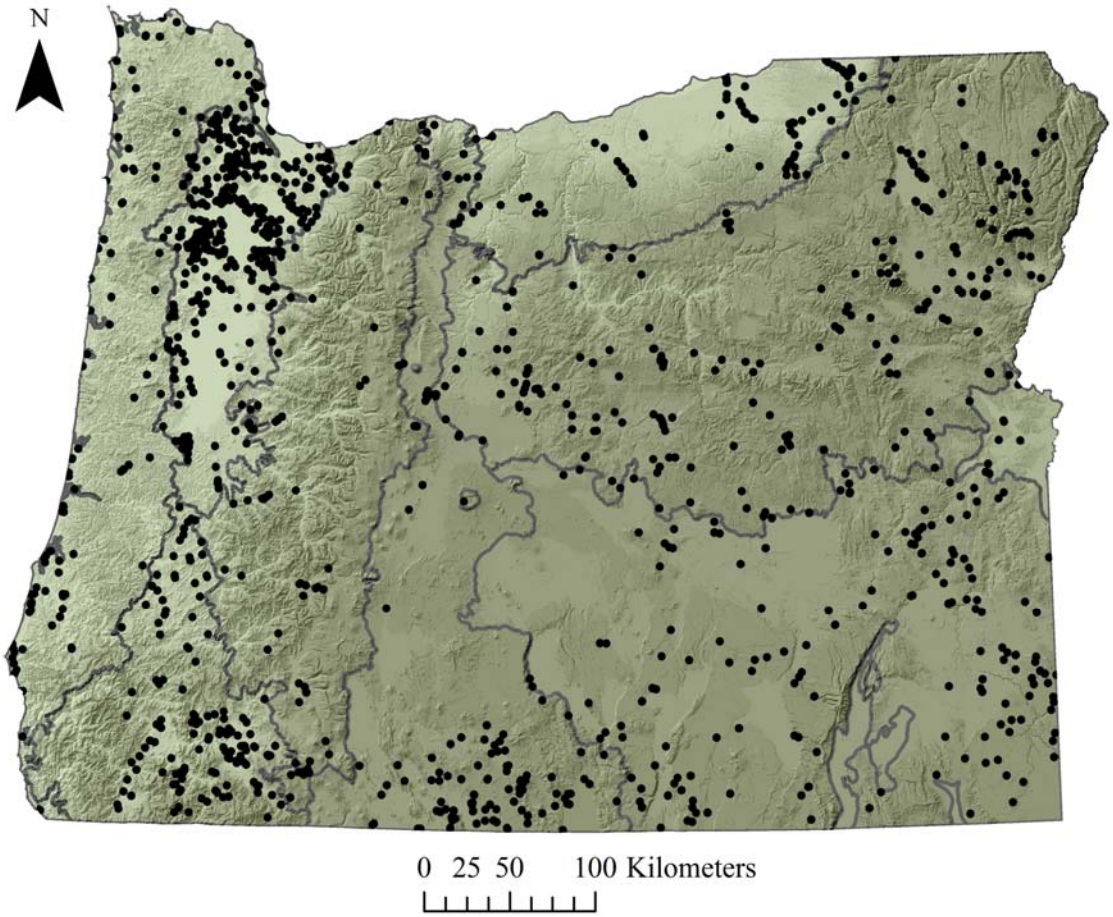


**Figure 4.8.** Pattern of the locations of small dams across the Oregon topography. Small dams are predominantly found in the lower elevations and tend to follow along foothills at the edges of the valleys.

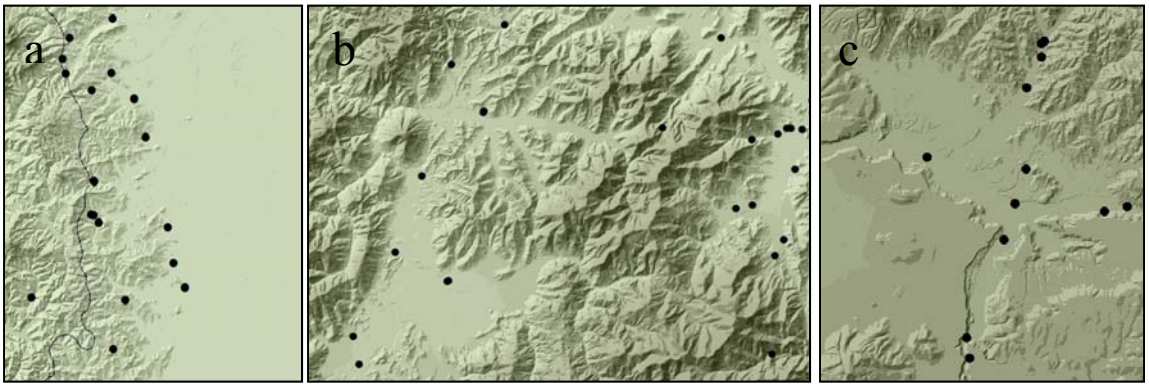


**Figure 4.9.** Images depicting the pattern of dam distribution at the edges of valleys and changes in slope at the foothills of mountains in the Willamette Valley (a), Applegate Valley (b), and eastern edge of the Deschutes River Valley (c).

4.3. Geomorphic impacts

Geomorphic impact analysis using Google Earth or OIE 0.5 m imagery was not possible due to the image resolution and the characteristics of streams where small dams are located. Google Earth is not currently available in sufficiently high resolution across Oregon to consistently see small dams (Figure 4.2a), much less take measurements from the imagery. Moreover, the small size of most streams meant that vegetation and shadow often obstructed the view of the majority of steam channel (Figure 4.2b). Furthermore, the actual image data (pixel values, etc.) are not extractable for further imagery analysis such as depth modeling (Fonstad and Marcus, 2005; Walther et al. in press).

Compared to the Google imagery, the 0.5 m OIE imagery made it possible to see more small dams (although not all, Figure 4.2c) and see greater portions of the streams at a resolution that potentially enabled morphological measurements. However, the location of small dams on small streams with narrow widths meant that riparian vegetation growing on the banks and associated shadows usually obscured the river (Figure 4.10). This made it impossible to see much of the river, much less remotely measure and quantify width, sinuosity, functional surfaces, active area, and geomorphic complexity above and below small dams. These obstructions were present, regardless of whether streams were in the semiarid landscapes of the Eastern Cascades (Figure 4.10a) or the cleared fields of the Willamette Valley (Figure 4.10b). Vegetation growing on the banks of a river is typically as large as or larger than vegetation outside of the riparian zone. In accordance with the river continuum concept, the riparian vegetation of small rivers is proportionately larger relative to stream width than that of large streams (Vannote et

al.,1980). Even when streams were not obstructed by overhanging vegetation, dense shadow would often obscure views of the river.

## 5. Summary and discussion

### 5.1. Imagery and data sets

Spatial resolution, image quality, overhanging vegetation, shadows, and look angle all place severe limitations on the use of aerial or satellite imagery to inventory small dams (Figures 4.2 and 4.10). Small dams only exacerbate this problem because of their size, their potential to be submerged, and their construction from local materials. Consideration of the time of acquisition to reduce shadows and the angle of incidence to reduce obstructions on the river edges would improve the imagery potential for use in small dam analysis.

Existing on-line data sets are also problematic. There is wide variation in the number and type of attributes within and between the ODFW and OWRD data sets. Since the data are collated from several sources, attribute values for particular fields are not always consistent even within the same data set. Analysis by attribute for all of the dams is not possible because of the discrepancies in how the attribute data are recorded and reported (Table 4.2). The lack of a consistent, comprehensive data set indicates that one cannot currently use publicly available data to inventory and analyze small dams.


**Figure 4.10.** Difficulties in evaluating small dam impacts on stream morphology. In the 0.5 m resolution OIE images, riparian vegetation partially blocks views of the river even in more sparsely vegetated ecoregions like the Eastern Cascades ecoregion (a). In agricultural regions, forest stream buffers can obscure the majority of channel, as in this example from the Willamette Valley (b). Small dam locations are circled.

The problem of different data sources is compounded when using both dam data sets. For example, it is unclear how the OWRD can show dams at locations where the ODFW data sets indicates dams <10 ft. in height (Table 4.1), since the OWRD data expressly focuses on dams greater than 10 ft. in height. Perhaps the smaller dams were lumped into the data set depending on the data available at the time. The absence of data on the impounded water volume in the ODFW data set is understandable as it is less pertinent to fish passage than dam height, but could be an important component in assessing impacts on downstream fish habitat. A more comprehensive data set, considering the multi-disciplinary needs of researchers, scientists, managers, and policy-makers that study and influence rivers, water resources, and aquatic species, is needed for greater ease in discourse and collaboration between them.

## 5.2. Distribution of small dams

In Oregon, the density of small dams is greatest in the areas with the greatest population densities. This is evidenced by the highest small dam densities in the Willamette Valley and Klamath Mountains ecoregions, which contain the Interstate Highway 5 corridor and the top twenty most-populated cities in Oregon and the highest growing populations (Loy et al. 2001). Furthermore, both regions have large areas of land in agricultural use for grass, orchards vegetables and vineyards and, east of the Cascades, grazing (Loy et al. 2001).

The Coast Range and Columbia Plateau ecoregions have the lowest median dam height values (Figure 4.6), possibly because the dams are located at the edges of the plateau and mountains or are one of many dams along the same river (Figure 4.11). The

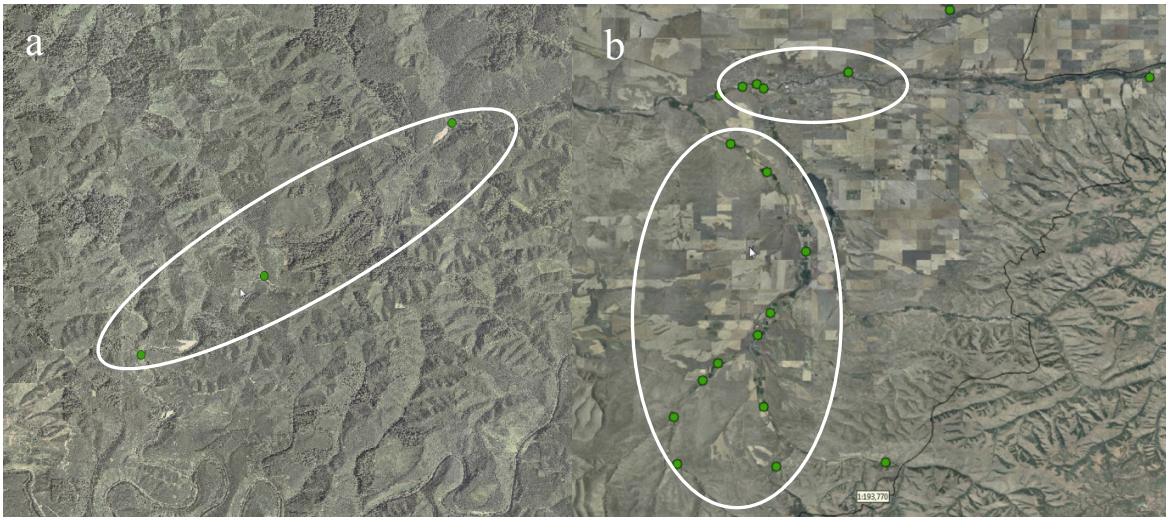


**Figure 4.11.** Lowest dam heights found in steep mountains or in sequence on the same river in the Coast Range (a) and Columbia Plateau (b). Dams are denoted in green and circle for visibility in (a) and for sequential location in (b).

reasons for this cannot be determined from the data sets, however, because although the ODFW data set includes an ownership attribute (private, federal, public utility, or blank if unknown), neither data set includes dam purpose as an attribute.

Dams in the Columbia Plateau have the highest median contributing drainage area per dam (Figure 4.7), probably because of the dry climate that provides little runoff per unit area. All of the ecoregions have a wide range of contributing areas, reflecting the geographic diversity in each ecoregion despite the combined similar characteristics on which the categorization is based.

Despite the wide range of physiographic characteristics and large number of dams, a pattern of similarity in the overall locations of the dams across the state seems to emerge from the distribution of small dams across Oregon. Illustrated in Figure 4.8, the clustering of dams at the foothills of mountains and in more densely populated areas

becomes apparent. This suggests, conceptually, that a model of the relationship of dam density to large changes in slope and population density could reflect this overall pattern (Figure 4.12). Dam density is greatest at foothills, where the change in slope is greatest, in more densely populated areas, and is least dense in mountains and valley centers, where smaller changes in slope occur, in less populated areas. This trend is observed, with some exceptions noted in Figure 4.8--where there are very wide valleys and, rarely, in mountains, throughout the state.

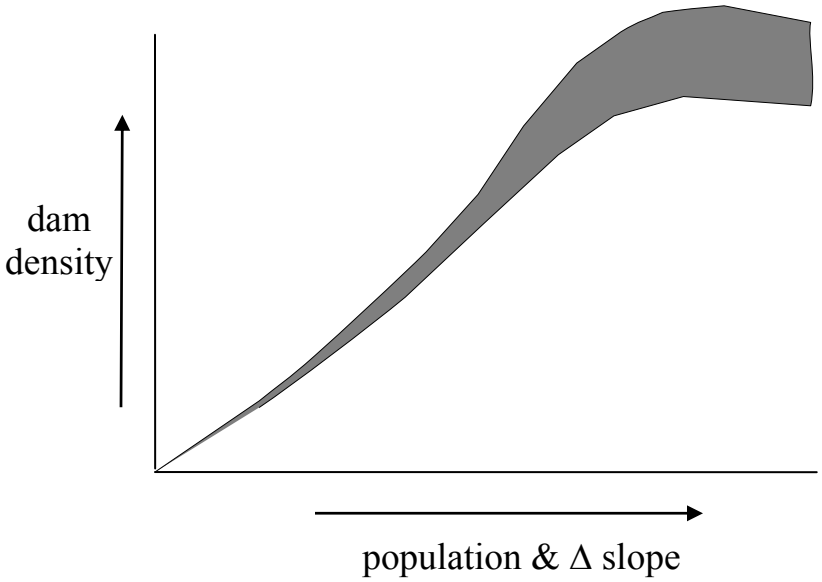


**Figure 4.12.** Conceptual model of the relationship of dam density to population density and change in slope. Dam density is skewed towards higher populations and greater changes in slope, to a degree. Dam density is greatest at foothills in more densely populated areas. Dams are found less frequently in areas of relatively equal slope such as mountains and valleys, or in areas of low population densities without a marked change in slope.

### 5.3. The problem of remote assessment of geomorphic impacts of small dams

The assessment of the geomorphic impacts of small dams using remotely sensed imagery is both a function of the nature of small dams and of imagery acquisition. Small dams tend to be located on small rivers, which are more difficult to see due to proportionately larger riparian vegetation, often densely clustered along the river even in otherwise open areas, and the shadows they cast (Figure 4.6a-4.6b). This is particularly true in optical aerial imagery, as both the time of day, lighting, and angle of acquisition all influence the resulting image. One possible solution would be to use LiDAR imagery which, if coupled with aerial imagery, might make it possible to map stream morphology above and below the dams.

## 6. Conclusions

Few un-dammed rivers remain in the U.S. The potential for dam removal has increased and the targets for removal are typically small dams (Doyle et al. 2000). Together with the fact that changes in small dams, physically and management-wise, are, in scale alone, less costly and less difficult, an understanding of the existing impacts on the river, as well as the effects of removal in different geographic and climate regions (or ecoregions) is needed. Csiki and Rhoads (2010) found similar sedimentological effects downstream of the dams in their study, but to different spatial extents. This suggests that there is no single rule for the type or scale of small dam impacts (and therefore removal responses). Furthermore, this study highlights that there are lot of small dams in Oregon, in the aggregate they may have a huge impact, and this deserves further study. Therefore,

more research is needed into the relationships of geographic, climatic, geologic, and dam characteristics and uses components of dams impacts, within spatial extents such as ecoregions, basins, and larger regional areas. This is not currently possible using the existing public databases of small dams. Though the data sets are large and contain numerous attributes, it is collectively not usable for geomorphic analysis--because it is not comprehensive and one cannot be certain of its quality.

The Willamette Valley is one example of basin scale data that has been compiled and produced by the Pacific Northwest Research Consortium (Hulse et al. 2002) for planning purposes, and includes dam location, history, management and utilization data (Payne, 2002). Geomorphic and in-channel characteristics would further aid in river-specific management. While some of the LiDAR and high resolution aerial imagery exist (not complete coverage of the state), the existing dam data needs to be updated for accuracy and combined into a comprehensive data set. With the LiDAR, imagery, and complete data, the possibilities for geomorphic assessment of small dams are greatly enhanced.

This work contributes important information on dam data to the almost non-existent data sets and geomorphic assessments on small dams in the U.S. (Chin et al. 2008 in Texas; Csiki and Rhoads, 2010 in Illinois) in the hopes of adding momentum for improvement and development on the state scale and sparking interest in eventually developing a national database. The multitude of water resource and aquatic species specialists working in our governmental agencies and consulting companies would greatly benefit from a comprehensive, accurate small dam data set for the studies they

currently undertake for planning and management. Furthermore, the collective data could drive new questions at larger scales that could continue to change and improve the way we think about and understand rivers, headwaters to sea.

# CHAPTER V

# SUMMARY

In this dissertation I examined human impacts of river regulation and several methods with which to do so. I evaluated a technique for bathymetric mapping, the effects of river regulation on sediment movement, and the spatial distribution of dams in Oregon. The goals of the research were to test a method of in-channel river characterization, to quantify the relative effects of diversion canals on sediment mobility, and to map small dams in Oregon and evaluate their geomorphic impacts. The results from the studies presented in Chapters II, III, and IV enhance our knowledge and understanding of the effects of river regulation at larger scales to inform environmental decision-making and river management.

On the lower McKenzie River, I evaluated the potential for mapping channel depths along the McKenzie River, OR, using 10 cm resolution optical aerial imagery with a hydraulically-assisted bathymetry (HAB-2) model. This study is the most rigorous test of the HAB-2 model to date. The sonar depths versus 2007 10 cm imagery modeled depths have a relatively low $R^2$ value (0.40), which improves only slightly with an Olympic filter to remove film granularity (0.48). The month-long gap between sonar and image acquisition may also contribute to the moderate fit of the model results to the sonar data. Modeled depth estimates for the 2008 0.5 m imagery fit the depth measurements more

closely ($R^2 = 0.89$). The better fit may reflect the collection of ground and image data at approximately the same time and discharge, as well as coarser spatial resolution, which created less sensitivity to changes in substrate size and colour. Results demonstrate that channel depths can be accurately mapped in many areas, with some imagery limitations. The HAB-2 model works well in the majority of the river, performing best in depths between 0.25-1.5 m. However, because the model is based on Beer's Law and the relationship of light to depth in water, the model does not do well in areas of shadow and surface turbulence. Still, the ability to characterize channel bathymetry and extract more representative cross-sections is an instrumental step in improving our ability to map aquatic habitat and hydrologically model river systems for restoration and planning.

Next, I analyzed the relative effects of a small dam and two diversion canals on grain size distribution along bars of the lower McKenzie River. First, I sampled bars for grain size distribution. The mean grain sizes above and below the dam show a classic coarsening pattern, which is not observed to the same degree below the tailraces. At the Walterville canal tailrace, the effect is much smaller and appears to be dampened by sediment input from Camp Creek located between the tailrace and the bars. Some degree of decrease in mean grain size is observed on most bars below a tributary. Overall, the typical pattern of downstream fining is disrupted at each feature and the coarsening below each feature is reduced at several tributaries, particularly in the "reduced water reaches" below canal outtakes. I calculated the stage height needed to mobilize the $D_{50}$ grain size and modeled the discharge value of that stage height at the bar cross-section. Most modeled discharge values necessary to mobilize bar sediments fall at or below the 2-year flood return interval, with the remaining at or below the 5-year flood return interval, generally

reflecting the $D_{50}$ values at each bar (20-115 mm). These results support the implementation of environmental flows which increase flows on the McKenzie River in an attempt to mimic the pre-regulation flow regime, as increased discharge on the river would primarily increase flow in the "reduced water" sections of the river and mobilize the larger sediment located in those reaches.

The third analysis of this work investigates the potential to document geomorphic impacts of small dams in Oregon at ecoregion extents using air photos and publically available data sets. This analysis highlights data disparity with respect to the collecting agency's mission and the difficulty of using remote sensing for small dams. Though the imagery was not useful in evaluating small dam impacts due to resolution and feature size, the data was useful in mapping the small dam distribution across Oregon and each ecoregion. The greatest number of dams per area is in the Willamette Valley ecoregion (0.021 dams/km$^2$), seven times greater than that of the state as a whole (0.003 dams/km$^2$). However, the greatest percentage of land located in the catchment of at least one small dam is greatest in the Cascades ecoregion (89%), almost a third more than that of the state (61%). The current data sets need upgrading, standardization, and consolidation in both attributes and collect methods to build a comprehensive database with the thought of how they would be used by the diverse range of scientist needed to solve problems and improve river habitat restoration and management. This assessment at the state and ecoregion scales elucidates the gaps in small dam data and can inform future research and data collection efforts.

Overall, this research suggests that, while the application of these techniques must be improved, our ability to observe, study, and understand rivers is enhanced by remote

sensing advancements and the combined use of these methods in river restoration and management. The importance of habitat diversity and connectivity in the riverscape is well-recognized, and insights from this work may apply to the up-scaling of river research from reach to basin scales. While incorporating more data into the already complex undertaking of understanding a river system adds time and expense, the geomorphic, hydrologic, and ecologic characteristics specific to each river are important in refining the limitations of management to achieve desired outcomes. Our work further highlights the importance of collaboration to incorporate the geomorphic component together with the hydrologic and ecologic components of dam management. Salmonid fish and other aquatic species depend on this complex combination of considerations to improve habitat on regulated rivers. Additional studies that integrate and new approaches and techniques (i.e., field surveys and sampling, remote sensing imagery--optical orthophotographs and LiDAR, modeling) and collaborate across disciplines and working groups, are needed and will help improve the extent to which we understand river systems at multiple scales.

## REFERENCES

Chapter I


Style used: Gibaldi, Joseph, ed. *MLA Handbook for Writers of Research Papers.* (any edition). New York: Modern Language Association of America.

Amoros, C., and G.E. Petts, eds. *Hydrosystèmes Fluviaux*. Paris: Masson, 1993. Print.

Amos, K.J., J.C. Croke, A.O. Hughes, J. Chapman, I. Takken, L. Lymburner. "A catchment-scale assessment of anabranching in the 143 000 $km^2$ Fitzroy River catchment, north-eastern Australia." *Earth Surface Processes and Landforms* 33 (2008): 1222-1241. Print.

Carbonneau, P.E., S.N. Lane, and N. Bergeron. "Feature based image processing methods applied to bathymetric measurements from airborne remote sensing in fluvial environments." *Earth Surface Processes and Landforms* 31 (2006): 1413-1423. Print.

Carbonneau, P.E., S.N. Lane, and N. Bergeron. "Catchment-scale mapping of surface grain size in gravel bed rivers using airborne digital imagery. *Water Resources Research* 40 (2004), doi: 10.1029/2003WR002759. Print.

Chessman, B.C., K.A. Fryirs, G.J. Brierley. "Linking geomorphic character, behaviour and condition to fluvial biodiversity: implications for river management. *Aquatic Conservation: Marine and Freshwater Ecosystems* 16 (2006): 267-288. Print.

Corenbilt, D., E. Tabacchi, J. Steiger, and A.M. Gurnell. "Reciprocal interactions and adjustments between fluvial landforms and vegetation dynamics in river corridors: A review of complementary approaches." *Earth-Science Reviews*, 84 (2007): 56-86. Print.

Doyle, M.W., and E.H. Stanley. "Exploring Potential Spatial-Temporal Links Between Fluvial Geomorphology and Nutrient-Periphyton Dynamics in Streams Using Simulation Models." *Annals of the Association of American Geographers*, 96 (2006): 687-698. Print.

Fonstad, M., and W.A. Marcus. "Remote sensing of stream depths with hydraulically assisted bathymetry (HAB) models." *Geomorphology* 72 **(**2005): 320-339. Print.

Gregory, K.J. "The human role in changing river channels." *Geomorphology* 79 (2006): 172-191. Print.

Kellerhals, R., M. Church, M., D.I. Bray. "Classification and analysis of river processes." *Journal of the Hydraulics Division* 102 (1976): 813-829. Print.

Kondolf, G.M., D.R. Montgomery, H. Piégay, and L. Schmitt. “Geomorphic classification of rivers and streams.” *Tools in Fluvial Geomorphology.* Eds. G.M. Kondolf andH. Piégay. Chichester, UK: J.Wiley and Sons, 2003. 169-202. Print.

Montgomery, D.R.., and J.M. Buffington. “Channel-reach morphology in mountain drainage basins.” *Geological Society of America Bulletin* 109 (1997): 596-611. Print.

Naiman, R.J., D.G. Lonzarich, T.J. Beechie, and S.C. Ralph. “General principles of classification and the assessment of conservation potential rivers.” *River Conservation and Management.* Eds. P.J. Boon, P. Calow, and G.E. Petts. New York: Wiley, 1992. 93-123. Print.

Orr, H.G., A.R.G. Large, M.D. Newson, C.L. Walsh. “A predictive typology for characterising hydromorphology.” Geomorphology 100 (2008): 32-40. Print.

Schmitt, L., G. Maire, P. Nobelis, J. Humbert. “Quantitative morphodynamic typology of rivers. A methodological study based on the French Upper Rhine basin.” *Earth Surface Processes and Landforms* 32 (2007): 1726-1746. Print.

Walther, S.C., W.A. Marcus, and M.A. Fonstad. “Evaluation of high resolution, true colour, aerial imagery for mapping bathymetry in a clear water river without ground-based depth measurements.” *International Journal of Remote Sensing*. In press. Print.

Ward, J.V., and J.A. Stanford. “Ecological Connectivity in Alluvial River Ecosystems and its Disruption by Flow Regulation.” *Regulated Rivers: Research and Management*, 11 (1995): 105-119. Print.

Chapter II

Style used: *International Journal of Remote Sensing*.

Brunner, G.W., 2002, HEC-RAS, River Analysis System User’s Manual. Hydrologic Engineering Center (HEC), pp.1-420 (Davis, CA: U.S. Army Corps of Engineers).

Campbell, J.B., 2007, *Introduction to Remote Sensing (4th ed.)*, pp. 1-626 (New York: The Guilford Press).

Carbonneau, P.E., Lane, S.N. and Bergeron, N., 2006, Feature based image processing methods applied to bathymetric measurements from airborne remote sensing in fluvial environments. *Earth Surface Processes and Landforms*, **31**, pp. 1413-1423.

Denny, M.W., 2003, *Air and Water: The Biology and Physics of Life’s Media*, pp. 1-360 (Princeton, NJ: Princeton University Press).

EA Engineering, Science, and Technology, 1991, The Fluvial Geomorphology of the Lower McKenzie River, pp. 1-66, Report prepared for Eugene Water and Electric Board (Bellevue, WA: EA Engineering, Science, and Technology).

ESRI, 2009, ESRI Geographer Information System (GIS) and mapping software. Information available online at: http://www.esri.com/index.html (accessed 9/12/09).

EWEB (Eugene Water and Electric Board), 2007, McKenzie Water Quality. Available online at: http://www.mckenziewaterquality.org/index.cfm (accessed 6/08/08).

Fonstad, M.A., and Marcus, W.A., 2005, Remote sensing of stream depths with hydraulically assisted bathymetry (HAB) models. *Geomorphology*, **72**, pp. 320-339.

Fonstad, M.A., Marcus, W.A., 2010, High resolution, basin extent observations and implications for understanding river form and process. *Earth Surface Processes and Landforms*. DOI: 10.1002/esp.1969.

Global Remote Sensing, 2008, *Hydrographic Survey Report: US Army Corps of Engineers Contract No. W9127N-04-D-0007 Delivery Order 10, McKenzie River*, pp. 1-51 (Portland, OR: GRS).

Gray, T., 2009. Personal communication about colour film scanning, Bergman Photographic Services, Inc., on 10/27/09.

Jarrett, R.D., 1984, Hydraulics of high-gradient streams. *Journal of Hydraulic Engineering*, **110** (11), pp. 1519-1539.

Jarrett, R.D., 1987, Errors in slope-area computations of peak discharges in mountain streams. *Journal of Hydrology*, Amsterdam, The Netherlands, **96**, pp. 53-57.

Lane, S.N., and Chandler, J.H., 2003, Editorial: the generation of high quality topographic data for hydrology and geomorphology: new data sources, new applications and new problems. *Earth Surface Processes and Landforms*, **28**, pp. 229-230.

Lane, S.N., Hardy, R.J., Elliott, L., and Ingham, D.B., 2002, High resolution numerical modelling of three-dimensional flows over complex river bed topography. *Hydrological Processes*, **16** (11), pp. 2261-2272.

Legleiter, C.J., Roberts, D.A., and Lawrence, R.L., 2009, Spectrally based remote sensing of river bathymetry. *Earth Surface Processes and Landforms*, **34**, pp. 1039–1059.

Legleiter, C.J., Roberts, D.A., Marcus, W.A., and Fonstad, M.A., 2004, Passive optical remote sensing of river channel morphology and in-stream habitat: Physical basis and feasibility. *Remote Sensing of Environment*, **93**, pp. 493-510.

Legleiter, C.J., Marcus, W.A., and Lawrence, R.L., 2002, Effects of sensor resolution on mapping in-stream habitats. *Photogrammetric Engineering and Remote Sensing*, **68** (8), pp. 801-807.

Lorang, M.S., Whited, D.C., Hauer, F.R., Kimball, J.S., Stanford, J.A., 2005, Using airborne multispectral imagery to evaluate geomorphic work across floodplains of gravel-bed rivers. *Ecological Applications*, **15** (4), pp. 1209-1222.

Magilligan, F.J., Renshaw, C., Svendsen, K.M., Nislow, N.H., and Kaste, J.M., 2007, The Effects of Flow Regulation by Dams on Channel Bed Sedimentation and Benthic Community Structure: Longitudinal Variation and the Role of Tributary Inputs. *AAG Annual Meeting Abstracts*, 3501 Fluvial Geomorphology II: Sediment and Channel Dynamics, p. 335**.**

Marcus, W.A., and Fonstad, M.A., 2008. Optical remote mapping of rivers at sub-meter resolutions and watershed extents. *Earth Surface Process and Landforms*, **33**, pp. 4-24.

Marcus, W.A., Legleiter, C.J., Aspinall, R.J., Boardman, J.W., and Crabtree, R.L., 2003, High spatial resolution hyperspectral mapping of in-stream habitats, depths, and woody debris in mountain streams. *Geomorphology*, **55**, pp. 363-380.

Marcus, W.A., Roberts, K., Harvey, L., and Tackman, G., 1992, An evaluation of methods for estimating Manning's n in small mountain streams. *Mountain Research and Development*, **12** (3), pp. 227-239.

McKean, J.A., Isaak, D.J., and Wright, C.W., 2008, Geomorphic controls on salmon nesting patterns described by a new, narrow-beam terrestrial-aquatic lidar. *Frontiers in Ecology and the Environment*, **6** (3), pp. 125-130.

Microsoft, 2009, Microsoft Office Products software-Excel. Information available online at: http://office.microsoft.com (accessed 9/10/09).

NOAA (National Oceanic Atmospheric Administration), 2005, ESA Recovery Planning for Salmon and Steelhead in the Willamette and Lower Columbia River Basins: Status of Planning Effort and Strategy for Completing Plans, December, 2005. Available online at: http://www.dfw.state.or.us/fish/esa/W-LC-Strategy.pdf (accessed 6/08/08).

OIE (Oregon Imagery Explorer), 2008, The Natural Resources Digital Library is housed at Oregon State University. Available online at: http://oregonexplorer.info/imagery/index.aspx (Imagery retrieved 8/15/08 for geo-referencing, 10/5/09 for DOQ HAB-2 analysis).

Ross, J.D., 2009, Personal communication about Ross 285B sounding data acquisition system, Ross Laboratories, Inc., on 9/9/09.

Smith, L.W., 2002, A Framework of Ecosystem Processes for Evaluating Effects of Dams on Endangered Species. *Northwest Science*, **76** (4), pp. 361-366.

Steffler, P., and Blackburn, J., 2002, *River2D: Two-dimensional Depth Averaged Model of River Hydrodynamics and Fish Habitat—Introduction to Depth Averaged Modeling and User's Manual*, pp. 1-120 (Edmonton: University of Alberta).

Stewart, G., Glasman, J.R., Grant, G.E., Lewis, S., and Ninneman, J., 2002, *Evaluation of Fine Sediment Intrusion into Salmon Spawning Gravels as Related to Cougar Reservoir Sediment Releases*, pp. 1-34 (Portland, OR: U.S. Army Corps of Engineers).

USGS (United States Geological Survey), 2005, *Biological Sciences in Oregon*, USGS FS 2006-3067, pp. 1-2 (Virginia: USGS and U.S. Department of the Interior).

Westaway, R.M., Lane, S.N., and Hicks, D.M., 2001, Airborne remote sensing of clear water, shallow, gravel-bed rivers using digital photogrammetry and image analysis. *Photogrammetric Engineering and Remote Sensing*, **67**, pp. 1271-1281.

Westaway, R.M., Lane, S.N., and Hicks, D.M., 2003, Remote survey of large-scale braided, gravel-bed rivers using digital photogrammetry and image analysis. *International Journal of Remote Sensing*, **24** (4), pp. 795-815.

Winterbottom, S.J., and Gilvear, D.J., 1997, Quantification of channel-bed morphology in gravel-bed rivers using airborne multispectral imagery and aerial photography. *Regulated Rivers: Research and Management*, **13** (6), pp. 489-499.

Wohl, E.E., 1998, Uncertainty in flood estimates associated with roughness coefficient. *Journal of Hydraulic Engineering*, **124** (2), pp. 219-223.

Chapter III

Style used: *River Research and Applications*.

Andrews ED. 1984. Bed-material entrainment and hydraulic geometry of gravel-bed rivers in Colorado. *Geological Society of America Bulletin* **95**: 371-378.

Applegate River Watershed Council (ARWC). 2007. *Applegate Basin Monitoring*. OWEB Grant 204-283 Final Report.

Arcement GJ Jr, Schneider VR. 1989. Guide for selecting Manning's roughness coefficients for natural channels and floodplains. *U.S. Geological Survey Water Supply Paper 2339.*

Baker VR, Ritter DF. 1975. Competence of rivers to transport coarse bedload material. *Bulletin of the Geological Society of America* **86**: 975-978.

Bathurst JC, Graf WH, Cao HH. 1987. Bed load discharge equations for steep mountain river. In *Sediment Transport in Gravel-bed Rivers*, Thorne CR, Bathurst JC, Hey RD (eds.). Wiley: Chichester, UK; 453-491.

Bell MC. 1986. *Fisheries handbook of engineering requirements and biological criteria*. U.S. Army Corps of Engineers, Office of the Chief of engineers, Fish Passage Development and Evaluation Program, Portland, Oregon.

Biggs BJF, Close ME. 1989. Periphyton biomass dynamics in gravel bed rivers: the relative effects of flows and nutrients. *Freshwater Biology* **22**: 209-231.

Bjornn TC, Reiser DW. 1991. Habitat Requirements of Salmonids in Streams. *American Fisheries Society Special Publication* **19**: 83-138.

Blott SJ, Pye K. 2001. Gradistat: A Grain Size Distribution and Statistics Package for the Analysis of Unconsolidated Sediments. *Earth Surface Processes and Landforms* **26**: 1237-1248, doi: 10.1002/esp.261.

Bradley WC, Fahnestock RK, Rowekamp ET. 1972. Coarse sediment transport by flood flows on Knik River, Alaska. *Bulletin of the Geological Society of America* **83**: 1261-1284.

Brown LR, Bauer ML. 2010. Effects of hydrologic infrastructure on flow regimes of California's central valley rivers: Implications for fish populations. *River Research and Applications* **26**: 751-765.

Brown MJ, Carter DL, Bondurant JA. 1974. Sediment in Irrigation and Drainage Waters and Sediment Inputs and Outputs for Two Large Tracts in southern Idaho. *Journal of Environmental Quality* **3**: 347-361.

Brown MJ, Bondurant JA, Brockway CE. 1981. Ponding Surface Drainage Water for Sediment and Phosphorous Removal. *Transactions of the ASAE*, Soil and Water Division.

Buffington JM, Montgomery DR. 1997. A systematic analysis of eight decades of incipient motion studies, with special reference to gravel-bedded rivers. *Water Resources Research* **33**: 1993-2029.

Buffington JM, Montgomery DR. 1999a. Effects of hydraulic roughness on surface textures of gravel-bed rivers. *Water Resources Research* **35**: 3507-3521.

Buffington JM, Montgomery DR. 1999b. Effects of sediment supply on surface textures of gravel-bed rivers. *Water Resources Research* **35**: 3523-3530.

Buffington JM, Montgomery DR, Greenberg HM. 2004. Basin-scale availability of salmonid spawning gravel as influenced by channel type and hydraulic roughness in mountain catchments. *Canadian Journal of Fisheries and Aquatic Sciences* **61**: 2085-2096.

Bunte K, Abt SR. 2001. Sampling Surface and Subsurface Particle-Size Distributions in Wadable Gravel and Cobble-Bed Streams for Analyses in Sediment Transport, Hydraulics, and Streambed Monitoring. *General Technical Report RMRS-GTR-74*. Fort Collins, CO: U.S. Department of Agriculture, Forest Service, Rocky Mountain Research Station; pp. 428.

Chien N. 1985. Changes in river regime after the construction of upstream reservoirs. *Earth Surface Processes and Landforms* **10**: 143-159.

Church M, Hassan MA. 2002. Mobility of bed materials in Harris Creek. *Water Resources Research* **38**: 1237, doi:10.1029/2001WR000753.

Collier M, Webb RH, Schmidt JC. 1997. *Dams and Rivers, A Primer on the Downstream Effects of Dams*. USGS Circular 1126; 94 pp.

Church M, Kellerhals R. 1978. On the statistics of grain size variation along a gravel river. *Canadian Journal of Fisheries and Aquatic Sciences* **15**: 1151-1160.

Church M, Hassan MA. 2002. Mobility of bed material in Harris Creek. *Water Resource Research* **38**: 1237-1248, doi: 10.1029/2001WR000753.

Coleman SE, Nikora VI. 2008. A unifying framework for particle entrainment. *Water Resources Research* **44**, doi: 10.1029/2007WR006363.

Cronin G, McHutchan Jr JH, Pitlick J, Lewis Jr WM. 2007. Use of shields stress to reconstruct and forecast changes in river metabolism. *Freshwater Biology* **52**: 1587-1601.

DOGAMI, 2009. Lidar Collection and Mapping, Oregon Lidar Consortium (OLC). Oregon Department of geology and Mineral Industries, http://www.oregongeology.org/sub/projects/olc/default.htm, accessed 10/6/2009.

Downs, P, Gregory K. 2004. *River Channel Management; Towards Sustainable Catchment Hydrosystems*. Hodder Arnold, London, UK, pp. 395.

DuBoys P. 1879. Le Rhône et les rivières à lit affouillable (River Rhone and tributaries of unconsolidated sediments). *Annum Ponts et Chaussées* **5**: 141-195.

Duncan MJ, Suren AM, Brown SLR. 1999. Assessment of streambed stability in steep, bouldery streams: development of a new analytical technique. *Journal of North American Benthological Society* **18**: 445-456.

EA Engineering, Science, and Technology, 1991. *The Fluvial Geomorphology of the Lower McKenzie River*. Bellevue, WA: EA Engineering, Science, and Technology for Eugene Water and Electric Board; 1-66.

Eberle LC, Stanford JA. 2010. Importance and seasonal variability of terrrestrial invertebrates as prey for juvenile salmonids in floodplain spring brooks of the Kol river (Kamchatka, Russian Federation). *River Research and Applications* **26**: 682-694, doi:10.1002/rra.1270.

EPA (Environmental Protection Agency). 2009. *National Water Program Research Strategy 2009-2014*. Office of Water (4304T), EPA 822-R-09-012; 1-57.

ESRI. 2009. ESRI Geographer Information System (GIS) and mapping software. Information available online at: http://www.esri.com/index.html (accessed 9/20/10).

EWEB (Eugene Water and Electric Board). 1991. Leaburg-Walterville Hydroelectric Project, Project No. 2496, Application for License, Vol. II, FERC, December 1991.

EWEB (Eugene Water and Electric Board), 2007. McKenzie Water Quality. Available online at: http://www.mckenziewaterquality.org/index.cfm (accessed 6/08/08).

Fassnacht H, McClure EM. 2003. Downstream Effects of the Pelton-Round Butte Hydroelectric Project on Bedload Transport, Channel Morphology, and Channel-Bed Texture, Lower Deschutes river, Oregon. *Water and Science Application* **7**: 175-207, doi: 10/1029/007WS12.

Flynn KM, Kirby WH, and Hummel PR. 2006a. *User's manual for program PeakFQ, Annual Flood Frequency Analysis Using Bulletin 17B Guidelines*. U.S. Geological Survey Techniques and Methods Book 4, Chapter B4, 1-42.

Flynn KM, Kirby WH, Mason RR, Cohn TA. 2006b. *Estimating magnitude and frequency of floods using the PeakFQ program*. U.S. Geological Survey Fact Sheet 2006-3143; 1-2.

Fonstad MA, Marcus WA. 2005. Remote sensing of stream depths with hydraulically assisted bathymetry (HAB) models. *Geomorphology* **72**: 320-339.

Folk RL, Ward WC. 1957. Brazos River bar: a study of the significance of grain size parameters. *Journal of Sedimentary Petrology* **27**: 3-26.

Fryirs KA, Brierley GJ, Preston NJ, Kasai M. 2007. Buffers, barriers and blankets: The (dis)connectivity of catchment-scale sediment cascades. *Catena* **70**: 49-67, doi: 10.1016/j.catena.2006.07.007.

Gessler J. 1971. Beginning and ceasing of sediment motion. In *River Mechanics*, Shen, HW (ed). Fort Collins; 1-22.

Gordon ND, McMahon TA, Finlayson BL, Gippel CJ, Nathan RJ. 2004. Stream Hydrology An Introduction for Ecologists. Wiley, Chichester, UK; pp. 429.

Graf WL. 1980. The effect of dam closure on downstream rapids. *Water Resource Research* **16**: 129-363.

Graf WL. 1996. Geomorphology and Policy for Restoration of Impounded American Rivers: What is 'Natural?'. In Rhoads BL, Thorn CE, (eds.). *The Scientific Nature of Geomorphology: Proceedings of the 27th Binghamton Symposium in Geomorphology*, 27-29 1996. Wiley, Chichester, UK, pp. 443-473.

Graf WH. 2005. Geomorphology and American dams: The scientific, social, and economic context. *Geomorphology* **71**: 3-26.

Graf WH. 2006. Downstream hydrologic and geomorphic effects of large dams on American rivers. *Geomorphology* **79**: 336-360.

Gran KB, Montgomery DR, Sutherland DG. 2006. Channel bed evolution and sediment transport under declining sand inputs. *Water Resources Research* **25**: 1161–1186.

Grant G, 2001. Dam removal: Panacea or Pandora for rivers? *Hydrological Processes* **15**: 1531-1532.

Gregory KJ. 2006. The human role in changing river channels. *Geomorphology* **79**:172-191.

Gregory S, Ashkenas L,Nygaard C. 2007. *Summary Report to Assist Development of Ecosystem Flow Recommendations for the Coast Fork and Middle Fork of the Willamette River, Oregon*. The Nature Conservancy and US Army Corps of Engineers. Portland, OR, pp. 237.

Hardy T, Palavi P, Mathias D. 2005. *WinXSPRO, A Channel Cross Section Analyzer, User's Manual, Version 3.0*. General Technical Report RMRS-GTR-146. Fort Collins, CO: United States Department of Agriculture, Forest Service, Rocky Mountain Research Station; pp. 94.

Harvey AM. 2002. Effective timescales of coupling within fluvial systems. *Geomorphology* **44**: 175-201.

Hoey T, Bluck B. 1999. Identifying the controls over downstream fining of river gravels. *Journal of Sedimentary Research* **69**: 40–50.

Hooke JM. 2003. Coarse sediment connectivity in river channel systems: a conceptual framework and methodology. *Geomorphology* **56**: 79-94.

Howard A, Dolan R. 1981. Geomorphology of the Colorado River in the Grand Canyon. *The Journal of Geology* **89**: 269-298.

Hunter, JW. 1973. *A discussion of game fish in the State of Washington as related to water requirements*. Report by the Washington State Department of Game, Fishery Management Division, to the Washington State Department of Ecology, Olympia.

Hynes HBN. 1970. *The Ecology of Running Waters*. Toronto: University of Toronto press.

IACWD (Interagency Advisory Committee on Water Data). 1982. *Guidelines for determining flood-flow frequency: Bulletin 17B of the Hydrology Subcommittee*. Reston, Va: Office of Water Data Coordination, U.S. Geological Survey; pp. 183, http://water.usgs.gov/osw/bulletin17b/bulletin_17B.html.

Jackson WL, Beschta RL. 1984. Influences of increased sand delivery on the morphology of sand and gravel channels. *Water Resources Bulletin* **20**: 527-533.

Johnson SL, Grant GE, Swanson FJ, Wemple BC. 1997. Lessons from a flood: an integrated view of the February 1996 flood in the McKenzie River basin. In *The Pacific Northwest Flood of 1996: Causes, Effects, and Consequences, Proceedings of the Flood Conference, Oct. 7-8, 1996, Portland, OR*, Laenaen A (ed.). American Institute of Hydrology and Oregon Water Resources Research Institute.

Johnson SL, Swanson FJ, Grant GE, Wondzell, SM. 2000. Riparian forest disturbances by a mountain flood--the influence of floated wood. *Hydrological Process* **14**: 3031-3050.

Kaufmann PR, Faustini JM, Larsen DP, Shirazi MA. 2008. A roughness-corrected index of relative bed stability for regional stream surveys. *Geomorphology* **99**: 150-170.

Knighton AD, 1980. Longitudinal changes in size and sorting of stream bed material in four English rivers. *Geological Society of America Bulletin* **91**: 55-62.

Knighton AD, 1987. River channel adjustment-the downstream dimension. In *River Channels-Environment and Process*, Richards K (ed.). Oxford: Basil Blackwell; pp. 391.

Knighton AD. 1991. Channel bed adjustment along mine-affected rivers of northeast Tasmania. *Geomorphology* **4**: 205-219.

Knighton AD. 1998. *Fluvial Forms and Processes*. London: Hodder Headline Group; pp. 383.

Kondolf GM. 1997. Hungry water: effects of dams and gravel mining on river channels. *Environmental Management* **21**: 533-551.

Kondolf GM. 2000. Assessing Salmonid Spawning Gravel Quality. *Transactions of the American Fisheries Society* **129**: 262-281.

Kondolf GM, Wilcock P. 1996. The flushing flow problem: Defining and Evaluating Objectives. *Water Resources and Research* **32**: 2589-2599.

Kondolf GM, Wolman MG. 1993. The sizes of salmonid spawning gravels. *Water Resources Research* **29**: 2275-2285.

Komar PD. 1987. Selective gravel entrainment and the empirical evaluation of flow competence. *Sedimentology* **34**: 1165-1176.

Lanzoni S, Tubino M. 1999. Grain sorting and bar instability. *Journal of Fluid Mechanics* **393**: 149-174.

Leopold LB, Maddock Jr. T. 1953. The hydraulic geometry of stream channels and some physiographic implications. *USGS Professional Paper* 252, pp. 57.

Lisle TE, Hilton S. 1992. The volume of fine sediment in pools: An index of sediment supply in gravel-bed streams. *Water Resources Bulletin* **28**: 371-383.

Lorang MS, Hauer FR. 2003. Flow competence and streambed stability: An evaluation of technique and application. *Journal of North American Benthological Society* **22**: 475-491.

Maidment, DR (ed.). 2002. Arc Hydro GIS for Water Resources. Redlands, CA: ESRI Press, pp. 203.

Mao L, Uyttendaele GP, Iroumé A, Lenzi MA. 2008. Field based analysis of sediment entrainment in two high gradient streams located in Alpine and Andine environments. *Geomorphology* **93**: 368-383.

May CL, Pryor B, Lisle TE, Lang M. 2009. Coupling hydrodynamic modeling and empirical measures of bed mobility to predict the risk of scour and fill of salmon redds in a large regulated river. *Water Resources Research* **45**, doi: 10.1029/2007WR006498.

Minshall GW. 1984. Aquatic insect-substratum relationships. In *The Ecology of Aquatic Insects*, Resh VH, Rosenberg DM. (eds.). New York: Praeger Scientific; pp. 358-400.

Montgomery DR, Buffington JM, Peterson NP, Schuett-Hames D, Quinn TP. 1996. Stream-bed scour, egg burial depths, and the influence of salmonid spawning on bed surface mobility and embryo survival. *Canadian Journal of Fisheries and Aquatic Sciences* **53**: 1061–1070, doi:10.1139/cjfas-53-5-1061.

Montgomery DR, Buffington JM. 1997. Channel-reach morphology in mountain drainage basins. *GSA Bulletin* **109**: 596-611.

Morris P, Williams D. 1999. A worldwide correlation for exponential bed particle size variation in subaerial aqueous flows. *Earth Surface Processes and Landforms* **24**: 835–847, doi: 10.1002/(SICI)1096-9837(199908)24:9<835: AID-ESP15>3.0.CO;2-G.

NOAA (National Oceanic and Atmospheric Administration) 2005. *ESA Recovery Planning for Salmon and Steelhead in the Willamette and Lower Columbia River Basins: Status of Planning Effort and Strategy for Completing Plans,* pp. 25.

Null SE, Deas ML, Lund JR. 2010. Flow and water temperature simulation for habitat restoration in the Shasta River, California. *River Research and Applications* **26**: 663-681, doi: 10.1002/rra.1288.

O'Connor J, Major J, Grant G. 2008. Down with the Dams: Unchaining U.S. Rivers. *Geotimes*, March. http://www.geotimes.org/mar08/article.html?id=feature_dams.html

Osmundson DB, Ryel RJ, Lamarra VL, Pitlick J. 2002. Flow-sediment-biota relations: Implications for river regulation effects on native fish abundance. *Ecological Applications* **12**(6): 1719-1739.

Papanicolaou AN, Diplas P, Evaggelopoulos N, Fotopoulos S. 2002. Stochastic Incipient Motion Criterion for Spheres under Various Bed Packing Conditions. *Journal of Hydraulic Engineering* **128**: 369-380.

Parker G, Klingeman PC, McLean DG, 1982. Bed load size distribution in paved gravel-bed streams. *Journal of Hydraulics Division ASCE* **108**: 544-571.

Petit F, Poinsard D, et Bravard J.-P. 1996. Channel incision, gravel mining and bedload transport in the Rhône River upstream of Lyon, France ("canal de Miribel"). *Catena* **26**: 209-226.

Poff NL, Ward JV. 1989. Implications of Streamflow Variability and Predictability for Lotic Community Structure: A Regional Analysis of Streamflow Patterns. *Canadian Journal of Fisheries and Aquatic Sciences* **46**: 1805-1818.

Poff NL, Allan JD, Bain MB, Karr JR, Prestegard KL, Richter BD, Sparks RE, Stromberg JC. 1997. The natural regime flow: a paradigm for river conservation and restoration. *Bioscience* **47**: 769-784.

Poff NL, Richter BD, Arthington AH, Bunn SE, Naiman RJ, Kendy E, Acreman M, Apse C, Bledsoe BP, Freeman MC, Henricksen J, Jacobson RB, Kennen JG, Merritt DM, O'Keefe JH, Olden JD, Rogers K, Tharme RE, Warner A. 2010. The ecological limits of hydrological alteration (ELOHA): a new framework for developing regional environmental flow standards. *Freshwater Biology* **55**:147-170, doi: 10.1111/j.1365-2427.2009.02204.x

Pohl M. 2004. Channel bed Mobility downstream from the Elwha dams, Washington. *The Professional Geographer* **56**: 422-431.

Potyondy J., Bunte K. 2002. Sampling with the us sah-97 hand-held particle size analyzer. Vicksburg, MS: Federal Interagency Sedimentation Project; pp. 1-6, http://fisp.wes.army.mil/Instructions%20US_SAH-97_040412.pdf

Recking A. 2009. Theoretical development on the effects of changing flow hydraulics on incipient bed load motion. *Water Resource Research* **45**, W04401, doi:1029/2008WR006826.

Rice SP, Church M. 1996. Sampling Surficial Fluvial Gravels: The Precision of Size Distribution Percentile Estimates. *Journal of Sedimentary Research* **663**: 654-665.

Rice SP, Greenwood MT, Joyce CB. 2001. Tributaries, sediment sources, and the longitudinal organisation of macroinvertebrate fauna along river systems. *Canadian Journal of Fisheries and Aquatic Sciences* **58**: 824-840.

Richter BD, Matthews R, Harrison DL, Wigington R. 2003. Ecologically sustainable water management: managing river flows for ecological integrity. *Ecological Applications* **13**: 206-224.

Richter BD, Warner AT, Meyer JL, Lutz K. 2006. A collaborative and adaptive process for developing environmental flow recommendations. *River Research and Applications* **22**: 297-318.

Risley J, Wallick JR, Waite I, Stonewall A. 2010. *Development of an environmental flow framework for the McKenzie River basin, Oregon*. U.S. Geological Survey Scientific Investigations Report 2010-5016, pp. 94.

Robinson RAJ, Slingerland RL. 1998. Origin of fluvial grain-size trends in a foreland basin: the Pocono formation of the Central Appalachian basin. *Journal of Sedimentary Research* **68**: 473–486.

Rubin DM, Topping DJ. 2001. Quantifying the relative importance of flow regulation and grain size regulation of suspended sediment transport $\alpha$ and tracking changes in grain size of bed sediment $\beta$. *Water Resources Research* **37**: 133-146.

Runyon J. 2000. *McKenzie River Subbasin Assessment Summary Report*. Portland, OR: Bonneville Power Administration (BPA) Report DOE/BP-23129-2, pp. 66.

Sennatt KM, Salant NL, Renshaw CE, Magilligan FJ. 2006. Assessment of methods for measuring embeddedness: application to sedimentation in flow regulated streams. *JAWRA* **Dec**: 1671-1682.

Shields A. 1936. Anwendung der Aehnlichkeitsmechanik und der Turbulenzforschung auf die Geschiebebewegung. *Mitteilungen der Preussiischen Versuchsanstalt fuer Wasserbau und Schiffhau*, Heft 26, Berlin, Germany. *Shields, A., 1936.* English translation by Ott WP, van Uchelen JC. *Hydrodynamics Laboratory Publication No. 167*, Hydrodynamics Lab., California Institute of Technology, Pasadena.

Sklar LS, Dietrich WE. 1998. River Longitudinal Profiles and Bedrock Incision Models: Stream Power and the Influence of Sediment Supply. *Geophysical Monograph* **107**: 237-260.

Sklar LS, Dietrich WE. 2001. Sediment and rock strength controls on river incision into bedrock. *Geology* **29**: 1087-1090.

Stallman JD, Bowers RJ, Cabera NC, Real de Asua R, Wooster JK. 2005. Sediment Dynamics in the Upper McKenzie River Basin, Central Oregon Cascade Range. *AGU Fall Meeting abstract*s #H51E-0411.

Stillwater Sciences. 2006. *Fluvial geomorphic processes and channel morphology at the Carmen-smith Hydroelectric Project, upper McKenzie basin, Oregon*. Final report. Arcata, CA: Stillwater Sciences for Eugene Water and Electric Board, Eugene, Oregon, pp. 105.

The Nature Conservancy, 2010. McKenzie River Environmental Flows Workshop, March 10-11, 2010. EWEB Headquarters, Eugene, Oregon.

Topping DJ, Rubin DM, Nelson JM, Kinzel III PJ, Corson IC. 2000. Colorado River Sediment Transport 2. Systematic Bed-Elevation and Grain-Size Effects of Sand Supply Limitation. *Water Resources Research* **36**: 543-570.

USGS, 2010. USGS National Streamflow Information Program (NSIP) streamflow data, http://waterdata.usgs.gov/nwis/rt, accessed 7/9/2009.

Walther SC, Marcus WA, Fonstad MA. in press. Evaluation of high resolution, true colour, aerial imagery for mapping bathymetry in a clear water river without ground-based depth measurements. *International Journal of Remote Sensing*.

Ward JV, Stanford JA (eds). 1979. *The Ecology of Regulated Streams*. Plenum Press: New York; pp. 398.

Weston DP, You J, Lydy MJ. 2004. Distribution and Toxicity of Sediment-Associated Pesticides in Agriculture-Dominated Water Bodies of California's Central Valley. *Environment Science and Technology* **38**: 2752–2759, doi: 10.1021/es0352193.

Wilcock PR. 2001. Toward a practical method for estimating sediment-transport rates in gravel-bed rivers. *Earth Surface Process and Landforms* **26**: 1395-1408.

Wohl E, Merritt D. 2005. Prediction of mountain stream morphology. *Water Resources Research* **41**: W08419, doi: 10.1029/2004WR003779.

Wolman MG. 1954. A method of sampling coarse river bed material. *Transactions of the AGU* **35**: 951-956.

Yen BC. 1992. *Channel Flow Resistance: Centennial of Manning's Formula*. Water Resources Publication, pp. 453.

Zar JH. 1999. Biostatistical Analysis, 4th ed. New Jersey: Prentice Hall, pp.663.

Chapter IV

Bach, L., 2008. Managing water releases to restore ecological flows in the McKenzie River. Oregon Watershed Enhancement Board Technical Assistance Grant Proposal, pp.13.

Bailey, R.G., 1995. Descriptions of the Ecoregions of the United States (2nd ed.). Publication No. 1391, Map scale 1:7,500,000, U.S. Department of Agriculture, Forest Service, 108 pp.

Chin, A., Laurencio, L.R., Martinez, A.E., 2008. The Hydrologic Importance of Small- and Medium-Sized Dams: Examples from Texas. The Professional Geographer 60(2), 238-251.

Chin, A., Harris, D.L., Trice, T.H., and Given, J.L., 2002. Adjustment of Stream Channel Capacity Following Dam Closure, Yegua Creek, Texas. Journal of the American Water Resources Association 38 (6), 1521-1531.

Csiki, S., Rhoads, B., 2010. Discontinuities caused by the presence of run-of-river dams on fluvial systems. GSA abstracts, Annual Meeting 2010.

Csiki, S., Rhoads, B., 2008. Fluvial geomorphological responses to the presence of run-of-river dams. AGU abstracts #H41I-08, Fall Meeting 2008.

Collier, M., Webb, R.H. , Schmidt, J. C., 1996. Dams and Rivers, A Primer on the Downstream Effects of Dams. USGS Circular 1126, 94 pp.

Doyle, M.W., Stanley, E.H., Luebke, M.A., Harbor, J.M., 2000. Dam removal: Physical, biological and societal considerations. ASCE Joint Conference on Water Resources, Engineering and Water Resources Planning and Management, 30 July-2August, Minneapolis, MN.

ESRI, 2009, ESRI Geographer Information System (GIS) and mapping software. Information available online at: http://www.esri.com/index.html (accessed 9/12/09).

Fonstad, M.A., Marcus, W.A., 2005. Remote sensing of stream depths with hydraulically assisted bathymetry (HAB) models. Geomorphology 72, 320-339.

Gesch, D.B., 2007. The National Elevation Dataset. In: Maune, D. (ed.), Digital Elevation Model Technologies and Applications: The DEM Users Manual, 2nd Edition. Bethesda, Maryland: American Society for Photogrammetry and Remote Sensing, p. 99-118.

Gesch, D., Oimoen, M., Greenlee, S., Nelson, C., Steuck, M., and Tyler, D., 2002. The National Elevation Dataset. Photogrammetric Engineering and Remote Sensing 68 (1), 5-11.

Google Earth, 2010. Program downloaded on-line from http://www.google.com/earth/index.html, accessed 7/10/2009.

Graf, W., 2006. Downstream hydrologic and geomorphic effects of large dams on American rivers. Geomorphology 79(3-4), 336-360.

Graf, W., 2005. Geomorphology and American dams: The scientific, social, and economic context. Geomorphology 71, 3-26.

Graf, W., 2001. Damage Control: Restoring the Physical Integrity of America's Rivers. Annals of the Association of American Geographers 91 (1), 1-27.

Graf, W., 1999. Dam Nation: A Geographic Census of Large American Dams and their Hydrological Impacts. Water Resources Research 35, 1305-1311.

Gregory, S., Ashkenas, L., Nygaard, C., 2007. Environmental Flows Workshop for the Middle Fork and Coast Fork of the Willamette River, Oregon. Summary Report by the Institute for Water and Watersheds and Oregon State University, pp.1-38.

Gregory, S.V., Bisson, P.A., 1997. Degradation and Loss of Anadromous Salmonid Habitat in the Pacific Northwest. In: Stouder, D.J. Bisson, P.A., Naiman, R.J. (eds.), Pacific salmon and their ecosystems: Status and future option. New York: Chapman and Hall, pp.685.

Hall, J.E., Holzer, D.M., and Beechie, T.J., 2007. Predicting river floodplain and lateral channel migration for salmon habitat conservation. Journal of the American Water Resources Association 43 (3), 786-797.

Harvey, A.M., 2002. Effective timescales of coupling with fluvial systems. Geomorphology 44, 175-201.

Hulse, D., Gregory, S., and Baker, J. (eds.), 2002. Willamette River Basin: trajectories of environmental and ecological change. Produced by the Pacific Northwest Ecosystem Research Consortium. Corvallis, OR: OSU Press, pp. 178.

Lackey, R.T., Lach, D.H., Duncan, S.L. (eds.), 2006. Salmon 2100: The Future of Wild Pacific Salmon. Bethesda, MD: American Fisheries Society, pp. 629.

Loy, W., Allan, S., Buckley, A.R., and Meacham, J.E., 2001. Atlas of Oregon, 2nd Edition.

Magilligan, F.J., Renshaw, C., Svendsen, K.M., Nislow, N.H., Kaste, J.M., 2007. The Effects of Flow Regulation by Dams on Channel Bed Sedimentation and Benthic Community Structure: Longitudinal Variation and the Role of Tributary Inputs. AAG Annual Meeting Abstracts, 3501.

Montgomery, D.R., 2003. King of Fish: The Thousand-Year Run of Salmon. Cambridge, MA: Westview Press, pp. 290.

Nilsson, C., Berggren, K., 2000. Alterations of Riparian Ecosystems Caused by River Regulation. BioScience 50 (9), 783-792.

ODFW (Oregon Department of Fish and Wildlife), 2009. Oregon Fish Passage Barriers. Natural Resources Information Management Program Fish Barrier Data. http://rainbow.dfw.state.or.us/nrimp/default.aspx?pn=fishbarrierdata

OIE (Oregon Imagery Explorer), 2005. Natural Resources Digital Library, Statewide 0.5 meter Aerial Imagery, http://oregonexplorer.info/imagery/.

Omernik, J.M. 1995. Ecoregions: A spatial framework for environmental management. In: Biological Assessment and Criteria: Tools for Water Resource Planning and Decision Making. Davis, W.S., and Simon, T.P. (eds.), Boca Raton, FL: Lewis Publishers, p. 49-62.

Omernik, J.M., and Bailey, R.G., 1997. Distinguishing between watershed and ecoregions. Journal of the American Water Resources Association 33, 935-949.

OWRD (Oregon Water Resources Department), 2009. Oregon dams stat set. http://www.wrd.state.or.us/OWRD/SW/dams_in_oregon.shtml, accessed 9/9/09.

Payne, S., 2002. Dams. In: Hulse, D., Gregory, S., and Baker, J. (eds.), Willamette River Basin: trajectories of environmental and ecological change. Produced by the Pacific Northwest Ecosystem Research Consortium. Corvallis, OR: OSU Press, p. 30-31.

Petts, G.E., Gurnell, A.M., 2005. Dams and Geomorphology: Research progress and future directions. Geomorphology 71, 27-47.

Salant, N.L., Renshaw, C.E., Magilligan, F.J., 2006. Short and long-term changes to bed mobility and bed composition under altered sediment regimes. Geomorphology 76, 43-53.

Smith, L.W., 2002. A Framework of Ecosystem Processes for Evaluating Effects of Dams on Endangered Species. Northwest Science 76(4), 361-366.

Stromberg, J.C., 1993. Instream flow models for mixed deciduous riparian vegetation within a semiarid region. Regulated Rivers: Research & Management, 8: 225–235. doi: 10.1002/rrr.3450080303.

Thorson, T.D., Bryce, S.A., Lammers, D.A., Wood, A.J., Omernik, J.M., Kagan, J., Pater, D.E., Comstock, J.A., 2003. Ecoregions of Oregon (color poster with map, descriptive text, summary tables, and photographs). Reston, Virginia, U.S. Geological Survey (map scale 1:1,500,000), found on-line at: http://www.epa.gov/wed/pages/ecoregions/or_eco.htm.

Vannote, R.L., Minshall, G.W., Cummins, K.W., Sedell, J.R., Cushing, C.E., 1980. The river continuum concept. Canadian Journal of Fisheries and Aquatic Sciences 37, 130-137.

Walther, S.C., Marcus, W.A., Fonstad, M.A., in press. Evaluation of high resolution, true colour, aerial imagery for mapping bathymetry in a clear water river without ground-based depth measurements. International Journal of Remote Sensing.

Ward, J.V., Stanford, J.A., 1983. Ecological Connectivity in Alluvial River Ecosystems and its Distribution by Flow Regulation. Regulated Rivers: Research and Management 11, 105-119.

Wipfli, M.S., Richardson, J.S., and Naiman, R.J., 2007. Ecological linkages between headwaters and downstream ecosystems: transport of organic matter, invertebrates, and wood down headwater channels. Journal of the American Water Resources Association 43 (1), 72-85.

Wohl, E.E., and Rathburn, S.L., 2003. Mitigation of sediment hazards downstream from reservoirs. International Journal of Sediment Research 18 (2), 97-106.